UNIVERSITAT DE BARCELONA

FACULTAT DE QUÍMICA

DEPARTAMENT DE QUÍMICA FÍSICA

Programa de Doctorat de Tecnologia de Materials

Bienni 2004-2006

Electrochemical preparation of Co-Ag nanostructured materials for GMR applications

Memòria que presenta JOSÉ MANUEL GARCÍA TORRES per optar al títol de Doctor per la Universitat de Barcelona

Directores de la tesi:

Dra. Elvira GÓMEZ VALENTÍN
Professora Titular de Química Física
Universitat de Barcelona

Dra. Elisa VALLÉS GIMÉNEZ
Professora Titular de Química Física
Universitat de Barcelona

CHAPTER 4

Co-Ag GRANULAR FILMS

4

Co-Ag GRANULAR FILMS

The work presented in this chapter analyzes the electrodeposition process and characterizes one kind of nanostructured material suitable to be implemented in magnetoresistive devices, the granular films. In this sense, the main objective of the present chapter is to prepare Co-Ag heterogeneous films from different and previously optimized electrolytic baths by means of electrodeposition. Different solutions were employed in order to compare the electrochemical, structural, magnetic and magnetotransport properties of the films prepared.

However, cobalt-silver electrodeposition is not an easy task as some problems are expected to occur during the codeposition process, the problems being related to the big difference in the standard potentials of both metals ($E°_{Co}$ = -0.28 V; $E°_{Ag}$ = +0.80 V) which in turn is increased by the inert character of cobalt in the electrodeposition. In this sense, the first step proposed in this study was to developed an electrolyte where overcoming these problems. Once the bath composition for silver deposition was optimized, the effect of the electrolyte over cobalt both deposition process and properties was studied. The results are shown in section 4.1.

In a second step, the viability of the electrodeposition technique to grow Co-Ag granular films from the developed electrolytic bath was demonstrated. The films prepared were deeply characterized by the appropriate techniques, i.e. XRD, XPS, TEM or electrochemical techniques among others. All these results will be presented in section 4.2.

Confirmed the viability to grow Co-Ag films by means of electrodeposition, the codeposition process from the very early deposition stages was studied. The objective was to gain knowledge about the way in which the properties varied with the growing films. The results are given in more detail in section 4.3.

The magnetotransport properties measurement followed by an optimization process of the films to improve the magnetoresistance values are presented in section 4.4. Moreover, results about the effect of impurities on the magnetoresistance effect will be drawn.

Finally and according to the previous results, a new bath was developed. A simpler electrolyte in terms of composition was employed to grow the Co-Ag films in order to avoid the inclusion of impurities onto the films. The microstructure/nanostructure of the deposits was greatly modified by changing the electrodeposition conditions, i.e. applied potential, deposition time or electrodeposition technique, in order to study their effect over the coating's properties, mainly the magnetotransport ones. The influence of the measurement temperature on the GMR will also be presented. All these results will be treated in section 4.5.

All the studies done have allowed getting some results about the preparation and characterization of the electrodeposited Co-Ag granular films which have been published in different international journals and will be included in the appropriate section.

4.1. Study of the electrodeposition process of the parents metals. Problems during Co-Ag codeposition

From an electrochemical point of view, the big difference in the standard potential of both metals represents the main problem when trying to perform Co-Ag codeposition. Moreover, some underlying problems appear due to its really big difference. On one hand, at the potentials where codeposition should take place (which are potentials equal or more negative than that for cobalt reduction onset) silver would be the metal preferentially deposited avoiding obtaining Co-Ag films with a modulated composition. Moreover, at these high negative potentials some side reactions, i.e. hydrogen evolution can take place disturbing the codeposition process. On the other hand, at such potentials dendritic growth of silver is expected (Figure 4.1(A)).

In this sense, previous to the Co-Ag codeposition it was necessary to raise some solutions to the existing problems. On one hand, Co(II) concentration in the electrolyte should be higher than that for silver in order to favour cobalt incorporation into the film. On the other hand, complexing agents were added to the electrolyte for different reasons:

- to delay the potential for silver reduction
- to improve the morphology of the silver matrix
- to favour cobalt incorporation into the deposit by making silver deposition unfavourable (Figure 4.1(B)).

Therefore, the first step proposed in this study was to develop an electrolyte able to obtain high quality/non-dendritic silver coatings at the codeposition potentials. Cyclic voltammetry combined with SEM examination were the main techniques employed to optimize the electrolyte. A basic study of the silver electrodeposition process was performed from the solution 0.01 mol dm^{-3} $AgClO_4$ + 0.2 mol dm^{-3} $NaClO_4$. Vitreous carbon was selected as the working electrode. The electrochemical study revealed some of the aforementioned problems (Figure 4.2, curve a). On one hand, at the conditions selected silver deposition took place at potentials (E_{Ag} ≈ +0.2 V) too far from that of cobalt (E_{Co} ≈ -0.8 V). On the other hand, hydrogen adsorption appeared at potentials corresponding to cobalt deposition. Moreover, at such negative potentials dendritic morphology for silver was detected.

Regarding the big difference in the reduction potentials of both metals, different silver complexing agents with a high complexing stability constant were tested (i.e. sodium citrate, potassium iodide, tartaric acid, thiourea, …). Among them, thiourea (TU) was the specie selected as the most negative potential for silver reduction was recorded due to its strongest complexing capacity. Shift in E_{Ag} of around 0.75 V to negative values was observed (Figure 4.2, curve b). Although it represented a very important shift on silver reduction, it was necessary to add some other species in order to improve silver deposits at the codeposition potentials. In this sense, different species and different concentrations were tested. Sodium gluconate and boric acid exerted a positive effect on silver films as both species delayed the potential at which dendritic growth was observed. However, the simultaneous presence of sodium gluconate and boric acid allowed expanding even more the potential range where obtaining deposits of good quality. Figure 4.3 clearly shows the morphological effect of all theses species. On the other hand, the side reaction was minimized adjusting the solution pH at 3.7 as more acidic baths leaded to an increase in the proton reaction-related current. Higher pH values were discarded as cobalt oxides could easily precipitate even in neutral media. The composition of the optimized electrolyte was: 0.01 mol dm^{-3} $AgClO_4$ + 0.2 mol dm^{-3} $NaClO_4$ + 0.1 mol dm^{-3} thiourea + 0.1 mol dm^{-3} sodium gluconate + 0.3 mol dm^{-3} boric acid.

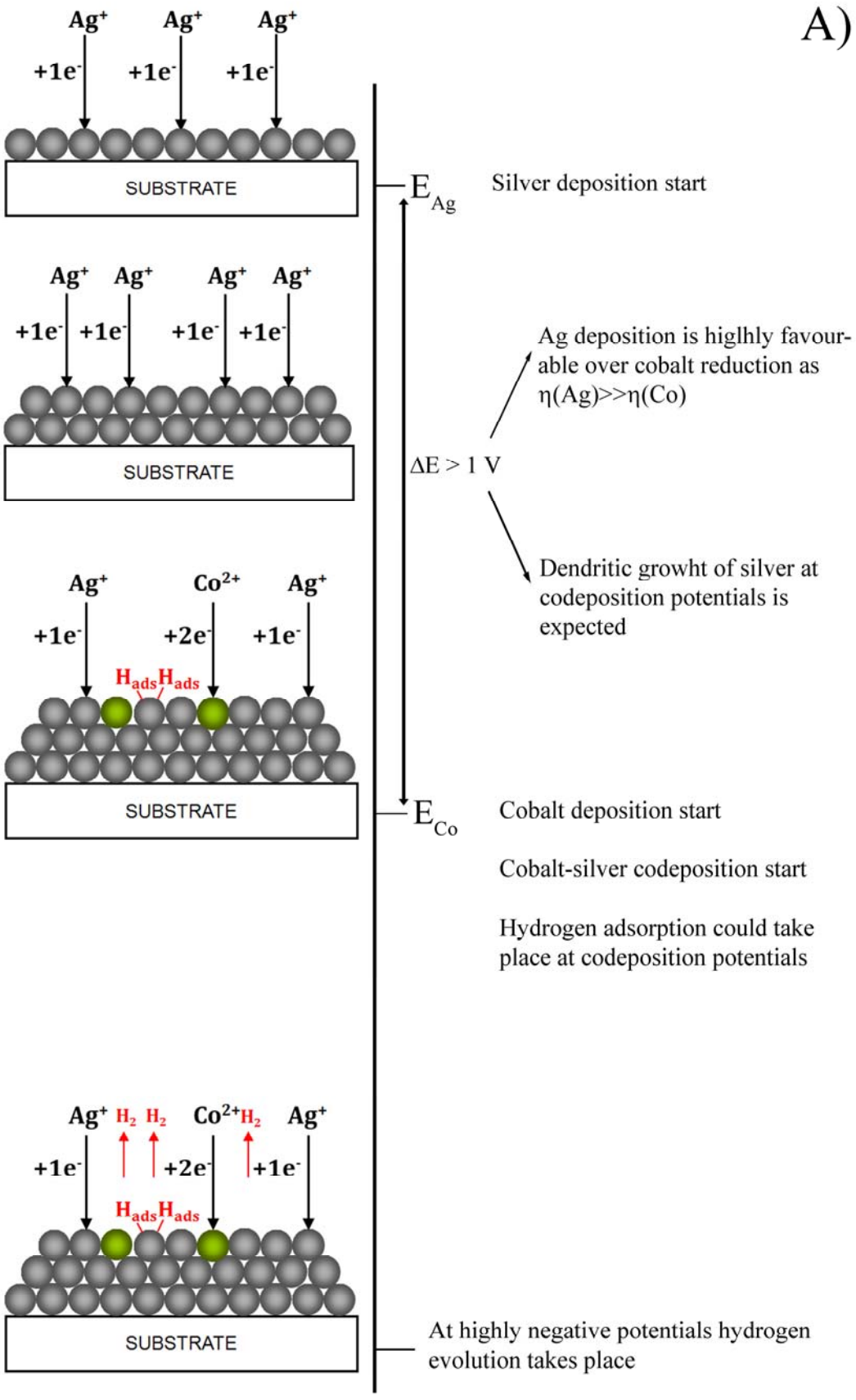

Figure 4.1.A) The scheme represents the possible problems during Co-Ag electrodeposition due to the great difference in the deposition potential of both metals.

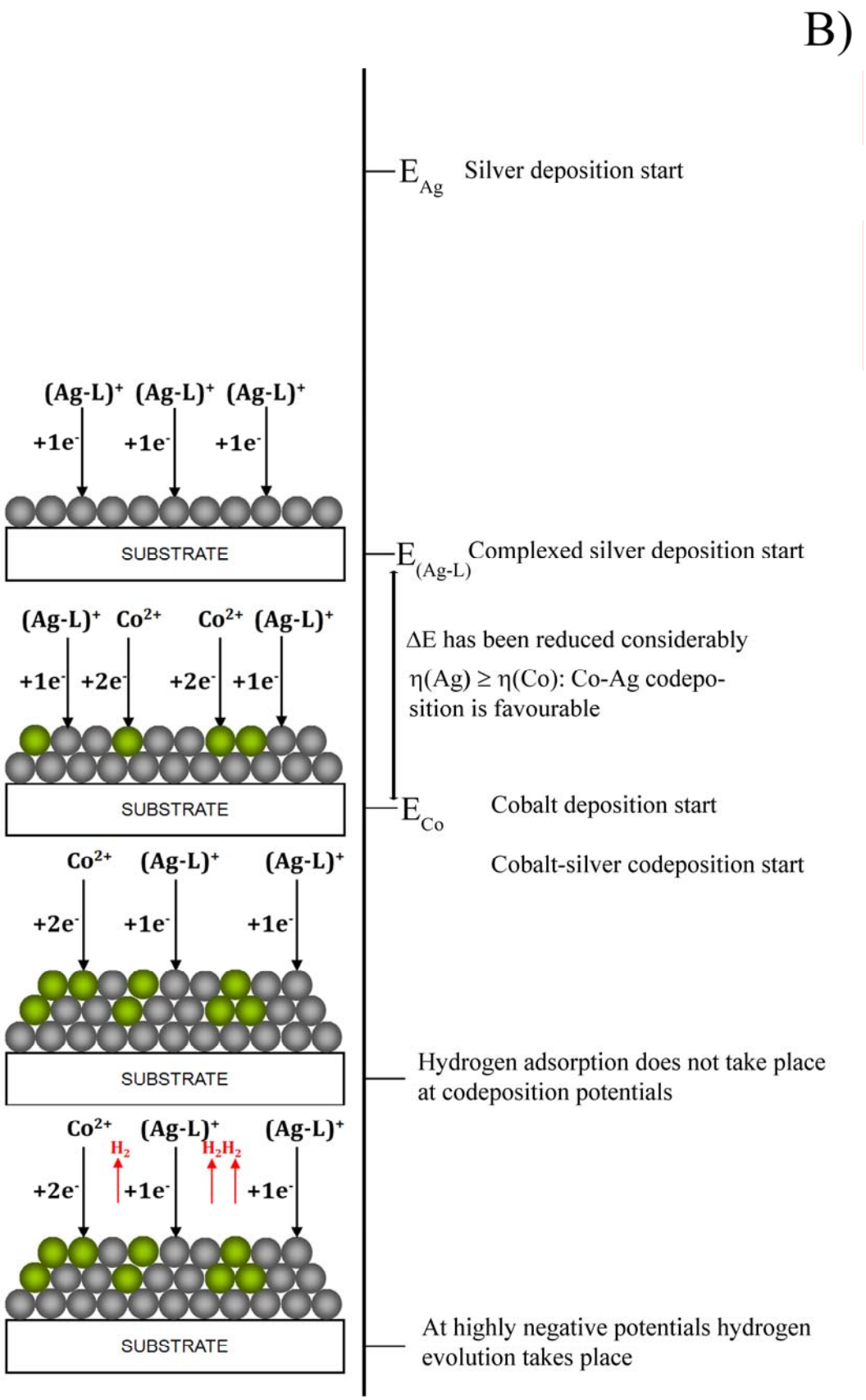

Figure 4.1.B) The scheme represents that the codeposition of Co-Ag can be favoured by the addition of a complexing agent (L).

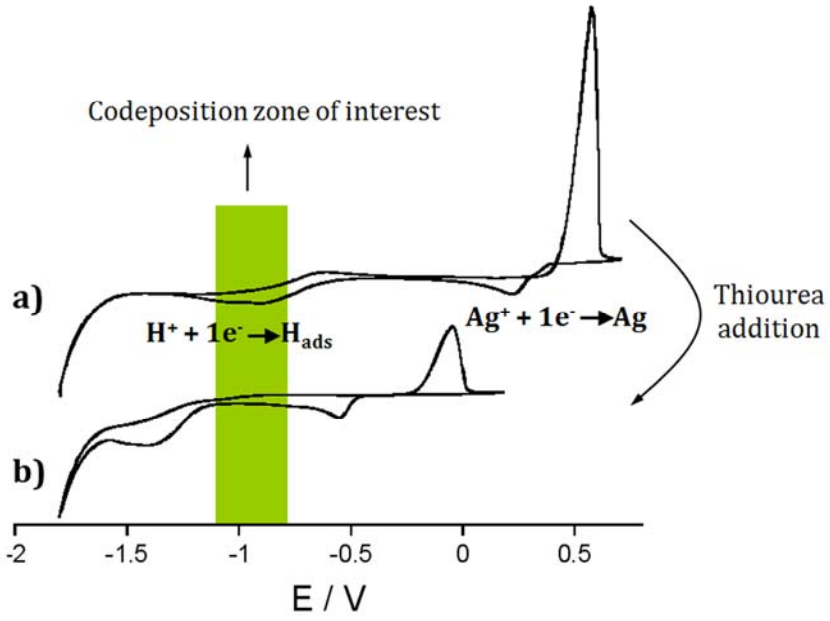

Figure 4.2. Influence of thiourea addition on the voltammetric response of silver

Also, the effect of each one of the present species in the electrolyte over both cobalt deposition and cobalt film properties was analyzed. The objective was to study the influence of those species over cobalt structure and magnetic properties. Cyclic voltammetry and current-time transients (*j-t* transients) clearly showed the effect of each species. Depending on the presence of thiourea (complexing capacity), sodium gluconate (complexing and adsorption capacity over the electrode) or boric acid (adsorption capacity) cobalt films with different structures were obtained: films with hcp structure but different crystalline orientations, films with a primitive cubic phase (ε-Co) never detected before by electrochemical methods or amorphous films were obtained. These structural differences were reflected in the magnetic properties of the films.

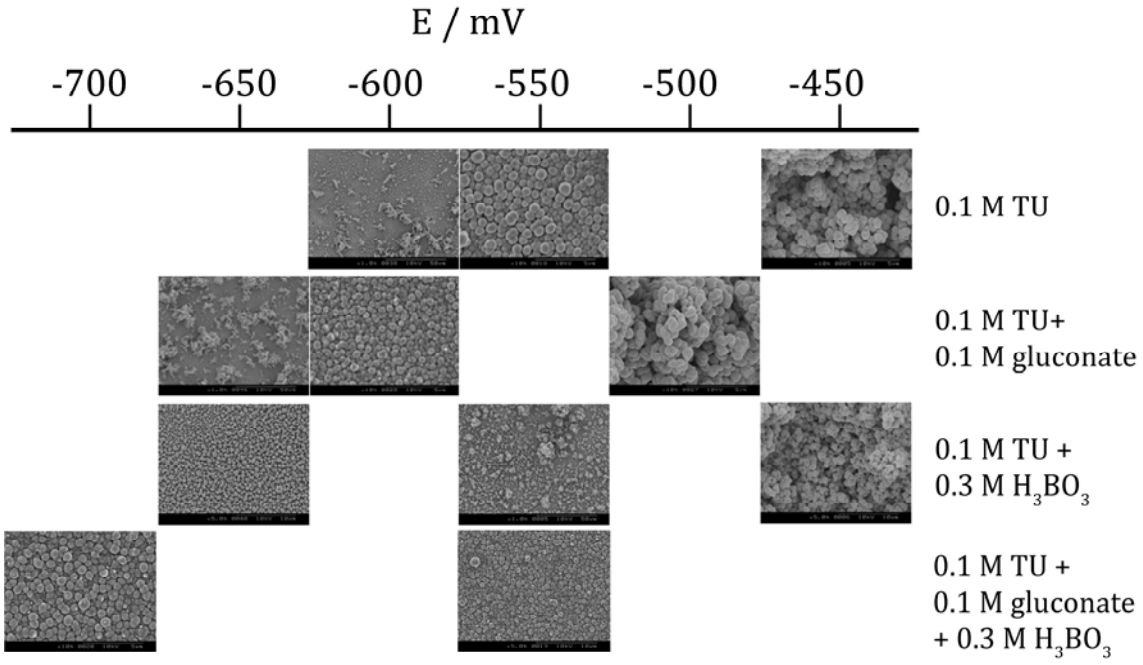

Figure 4.3. Influence of the species present in the bath on the morphology of silver films.

Group of articles included in section 4.1.

Page 57: Study and preparation of silver electrodeposits at negative potentials

Elvira Gómez, Jose Garcia-Torres and Elisa Vallés, Journal of Electroanalytical Chemistry 594 (2006) 89

Page 67: Electrodeposition of silver as a precursor matrix of magnetoresistive materials

E. Gómez, J. Garcia-Torres and E. Vallés, Materials Letters 61 (2007) 1671

Page 73: Modulation of magnetic and structural properties of cobalt thin films by means of electrodeposition

Jose Garcia-Torres, Elvira Gómez and Elisa Vallés, Journal of Applied Electrochemistry 39 (2009) 233

Study and preparation of silver electrodeposits at negative potentials

Available online at www.sciencedirect.com
SCIENCE DIRECT®
Journal of Electroanalytical Chemistry 594 (2006) 89–95
Journal of Electroanalytical Chemistry
www.elsevier.com/locate/jelechem

Study and preparation of silver electrodeposits at negative potentials

Elvira Gómez *, José García-Torres, Elisa Vallés

Electrodep. Departament Química Física, Facultat de Química, Universitat de Barcelona, Martí i Franquès, 1, 08028 Barcelona, Spain

Received 28 February 2006; received in revised form 22 May 2006; accepted 25 May 2006
Available online 12 July 2006

Abstract

Electrodeposition of silver films, potentially useful as a matrix for cobalt–silver magnetoresistive materials, has been studied. Silver electrodeposition at negative potentials has been analyzed in order to attain deposition potentials next to those of cobalt. The study of the process in an acidic perchlorate medium showed the necessity of using a complexing agent to shift both silver electrodeposition and proton reduction to negative potentials. This was achieved by adding thiourea which allowed silver electrodeposition in a wide range of potentials where secondary proton reduction process was not significant. Scanning electron microscopy analysis showed that the presence of thiourea in the bath was beneficial, since the silver films completely coated the substrate. Furthermore, the silver deposits obtained were compact, uniform, fine grained but rough. To further improve deposit quality, organic (sodium gluconate) and inorganic (boric acid) substances were added to the electrolytic bath, revealing a substantial improvement in the deposits obtained. Thus, conditions favourable to silver–cobalt codeposition have been determined.
© 2006 Elsevier B.V. All rights reserved.

Keywords: Silver; Electrodeposition; Thiourea; Thin films

1. Introduction

Metal electrodeposition allows to prepare patterns ranging micrometric to nanometric size by setting appropriate growth rate conditions, such as composition, hydrodynamic conditions, temperature and applied potential.

Advances in electronic devices imply their miniaturization and higher frequency operation, which in turn require using high-conductivity wiring. In this field, copper is mainly used as wiring material. But for certain applications copper needs to be replaced by silver due to its better electrical properties [1]. Generally these silver connections were produced by electrodeposition process using cyanide baths because silver electrodeposits prepared from a simple salt do not lead to coherent deposits [2]. Despite the high quality of the deposits obtained from the alkaline cyanide solutions, these plating baths are strongly toxic. Thus, developing alternative baths, which could replace the cyanide ones, is of important environmental and economical interest [3,4].

On the other hand, in recent years the development of magnetoresistive materials, in which ferromagnetic material is included in a non-ferromagnetic matrix has attracted much interest [5–7]. The possibility to obtain this kind of materials by means of electrodeposition is contrastable [8,9]. Silver is an excellent matrix to include ferromagnetic metal [10]. In this line, our interest is the design of silver baths to allow the simultaneous electrodeposition of cobalt in order to prepare magnetoresistive films. Yet, simultaneous deposition of silver and cobalt is difficult due to the great difference between their standard potentials. The use of a complexing agent as thiourea (TU) is proposed to shift the silver deposition process to negative values, without shifting of cobalt deposition process. TU is a known complexing agent for silver cations [11], but not for Co(II) [12].

As a previous stage for deposition of cobalt–silver system, silver electrodeposition in a TU-containing bath will

* Corresponding author. Fax: +34 934021231.
E-mail address: e.gomez@ub.edu (E. Gómez).

0022-0728/$ - see front matter © 2006 Elsevier B.V. All rights reserved.
doi:10.1016/j.jelechem.2006.05.030

be developed, with the goal of making high-quality silver deposits at very negative potentials which will act as good matrixes for magnetoresistive materials. TU is a good complexing agent, having a marked tendency to give coordinate bonds with many univalent and multivalent ions, and is therefore considered one of the most important masking agents having sulphur as donor atom. Different thiourea–silver complexes have been found in the Ag(I)–TU–H_2O system depending on the ligand:silver ratios in the bath. Evidence of presence of complexes 1:1, 2:1, 3:1, 4:1, 3:2 are referred by different authors, having all high thermodynamic stabilities, in aqueous solution relative to the uncomplexed species [13,14].

Our main aim is to analyze the thiourea influence in the silver electrodeposition process in acid solutions, studying the different processes involved during the deposition. TU excess will be selected in order to attain the more negative deposition potentials possible for silver deposition. Voltammetric techniques and potentiostatic current–time transient techniques will be used in this study.

2. Experimental

The study of the electrodeposition process and deposit preparation was performed in a conventional three-electrode cell using a microcomputer-controlled potentiostat/galvanostat Autolab with PGSTAT30 equipment and GPES software. Chemicals used were $AgNO_3$ and thiourea (CSN_2H_4), all of analytical grade. Finally, boric acid and sodium gluconate were used. The silver concentration was mainly maintained at 0.01 mol dm^{-3} and $NaClO_4$ was kept constant at 0.2 mol dm^{-3}. Perchlorate anion was selected as supporting electrolyte in order to avoid possible complexing effects. The pH was adjusted usually to 3.7 by adding $HClO_4$ to the solution. All solutions were freshly prepared with water doubly-distilled and then treated with a Millipore Milli Q system. Before the experiments, solutions were de-aerated with argon and maintained under argon atmosphere during the electrochemical experiments. Temperature was kept at 25 °C except when studying temperature influence.

Deposit morphology was examined with a Hitachi S 2300 scanning electron microscope. The samples for SEM analysis were rinsed with water and dried in an argon stream. Deposit composition was determined by inductively coupled plasma optical emission spectrometry (ICP-OES) with a Perkin Elmer Optima 3200 RL after deposits dissolution using 3% HNO_3.

Vitreous carbon (Metrohm, 0.0314 cm^2) and, in some experiments, silver wire were used as working electrodes. The former was polished to a mirror finish before each experiment using alumina of different grades (3.75 and 1.85 μm) and cleaned ultrasonically for 2 min in water. The reference electrode was Ag|AgCl|1 mol dm^{-3} NaCl mounted in a Luggin capillary containing 0.2 mol dm^{-3} $NaClO_4$ solution. All potentials are referred to this electrode. The counter electrode was a platinum spiral.

Voltammetric and linear scans or stripping experiments were used to analyse the deposition process. Deposits were prepared potentiostatically under moderate stirring ($\omega =$ 100 rpm) using a magnetic stirrer.

3. Results

In order to analyse the influence of complexing agent on the silver deposition, it is interesting to compare the electrochemical response for the electrolyte in the presence and absence of thiourea. This study began with the analysis of silver deposition on vitreous carbon in perchlorate medium. Silver deposition process was mainly investigated using cyclic voltammetry using a potential sweep equal to 50 mV s^{-1}.

3.1. Silver deposition from free-thiourea bath

Scanning the potential between hydrogen and oxygen evolution, two main reduction (peaks I and II) and one oxidation features were observed (Fig. 1 curve a). Curve b in Fig. 1 shows the voltammogram corresponding to the blank solution for which no remarkable features were observed within this potential range.

A nucleation loop was observed when the scan was reversed at the beginning of the first reduction peak (peak I) (Fig. 2(A) curve a) which is a characteristic feature of a nucleation process. Increasing the cathodic limit, a clear reduction peak followed by a progressive current decay was recorded (Fig. 2(A) curves b–d). This first peaks' appearance was clearly related with a mass control process, since if the solution was stirred, the reduction current maintained a constant value (Fig. 2(B)). Therefore, peak (I) was related to nucleation and three-dimensional growth of silver deposition. A single oxidation peak corresponding to silver oxidation was also observed.

Reduction peak (II) was pH-dependent. Although modification of solution pH did not qualitatively affect the vol-

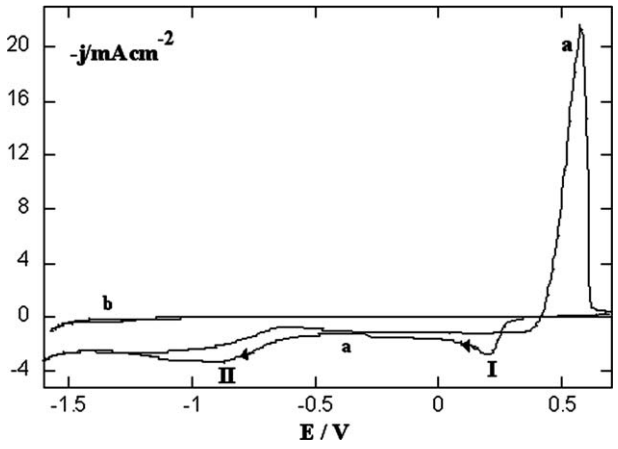

Fig. 1. Cyclic voltammograms of: curve (a) 0.01 mol dm^{-3} $AgNO_3$ + 0.2 mol dm^{-3} $NaClO_4$ solution, pH 3.7, curve (b) 0.2 mol dm^{-3} $NaClO_4$ solution, pH 3.7 (blank solution). Vitreous carbon electrode.

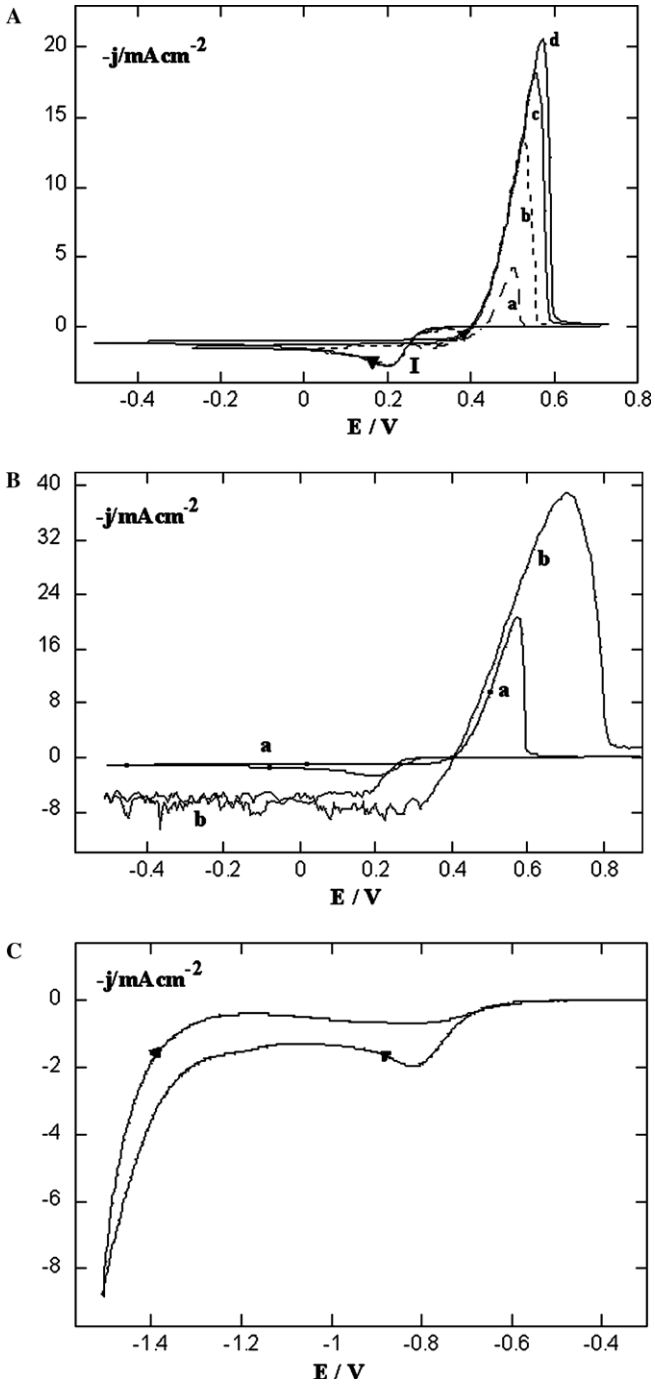

Fig. 2. Cyclic voltammograms of 0.01 mol dm^{-3} $AgNO_3$ + 0.2 mol dm^{-3} $NaClO_4$ solution, pH 3.7. (A) Different cathodic limits. Curves: (a) 260 mV, (b) 0 mV, (c) −250 mV and (d) −500 mV. (B) Curves (a) quiescent conditions, (b) stirred conditions. Vitreous carbon electrode. (C) Cyclic voltammogram of blank solution. Silver wire electrode.

tammetric response, more charge was involved in peak (II) when the pH was decreased, while the charge of peak (I) remained constant. In the voltammetric response of a silver electrode in a blank solution (0.2 mol dm^{-3} $NaClO_4$, pH 3.7), a similar reduction process was observed, a clear reduction peak appearing (Fig. 2(C)). This clearly increased both when the pH of the blank solution was decreased and when solution was stirred. Then, the second reduction process detected during silver electrodeposition (peak II) was assigned to proton reduction [15].

Voltammetric holds of different duration, followed by scan reversing were performed during the cathodic scan. During the hold, solution was stirred. Holding the potential during 30 s in the potential range corresponding to peak (I), an increase in the charge involved under the oxidation peak was observed (Fig. 3 curve a), that increased upon increasing the hold time. However, when the hold was made in the peak (II) potential range, a sudden negative current increase was observed (at around 110 mV), revealing a new reduction current during the anodic scan (Fig. 3 curves b and c). This rapidly decayed to positive values, producing an oxidation band placed before the main oxidation peak, which involved a charge similar to that recorded when no scan holding was performed (Fig. 3 curves d and e). An increase in hold duration increased both negative stepped current value and the charge involved in the band that appeared prior to the main oxidation peak. The charge under the main oxidation peak remained constant independently of the hold duration.

Once the general electrochemical behaviour of silver deposition from a complexing-free bath has been determined, the effect of thiourea addition was studied.

3.2. Voltammetric behaviour of thiourea

As a first step, the general trends of electrochemical behaviour of the thiourea (0.1 mol dm^{-3}) in perchlorate medium on different substrata were analysed. Vitreous carbon, silver wire and freshly silver deposits over vitreous carbon were selected for this purpose.

Thiourea reduction was not observed on any substrate. On vitreous carbon a wider potential range between the start of thiourea oxidation and the beginning of hydrogen evolution (+300 mV, −1700 mV) was found, and no

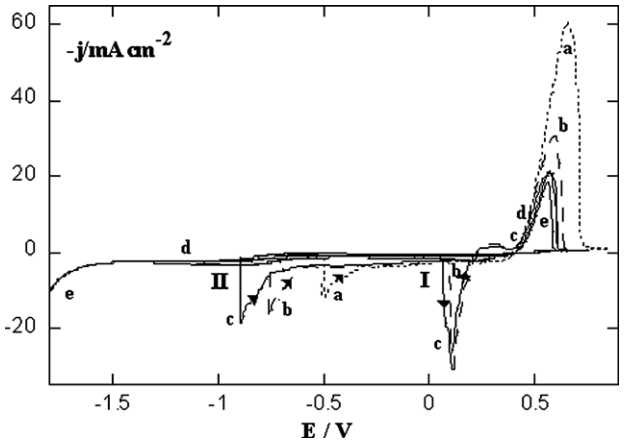

Fig. 3. Voltammograms of 0.01 mol dm^{-3} $AgNO_3$ + 0.2 mol dm^{-3} $NaClO_4$ solution, pH 3.7. Holds during 30 s at: (a) −500 mV (···), (b) −750 mV (---) and (c) −900 mV (continuous line). Cyclic voltammograms at different cathodic limits (d) −1100 mV and (e) −1700 mV. Vitreous carbon electrode.

significant current value was recorded (Fig. 4 curve a). On silver wire electrode, this range was reduced and a process related to proton reduction prior to hydrogen evolution was observed (Fig. 4 curve b). Intermediate behaviour was obtained on a vitreous carbon electrode over which different silver charges were deposited (Fig. 4 curve c).

3.3. Silver deposition from 0.1 mol dm^{-3} thiourea bath

Thiourea presence in the bath provoked an important shift of both silver deposition process onset and an important diminution of the current involved during the process. The heights of both reduction and oxidation peaks were lower than those observed in TU-free baths. On the other hand, the general trends of the silver deposition process were similar to those observed for silver deposition from the complexing-free bath; a reduction peak (peak I′), related to mass control process of silver deposition, appeared during the negative scan. The silver oxidation peak appeared at more negative potentials than on TU-free baths (Fig. 5 curves a–c). Lengthening the scan, the second reduction process prior to the hydrogen evolution, related to proton reduction (peak II′), appeared at around −1300 mV (Fig. 5 curve d). The exact anodic peak location depended on cathodic limit. When this was increased, the oxidation process became easier.

In an attempt to separate the various contributions in the voltammetric response, the concentration of silver (I) was reduced to 0.003 mol dm^{-3}. The general shape of the voltammogram was, then, similar although peak II′ appeared at a more negative potential and the charge involved was lower (Fig. 6), as corresponded to the lesser silver quantity deposited in the voltammetric scan.

In order to investigate pH influence on the silver deposition process, voltammograms were recorded from baths at different pH values, but this brought no modification in the Ag(I) reduction peak (peak I′). Yet, on decreasing pH, the charge involved in the second reduction process (peak II′) increased and the oxidation peak became centred at more positive potentials. At a given pH, the charge involved on this second reduction process increased under stirred conditions.

The study of temperature influence revealed that the first deposition process was very sensitive to this parameter, an increase of around 10 °C, advancing current appearance by almost 100 mV, although reduction peak height remained unaffected, as is also the case for the process related to hydrogen reaction. Deposits obtained at higher temperatures oxidized easier in the temperature range studied.

3.4. Morphological analysis

Deposits were prepared in order to image deposit morphology as a function of the experimental conditions. Silver deposits were prepared potentiostatically under stirred conditions in order to maintain the contribution of

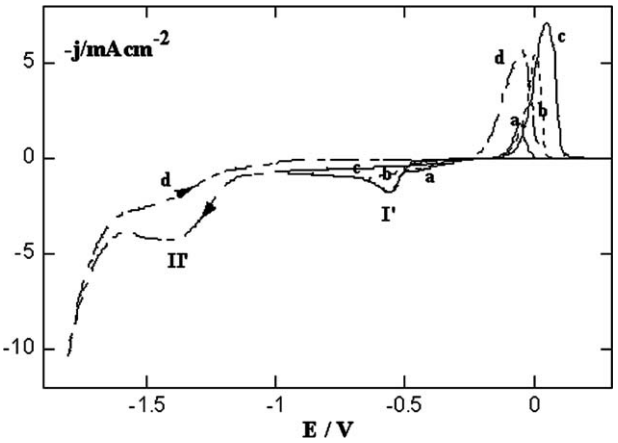

Fig. 5. Cyclic voltammograms of 0.01 mol dm^{-3} $AgNO_3$ + 0.1 mol dm^{-3} thiourea + 0.2 mol dm^{-3} $NaClO_4$ solution, pH 3.7. Different cathodic limits, curves: (a) −500 mV, (b) −650 mV, (c) −1000 mV and (d) −1800 mV. Vitreous carbon electrode.

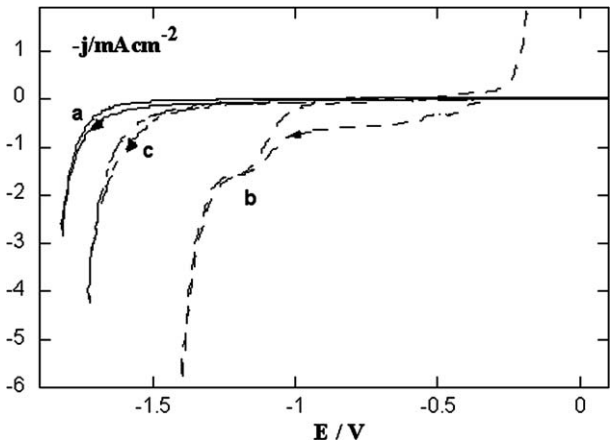

Fig. 4. Cyclic voltammograms of 0.1 mol dm^{-3} thiourea + 0.2 mol dm^{-3} $NaClO_4$ solution, pH 3.7. Curves: (a) vitreous carbon, (b) silver wire and (c) −55 mC of freshly silver deposited over vitreous carbon.

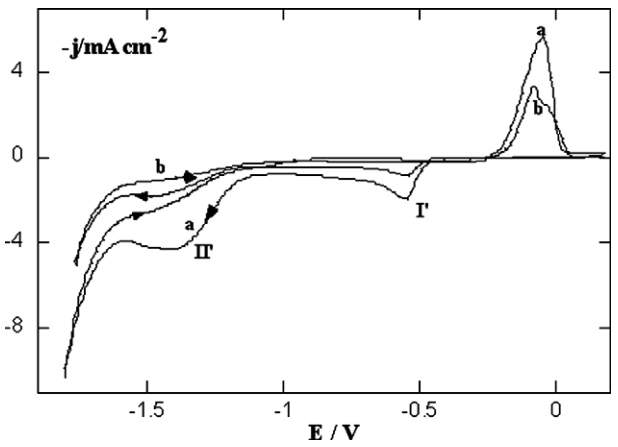

Fig. 6. Cyclic voltammograms of x mol dm^{-3} $AgNO_3$ + 0.1 mol dm^{-3} thiourea + 0.2 mol dm^{-3} $NaClO_4$ solution, pH 3.7 (TU bath). (a) $x = 0.01$ and (b) $x = 0.003$.

electroactive species to the electrode. For each analysed bath the deposition potentials were selected according to the shift in the appearance of reduction current observed in the voltammetric curves. Taking into account the important temperature influence, an accurate control of temperature was necessary during the deposition process.

The objective was to analyse potential influence on the process and to establish the relationships between the deposition potential, solution composition and deposit morphology and appearance, all at relatively high deposition times. Our interest is to find conditions which lead to deposits with satisfactory appearance and morphology.

SEM pictures are quite revealing, showing marked differences in morphology between electroplates obtained in presence or absence of complexing agent whatever the conditions. Fig. 7(A) shows the morphological details of silver deposits electrogrown from TU-free bath. Isolated crystals of variable size were observed and did not evolve into compact deposits on increasing deposition charge. Deposits showed dendritic growth when the potential was made more negative.

Substantial changes were observed when the deposits obtained from a TU bath were analyzed. Those were compact, homogeneous and formed by similarily-sized, small grains (Fig. 7(B)). The variation of the plating potential was in agreement with the morphology of the deposits, since a decrease in the deposition potential led to fine-grained deposits. But in all cases, by decreasing the deposition potential, dendritic growth was observed (Fig. 7(C)). Since thiourea species get adsorbed over silver surface [16], a parallel compositional analysis was made in order to establish the possible incorporation of thiourea in the deposit. The deposits were prepared at different potentials under different charge values, and then rinsed and immersed in sufficient water in order to remove any thiourea that might proceed from the bath. When a compact deposit was obtained, the ICP compositional analysis revealed that sulphur presence was lower than 0.2 wt.%, indicating that thiourea incorporation was quite low (<0.5 wt.%). Even when a dendritic deposit was formed the maximum TU percentage was no greater than 2 wt.%.

The viability of this formulation was tested by adding cobalt to the solution; cobalt began to deposit around two-three hundred millivolts more negative than the potentials at which good silver deposits were obtained.

3.5. Influence of gluconate and boric acid presence

In order to obtain finer-grained deposits, and also to be able to operate at more negative potentials, the effect of other species, susceptible of improving TU influence, were studied, boric acid and gluconate salt being selected. Concentration of the latter was established at 0.1 mol dm^{-3}, while that of the former was 0.3 mol dm^{-3}.

The study began by recording the voltammetric response of silver deposition from these modified baths, which was found to be similar to that previously recorded from the TU-bath, although boric acid addition slightly advanced and gluconate presence slightly delayed the start of the process. With this in mind, deposits were prepared potentiostatically at deposition rates similar to those applied to obtain the deposits in absence of these species. This was necessary in order to compare the effect of the foreign species on final deposit morphology.

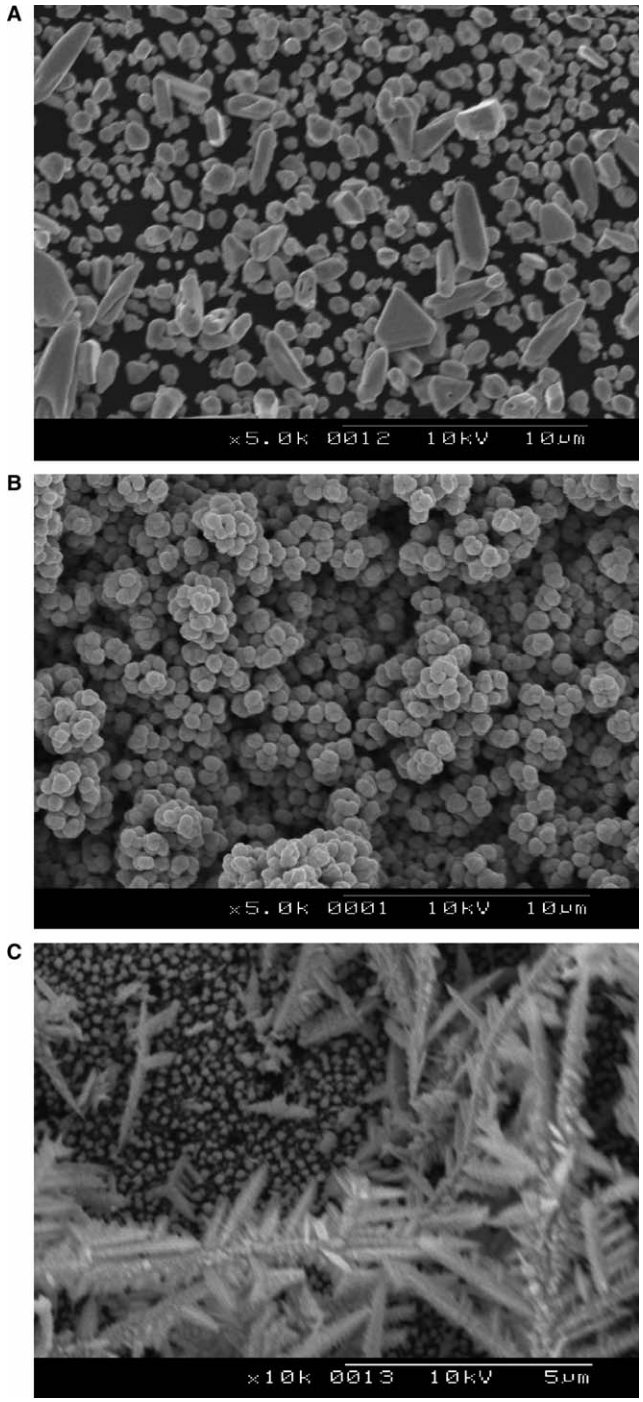

Fig. 7. Scanning electron micrographs of silver deposits obtained from 0.01 mol dm^{-3} $AgNO_3$ + x mol dm^{-3} thiourea + 0.2 mol dm^{-3} $NaClO_4$ solution, pH 3.7. $Q = -50$ mC. (A) $x = 0$, $E_{dep} = 300$ mV. (B) $x = 0.1$, $E_{dep} = -450$ mV. (C) $x = 0.1$, $E_{dep} = -700$ mV.

At all potentials, gluconate presence in the TU-bath improved deposit quality (Fig. 8(A)). Grain size was reduced and compact, fine-grained deposits being obtained (Fig. 8(B)). However, gluconate presence was unable to retard the start of dendritic growth over the initial deposit at a given deposition rate. Gluconate presence improved deposit morphology but it was only able to extend by a few millivolts the potential range at which deposits were adequate.

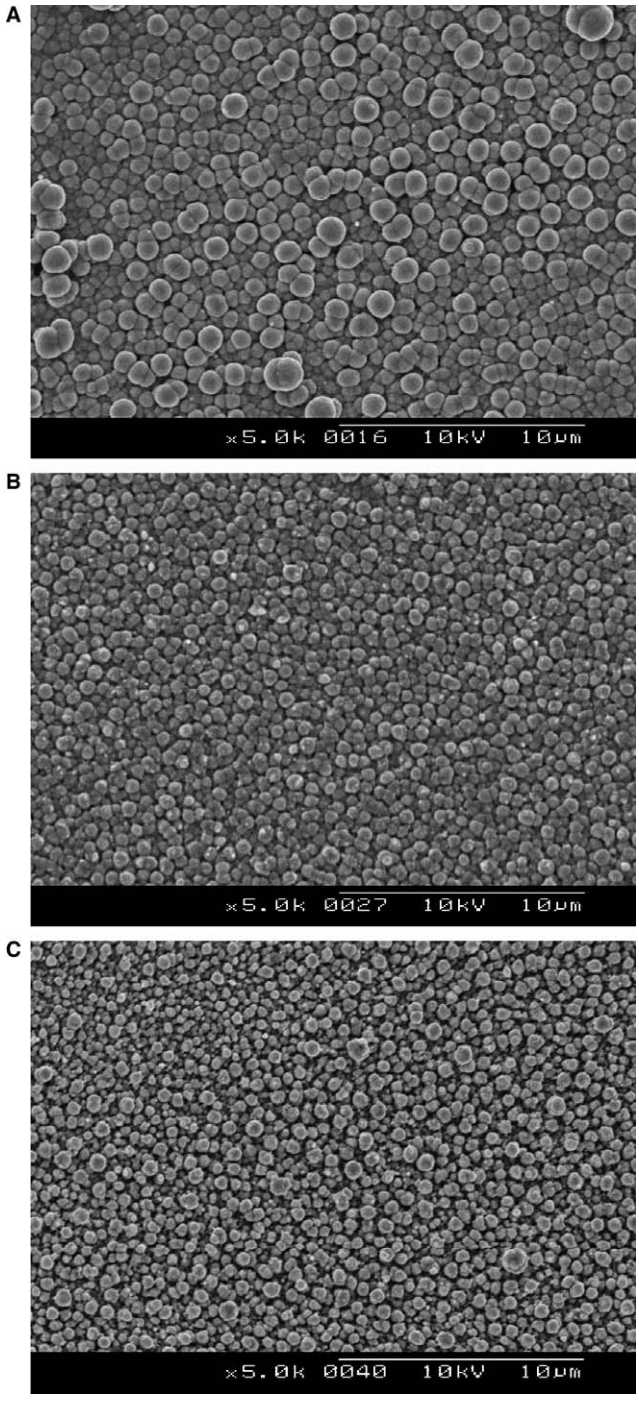

Fig. 8. Scanning electron micrographs of silver deposits of $Q = -50$ mC, obtained from: (A) TU bath at $E_{dep} = -550$ mV. (B) TU bath + 0.1 mol dm^{-3} gluconate at $E_{dep} = -600$ mV. (C) TU bath + 0.3 mol dm^{-3} boric acid at $E_{dep} = -630$ mV.

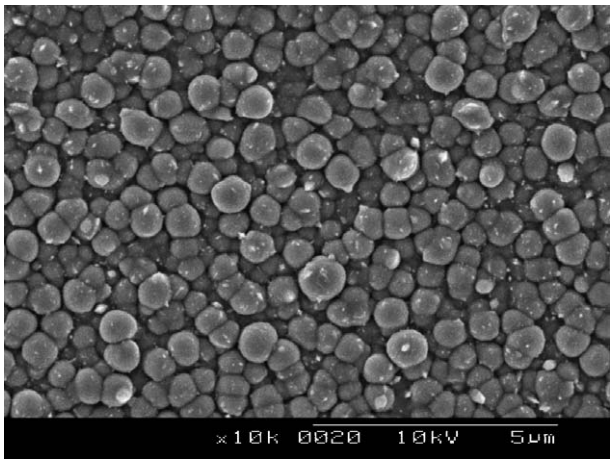

Fig. 9. Scanning electron micrograph of silver deposit obtained at $E = -700$ mV from 0.01 mol dm^{-3} $AgNO_3$ + 0.1 mol dm^{-3} thiourea + 0.1 mol dm^{-3} gluconate + 0.3 mol dm^{-3} boric acid + 0.2 mol dm^{-3} $NaClO_4$ solution, pH 3.7. $Q = -50$ mC.

When boric acid was present in the bath, its effect was not relevant at the low deposition potentials and deposits similar to those obtained from boric-free baths were obtained. Its effect became significant upon decreasing the applied potential, because its presence seems to inhibit vertical growth, enlarging the potential range at which homogeneous, fine-grained deposits can be obtained. Fig. 8(C) shows the deposit obtained at the same deposition potential at which dendritic growth appeared, both in thiourea and in gluconate-thiourea baths.

Both gluconate and boric acid separately seemed to improve silver deposits. Then, the next step would be to study the effect of simultaneous gluconate and boric presence in the bath on the deposits' quality. Then, good quality deposits were obtained (Fig. 9) applying more negative deposition potentials than those used in absence of gluconate or boric acid in the bath.

4. Discussion and conclusions

The study performed allowed us to select the potential range in which only silver electrodeposition occurs, avoiding secondary processes. Over vitreous carbon electrodes, two reduction processes have been detected: the first one corresponds to the electrodeposition of silver by means nucleation and three-dimensional growth, while the second is attributed to hydrogen reaction over the freshly-deposited silver. Hydrogen reaction over the electrodeposited silver is favoured at very negative potentials and by decreasing the solution pH.

The hydrogen evolution reaction on silver electrodes follows the Volmer–Heyrowski mechanism, in which H_{ads} is formed as reaction intermediate, a prewave appearing in perchlorate medium corresponding then to H_{ads} formation [15]. From our voltammetric results, we can deduce that

the H_{ads} formed on the freshly-deposited silver remains adsorbed, hindering ulterior silver deposition. When hold experiments were made during voltammetric scans in the potential zone corresponding to H_{ads} formation, an important reduction current at positive potentials was detected after reversing the scan. This negative current ought to be due to the reduction of Ag(I) accumulated in the electrode surrounding when hydrogen desorption occurs.

On the other hand, to allow the codeposition of silver and cobalt it will be necessary to approach their deposition potentials, shifting the silver deposition process to negative values. Simultaneously, it will be necessary to shift the proton reduction process too. The presence of thiourea in the bath accomplishes these requirements, because it adsorbs both on vitreous carbon and silver electrodes [16] shifting the prewave and hydrogen evolution process. Thiourea presence delayed the undesired hydrogen reaction to very negative potentials, so that the potential range useful to codeposit silver and cobalt with low hydrogen evolution is enlarged. This behaviour was previously detected also for silver electrodeposition process in presence of thiourea in basic perchlorate medium [17].

The selected solution, containing 10:1 thiourea:silver(I) ratio, shifts the onset of silver deposition by some 750 mV towards negative values. Also, it is confirmed that for obtaining compact deposits, a complexing agent is necessary. TU promotes the formation of smooth, homogeneous, finer-grained deposits. Grain size reduction is a consequence of the decrease in the plating potential that results in an increase of nucleation over growth rate. Good silver deposits are obtained at potentials around 300 mV more positive that those corresponding to cobalt deposition in the same bath.

Another item researched was the possible incorporation of sulphur in the deposit. Due to its interest, once the conditions at which sulphur was incorporated were established, in order to minimise it. Silver deposits obtained in presence of TU at moderate deposition potentials were shown to incorporate low sulphur content. This low incorporation is favoured by the fact that TU does not get reduced in spite of the high TU:Ag(I) ratio used. Sulphur content in the deposits increases when dendritic growth develops, probably due by occlusion of solution into the dendritic deposit.

In order to widen the possibility to obtain deposits at more negative potential maintaining the quality of silver deposits obtained, gluconate addition was tested and proved to improve deposit smoothness. Gluconate also homogenizes the deposits providing finer-grained ones but it is unable to extend the potential range at with compact deposits might be obtained.

While boric acid effect is unclear, it is well-known that in some way it promotes the correct deposit growth, when hydrogen reactions are involved. Thus, boric acid was added to the thiourea bath. Although at the lower deposition potentials its presence was not relevant, at the more negative potentials, it does minimize vertical growth and delays the appearance of dendritic growth by around 100 mV in respect to that observed in TU-only baths.

The beneficial effect on deposits of both gluconate and boric acid observed separately has been improved in a discreet way when they are used together. It becomes thus possible to obtain good quality silver deposits at around −700 mV.

The knowledge of silver deposition processes in presence of these species will allow modifying conveniently the deposition parameters, approaching silver deposition and cobalt deposition potentials and thus allowing codeposition to take place. This complex bath could be useful to simultaneous cobalt–silver deposition because it has been checked that in this bath cobalt deposits around −800 mV over the freshly deposited silver.

Acknowledgements

The authors wish to thank the Serveis Cientificotècnics (Universitat de Barcelona) for the use of their equipment. This paper was supported by contract MAT 2003-09483-C02-01 from the *Comisión Interministerial de Ciencia y Tecnología (CICYT)*.

References

[1] T. Ida, M. Yoshino, J. Sasano, I. Matsuda, T. Osaka, Surf. Finis. Soc. Jpn. 55 (2004) 212.
[2] A.T. Dimitrov, S. Hadzi-Jordanov, K.I. Popov, M.G. Pavlovic, V. Radmilovic, J. Appl. Electrochem. 28 (1998) 791.
[3] G.M. Zarkadas, A. Stergion, G. Papanastasiou, J. Appl. Electrochem. 31 (2001) 1251.
[4] G.M. Zarkadas, A. Stergion, G. Papanastasiou, Electrochim. Acta 50 (2005) 5022.
[5] H. Takeda, A. Fujita, K. Fukamichi, J. Appl. Phys. 91 (2002) 7780.
[6] C.L. Chien, J.Q. Xiao, S. Jiang, J. Appl. Phys. 73 (1993) 5309.
[7] J.Q. Wang, G. Xiao, Phys. Rev. B 49 (1994) 3982.
[8] H. Zaman, A. Yamada, H. Fukuda, Y. Ueda, J. Electrochem. Soc. 145 (1998) 565.
[9] E. Gómez, A. Labarta, A. Llorente, E. Vallés, J. Electroanal. Chem. 517 (2001) 63.
[10] S. Kenane, J. Voiron, N. Benbrahim, E. Chainet, F. Robaut, J. Magn. Magn. Mater. 297 (2006) 99.
[11] B. Reents, W. Plieth, V.A. Macagno, G.I. Lacconi, J. Electroanal. Chem. 453 (1998) 121.
[12] A. Bellomo, D. de Marco, A. de Robertis, Talanta 20 (1973) 1225.
[13] P.M. Heinrichs, J.J.H. Ackerman, G.E. Maciel, J. Am. Chem. Soc. 99 (1977) 2544.
[14] A.E. Martell, R.M. Smith, Critical Stability Constants, vol. 3, Plenum Press, New York, 1977.
[15] D. Diesing, H. Winkes, A. Otto, Phys. Status Solidi A 159 (1997) 243.
[16] M. Fleishmann, G. Sundholm, Z.Q. Tian, Electrochim. Acta 31 (1986) 907.
[17] J. Bukowska, K. Jacowska, J. Electroanal. Chem. 367 (1994) 41.

Electrodeposition of silver as a precursor matrix of magnetoresistive materials

Available online at www.sciencedirect.com
ScienceDirect
Materials Letters 61 (2007) 1671–1674
materials letters
www.elsevier.com/locate/matlet

Electrodeposition of silver as a precursor matrix of magnetoresistive materials

E. Gómez *, J. García-Torres, E. Vallés

Electrodep. Departament Química Física, Facultat de Química, Universitat de Barcelona, Martí i Franquès, 1. 08028 Barcelona, Spain

Received 15 March 2006; accepted 22 July 2006
Available online 10 August 2006

Abstract

The design of a bath able to electrodeposit silver at a relatively high negative potential was attained. The preparation of silver films at negative potentials in conditions at which dendritic growth is avoided, makes the process useful in silver-matrix magnetoresistive materials manufacture. Thiourea as a complexing agent was able to accomplish this purpose. Results indicate that thiourea bath produces homogeneous and fine-grained silver deposits with low sulfur content, avoiding hydrogen reaction in the potential range at which coherent deposits were obtained. Morphological and structural analysis were made as a function of temperature and the presence in the bath of other species.
© 2006 Elsevier B.V. All rights reserved.

Keywords: Silver; Electrodeposition; Films; Thiourea

1. Introduction

Magnetoresistive thin films have attracted great attention for their application in sensor devices [1,2]. Silver is a good element to be used as a matrix to contain ferromagnetic materials in order to prepare potentially magnetoresistive materials. Since silver and cobalt are immiscible according to the phase equilibrium diagram, a cobalt–silver couple would be an interesting system as a magnetoresistive material [3–5].

Metal electrodeposition is a very interesting subject to the microelectronics industry; silver deposits are mainly obtained by electrodeposition [6,7], which has also proved to be an alternative tool to prepare homogeneous or heterogeneous thin films [8]. This method makes it possible to modify the morphology and/or structure of deposits by varying the electrodeposition conditions (electrolyte composition, temperature, solution pH and electrochemical parameters), while working both at ambient pressure and temperature, thus requiring relatively inexpensive equipment.

The aim of the present study is to develop a basic bath for silver deposition, which afterwards, will be useful in cobalt codeposition. The challenge is to reduce the tendency of the noble metal to deposit, delaying the deposition process to values similar to those at which the parent metal is able to deposit, avoiding dendritic growth and preserving deposit properties. Moreover, the negative potentials might favour grain size reduction, thus making more desirable the final deposits due to their expected nanostructure. Electrodeposition conditions will be adequate to allow codeposition and to obtain materials that fulfil final application requisites.

Coherent silver deposits are obtained only when certain organic and/or inorganic species are present in the bath, but, regardless of the conditions of deposition, the deposits prepared from simple salt solutions are not compact [9]. Various additives and complexing agents have been reported in the literature [10–14].

In this regard, and due to the very different electrochemical characteristics of silver and cobalt, the objective is to delay silver deposition process. Thiourea (TU) was selected as the main complexing agent [15,16]. Furthermore, the final deposit must be coherent and able to act as a matrix of magnetoresistive material.

2. Experimental details

The electrochemical study was performed in a three-electrode cell using a microcomputer-controlled potentiostat/galvanostat Autolab. The chemicals used were $AgClO_4$, CSN_2H_4 (TU) and

* Corresponding author. Tel.: +34 934021234; fax: +34 9 34021231.
E-mail address: e.gomez@ub.edu (E. Gómez).

0167-577X/$ - see front matter © 2006 Elsevier B.V. All rights reserved.
doi:10.1016/j.matlet.2006.07.096

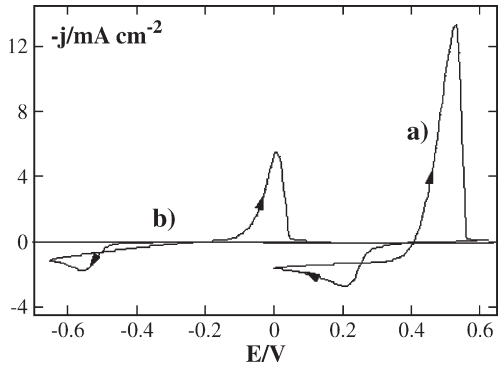

Fig. 1. Cyclic voltammograms of 0.01 mol dm^{-3} $AgClO_4$ + 0.2 mol dm^{-3} $NaClO_4$ + x mol dm^{-3} thiourea solution, pH = 3.7. a) x = 0, b) x = 0.1.

$NaClO_4$ as supporting electrolyte, all of analytical grade. Sporadically boric acid and sodium gluconate were also used. Analytical concentrations were 0.01 M for silver, 0.1 M for thiourea and 0.2 M for supporting salt. The solution pH was selected at 3.7. All solutions were freshly prepared with water treated with a Millipore Milli Q system, de-aerated with argon and maintained under argon atmosphere during the electrochemical experiments.

Vitreous carbon, polished to a mirror finish before each experiment was used as the working electrode. The reference electrode was Ag|AgCl|1 mol dm^{-3} NaCl mounted in a Luggin capillary containing 0.2 M $NaClO_4$ solution. The counter electrode was a platinum spiral.

Deposit morphology was examined by SEM. The deposits composition was determined by inductively coupled plasma optical emission spectrometry (ICP-OES). X-ray diffractograms were recorded using a Bragg–Brentano Siemens D-500 diffractometer. Diffraction diagrams were obtained in the 10–110° 2θ range with a step range of 0.05° and a measuring time of 5 s per step.

Cyclic voltammetry was used to establish the potential range and to reveal relevant features of the process, and step techniques to prepare the deposits.

3. Results and discussion

As TU forms different complexes with silver, a preliminary study was carried out in order to optimise the TU:Ag(I) bath ratio. A ratio of 10:1 was selected in order to assure that only a main complex was present in the solution.

At the selected conditions, the effect of thiourea present in the bath was evident from the comparison between the voltammetric response in the presence and absence of thiourea (Fig. 1). An important shift of the onset of the reduction current took place. In the absence of thiourea, current was detected around +300 mV (Fig. 1 curve a), whereas when thiourea was present in the bath, no current was observed up to around −450 mV (Fig. 1 curve b).

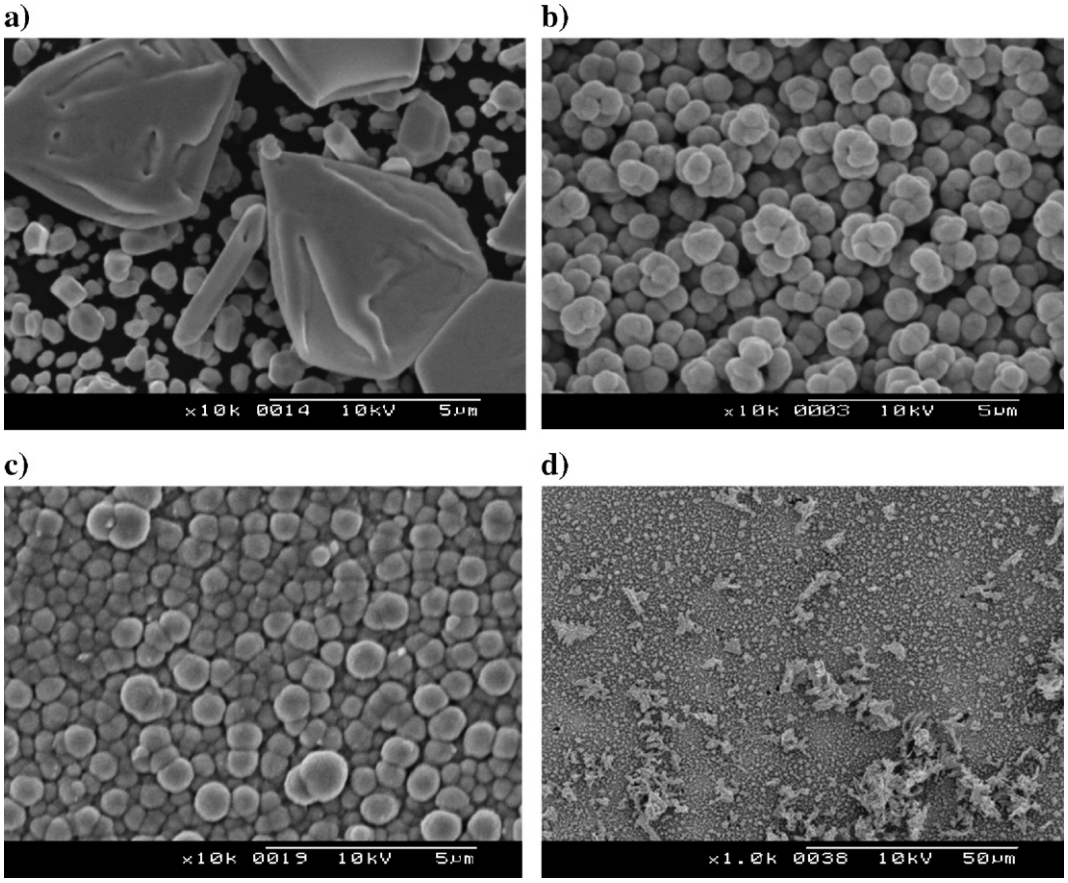

Fig. 2. Scanning electron micrographs of silver deposits of Q = −1.6 C cm^{-2}, obtained at 25 °C from 0.01 mol dm^{-3} $AgClO_4$ + 0.2 mol dm^{-3} $NaClO_4$ + x mol dm^{-3} thiourea solution, pH = 3.7: a) x = 0, E_{dep} = 300 mV, b) x = 0.1, E_{dep} = −450 mV, c) x = 0.1, E_{dep} = −550 mV and d) x = 0.1, E_{dep} = −650 mV.

Silver deposition occurred in both media by means of a nucleation and three-dimensional growth process: reduction current was observed in the anodic scan at potentials more positive than those in the cathodic one. In the thiourea bath the height of the reduction peak was reduced, probably due to a decrease of the diffusion coefficient. Voltammetric experiments indicated that the silver deposition process is sensitive to the solution stirring but not to the pH change in acidic solutions.

Deposits were prepared under agitation in order to assure the contribution of the electroactive species to the electrode. In contrast to the non-coherent deposits observed in a TU-free bath (Fig. 2a), its presence caused an important beneficial change in the morphology, and compact and fine-grained deposits were obtained (Fig. 2b). Decreasing the potential, the deposits became smooth and uniform (Fig. 2c). Compositional analysis of those deposits indicated that sulphur content was always lower than 0.5%. However, a new decrease in the applied potential showed that dendritic growth was developed over the first coherent deposit (Fig. 2d). So, it was concluded that the lowest potential at which uniform deposits of several microns could be obtained in the thiourea bath was −600 mV, insufficient to achieve a silver–cobalt homogeneous codeposition. Structural analysis indicated that the deposits obtained from thiourea bath showed the fcc structure without preferred orientation. In all cases the peak width was wide, indicating that a small grain size was formed. By means of the Scherrer equation it was possible to estimate grain mean size, being around 27 nm.

The silver deposition process exhibits a great temperature influence: a variation of a few degrees moving the onset of the deposition process significantly (Fig. 3). This behaviour could be used to delay the process towards more negative potentials. Imaging the deposits obtained at 15 °C, the morphological change observed with the applied potential was similar to the observed for the deposits obtained at 25 °C. Dendritic growth was evident at −700 mV. Structural analysis of the deposits obtained at different temperatures indicated that the temperature diminution did not involve structural modification but did increase grain size.

In order to improve the deposit morphology and to extend the potential range at which coherent deposits might be obtained, slowing down the appearance of dendritic growth, sodium gluconate, tartaric and boric acid were also added to the bath. Tartaric was discarded because no beneficial effect was observed.

An exhaustive concentration study was made, in order to optimise the electrodeposition conditions. In all cases, no additive level concentrations of these species were used, and these were always kept at complexing agent or buffer level. Both gluconate and boric concentrations were varied between 0 and 0.3 M, the temperature

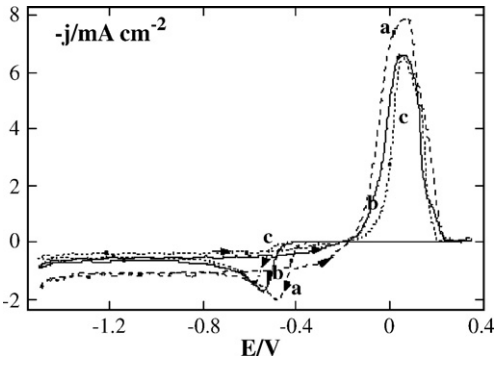

Fig. 3. Cyclic voltammograms of 0.01 mol dm^{-3} $AgClO_4$+0.2 mol dm^{-3} $NaClO_4$+0.1 mol dm^{-3} thiourea solution, pH=3.7, at different temperatures: a) 35 °C, b) 25 °C and c) 15 °C.

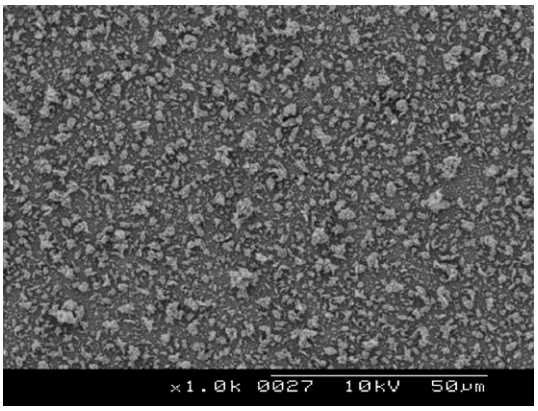

Fig. 4. Scanning electron micrograph of silver deposit of Q=−1.6 C cm^{-2}, obtained from 0.01 mol dm^{-3} $AgClO_4$+0.1 mol dm^{-3} thiourea+0.1 mol dm^{-3} gluconate+0.3 mol dm^{-3} boric acid+0.2 mol dm^{-3} $NaClO_4$ solution, pH=3.7, T=25 °C, and E_{dep}=−750 mV.

varying between 15 and 25 °C. For all the temperatures studied voltammetric response was recorded in all cases, showing that no new features appeared during the scan. Temperature effect was similar to that observed on thiourea bath.

The presence of gluconate delayed slightly the onset of voltammetric current and advanced the hydrogen reaction over freshly-deposited silver. Upon increasing its concentration, the current of the silver reduction peak decreased and the hydrogen reduction process was favoured. This last effect was undesirable because hydrogen reaction took place at potentials close to those at which cobalt would deposit in this bath (around −800 mV), being a new factor to consider. Morphological analysis showed that the addition of gluconate favoured deposit smoothness by reducing grain size. However, upon increasing gluconate concentration the final deposits were formed by chains of twinned grains that lead to deposits with a characteristic of highly rough morphology. This morphological effect, joined to the favoured hydrogen reaction, made it inadvisable to raise gluconate concentration. Optimum gluconate concentration was found thus to be 0.1 M.

Boric acid addition to the thiourea bath had a very slight effect on the electrochemical response. However, it did delay dendritic growth appearance although increasing concentration did not improve deposit quality. Similar results were obtained when boric acid was added to the solution containing both complexing agents.

A bath containing 0.1 M thiourea, >0.1 M boric acid and 0.1 gluconate produced fine-grained deposits (Fig. 4) over which dendritic growth did not appear at relatively negative potentials (greater than −800 mV).

Structural analysis of the deposits obtained in all conditions showed that the deposits maintained their fcc structure, and only in the bath containing thiourea and boric acid was observed a slight preferential orientation of (111). A discrete refinement of the grain size was observed with the addition of the new species to the bath. Low temperature favoured grain size increase.

4. Conclusions

The results obtained could be summarized as follows

- Thiourea was a convenient complexing agent for the preparation of homogeneous deposits of nanometric grain size in a wide negative range of potentials.

– Lowering the temperature increased the grain size and delayed dendritic growth.
– Boric acid addition delayed dendritic growth appearance.
– Gluconate addition reduced the grain size.

A deposition bath containing 0.1 M thiourea, 0.1 M gluconate and boric acid >0.1 M will be therefore selected as a matrix silver bath to prepare silver–cobalt deposits.

Acknowledgements

The authors wish to thank the Serveis Cientificotècnics (Universitat de Barcelona) for the use of their equipment. This paper was supported by contract MAT 2003-09483-C02-01 from the *Comisión Interministerial de Ciencia y Tecnología (CICYT)*.

References

[1] J. Schotter, P.B. Kanip, A. Becker, A. Pühler, D. Brunkmann, W. Schepper, H. Bruckl, G. Keiss, IEEE Trans. Magn. 38 (2002) 3365.
[2] M. Tondra, M. Porter, R.J. Lipert, J. Vac. Sci. Technol., A, Vac. Surf. Films 18 (2000) 1124.
[3] A. Berkowitz, J.R. Mitchell, M.J. Carey, A.P. Young, D. Rao, A. Starr, S. Zhang, F.E. Spada, F.T. Parker, A. Hutten, G. Thomas, J. Appl. Phys. 73 (1993) 5320.
[4] J.M.D. Coey, A.J. Fagan, R. Skomski, J. Gregg, K. Ounadjela, S.M. Thompson, IEEE Trans. Magn. 30 (1994) 666.
[5] A.J. Fagan, M. Viret, J.M.D. Coey, J. Phys., Condens. Matter 7 (1995) 8953.
[6] A.J. Dimitrov, S.H. Jordanov, K.I. Popov, M.G. Pavlovic, V. Radmilovic, J. Appl. Electrochem. 28 (1998) 791.
[7] T. Iida, M. Yoshino, J. Sasano, I. Matsuda, T. Osaka, J. Surf. Finish. Soc. Jpn. 55 (2004) 212.
[8] H. Zaman, A. Yamada, H. Filuda, Y. Ueda, J. Electrochem. Soc. 145 (1998) 565.
[9] G.M. Zarkadas, A. Stergiou, G. Papanastasiou, Electrochim. Acta 50 (2005) 5022.
[10] E. Michailova, A. Milchev, J. Appl. Electrochem. 21 (1991) 170.
[11] C. Ramirez, E.M. Arce, M. Romero-Romo, M. Palomar-Pardave, Solid State Ionics 169 (2004) 81.
[12] G.M Zarkadas, A. Stergiou, G. Papanastasiou, J. Appl. Electrochem. 31 (2001) 1251.
[13] G.M. de Oliveira, L.L. Barbosa, R.L. Broggi, I.A. Carlos, J. Electroanal. Chem. 578 (2005) 151.
[14] A. Hubin, H. Terryn, J. Vereecken, R.D. Keyzer, Electrochim. Acta 30 (1985) 1399.
[15] P.M. Henrichs, J.J.H. Ackerman, G.E. Maciel, J. Am. Chem. Soc. 99 (1977) 2544.
[16] A. Bellomo, D. de Marco, A. de Robertis, Talanta 20 (1973) 1225.

Modulation of magnetic and structural properties of cobalt thin films by means of electrodeposition

J Appl Electrochem (2009) 39:233–240
DOI 10.1007/s10800-008-9661-9

ORIGINAL PAPER

Modulation of magnetic and structural properties of cobalt thin films by means of electrodeposition

Jose García-Torres · Elvira Gómez · Elisa Vallés

Received: 28 March 2008 / Accepted: 3 September 2008 / Published online: 23 September 2008
© Springer Science+Business Media B.V. 2008

Abstract Cobalt electrodeposits were prepared from an electrolytic bath containing cobalt perchlorate. The effect of different species, organic (thiourea and sodium gluconate) and inorganic (boric acid), on the crystallographic structure, morphology, magnetic properties and electrochemical behaviour of cobalt electrodeposits was investigated. Amorphous cobalt, hcp cobalt and a non-usual primitive cubic cobalt phase were observed depending on the bath composition. Depending on the structure, different morphologies and magnetic properties were found. Coercivity values of the cobalt coatings ranged from around 15 Oe for amorphous, nodular deposits to 380 Oe for cobalt coatings showing acicular morphology and hcp structure with a (002) preferred orientation. Knowledge of the influence of the species on the properties of cobalt makes it possible to obtain tailored cobalt films.

Keywords Cobalt coatings · Electrodeposition · Magnetic properties · Crystal structure

1 Introduction

Electrodeposition is an efficient tool for preparing films for new technological applications. This method is cheaper in terms of equipment and less time consuming than other available deposition techniques. One of the metals successfully deposited by this method is cobalt. The electrodeposition of cobalt metallic layers and alloys is of considerable interest due to its potential applications in several fields [1, 2], especially in microelectronics for magnetic recording systems [3, 4]. Cobalt is one of the most important ferromagnetic components of magnetic thin film materials. Electrodeposition is also of interest for the preparation of cobalt and cobalt alloys because it makes it possible to modulate the structure of deposits and, hence, their magnetic properties. Depending on the preparation conditions, i.e. electrolyte composition, temperature, applied potential and presence of additives, materials with different structures, morphologies and magnetic properties can be obtained. The effects of bath compositions as well as the influence of solution parameters (pH, temperature) and electrodeposition conditions have been reported [5–7].

Our research is focused on the electrolytic preparation of cobalt based materials, one of our objectives being the preparation of nanostructured heterogeneous Co–Ag deposits. The electrolytic bath developed for this purpose contains various species: thiourea, sodium gluconate and boric acid [8, 9]. Given that the constituents of the electrolytic bath influence the deposit properties, the objective of the present study is to determine the effect of each one of the non-electroactive species present in the Co–Ag bath on the properties of pure-cobalt electrodeposits. The study focuses not only on the influence of each non-electroactive species and their combinations on deposits characteristics but also on establishing the relationship between the morphology, structure and magnetic properties of cobalt films prepared from the different electrolytic baths. This study seeks to obtain background information about the effect of each species present in the bath on the cobalt coatings and hence to facilitate the preparation of Co–Ag deposits with tailored properties.

J. García-Torres · E. Gómez · E. Vallés (✉)
Electrodep, Departament de Química Física and Institut de Nanociència i Nanotecnologia (IN 2 UB), Universitat de Barcelona, Martí i Franquès 1, 08028 Barcelona, Spain
e-mail: e.valles@ub.edu

2 Experimental section

Electrodeposition of cobalt coatings was performed from different baths summarized in Table 1. Chemicals used were $Co(ClO_4)_2$, CSN_2H_4 (thiourea), H_3BO_3, $C_6H_{11}NaO_7$ (sodium gluconate) and $NaClO_4$, all of analytical grade. All solutions were freshly prepared with water treated with a Millipore Milli Q system, de-aerated with argon and maintained under argon atmosphere during the electrochemical experiments. The pH of the bath selected for electrodeposition was maintained at 3.7. In all cases temperature was kept constant at 25 °C.

Electrodeposition was performed in a conventional three-electrode cell using a microcomputer-controlled potentiostat/galvanostat Autolab with PGSTAT30 equipment and GPES software. Cobalt films were deposited on vitreous carbon substrates. In order to avoid the possible influence of epitaxial control, amorphous substrate (vitreous carbon) was selected to analyze the influence of only bath composition and deposition conditions. The vitreous carbon electrode was previously polished to a mirror finish by using alumina of different grades (3.75 and 1.87 μm) and ultrasonically cleaned for 2 min in water before each experiment. The counter-electrode was a platinum spiral. The reference electrode was Ag|AgCl|NaCl 1 M mounted in a Luggin capillary containing 0.2 M $NaClO_4$ solution.

Voltammetric experiments were carried out at 50 mV s^{-1}, scanning towards negative potentials. Only one cycle was run in each voltammetric experiment. Deposits were prepared potentiostatically under stirring conditions ($\omega = 100$ rpm) using a magnetic stirrer. Cobalt deposit nominal thicknesses were estimated from the deposition charge without taking into account the efficiency of the process.

Deposit structures were studied by means of X-ray powder diffraction (XRD), using a conventional Bragg-Brentano diffractometer Siemens D-500. The Cu Kα radiation ($\lambda = 1.5418$ Å) was selected by means of a diffracted beam curved graphite monochromator. X-Ray powder diffraction diagrams were obtained in the 10–130° 2θ range with a step range of 0.05° and a measuring time of 30 s per step. Morphology of deposits was observed using Hitachi S 2300 and Jeol JSM 840 scanning electron microscopes. A SQUID magnetometer was used to take the magnetic measurements at room temperature.

Table 1 Composition of the baths used to obtain cobalt coatings

Bath	Concentration (mol dm^{-3})				
	$Co(ClO_4)_2$	$NaClO_4$	Thiourea	Sodium gluconate	H_3BO_3
A	0.1	0.1	0	0	0
B	0.1	0.1	0.1	0	0
C	0.1	0.1	0	0.1	0
D	0.1	0.1	0	0	0.3
E	0.1	0.1	0.1	0.1	0.3

3 Results and discussion

3.1 Electrochemical study of the deposition process

Different electrolytic baths (A–E) (Table 1) were selected to prepare cobalt deposits. For each bath, cyclic voltammetry and potentiostatic techniques were used to give a phenomenological description of the deposition process. The potentiostatic technique was also used as the method to obtain cobalt deposits.

Cyclic voltammogram (Fig. 1, curve a) recorded from the additive-free bath (bath A), showed a clear reduction peak corresponding to cobalt electrodeposition. The reduction peak was related to a mass transfer controlled process because when the solution was stirred, the reduction current maintained a constant value. Reversing the scan at potentials corresponding to the onset of the reduction current, a clear current loop was observed corresponding to the nucleation and growth process of cobalt. Two oxidation peaks were observed during the anodic sweep. The peak at more positive potentials corresponds to cobalt oxidation. Meanwhile, the most negative peak is assigned to the oxidation of the hydrogen formed during the negative scan favoured by cobalt deposition. The charge associated with this peak decreased when the same voltammetric scan was performed under stirring conditions, suggesting that H_2 was removed from the electrode when stirring. A similar oxidation peak was detected in voltammetric curves recorded under stationary conditions for cobalt and cobalt alloy deposition processes in other baths at high cathodic limits [10, 11].

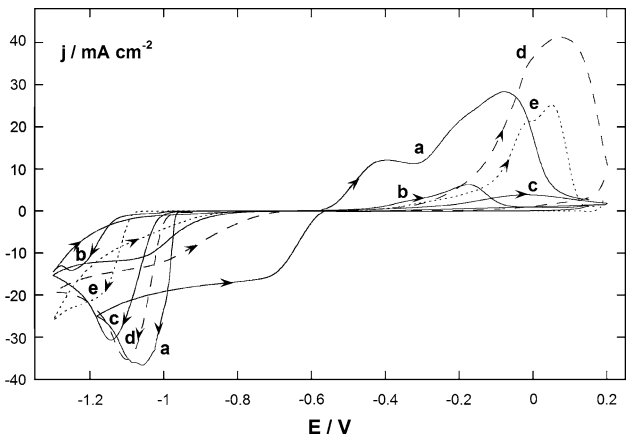

Fig. 1 Cyclic voltammograms of: (a) bath A, (b) bath B, (c) bath C, (d) bath D and (e) bath E

When different additives were added to the simplest bath, A, a shift in the onset of the cobalt deposition process as well as a decrease in the peak current, were observed in some cases. In all cases a nucleation loop was observed, reversing the scan at the onset of the deposition process. The presence of thiourea in the bath (bath B) (Fig. 1, curve b) caused not only an important delay in the onset of the cobalt deposition process but also a decrease in the current peak. Thiourea forms a complex with cobalt [12], and this Co-thiourea complex is chiefly responsible for the shift observed at the onset of the reduction process as well as the decrease observed in the peak current (as a consequence of a sharp decrease in the diffusion coefficient with respect to that of free cobalt ions). On the other hand, under these conditions no clear reduction peak was developed due to the close and simultaneous hydrogen evolution.

The addition of either sodium gluconate (bath C) (Fig. 1, curve c) or boric acid (bath D) (Fig. 1, curve d) had a lesser effect on the cobalt electrodeposition process than thiourea, although a clear shift of the onset of the deposition process as compared to the additive-free bath (bath A) was observed. With the presence of sodium gluconate, there was not only a delay in the cobalt reduction but also a decrease in the current peak. Two factors may explain the voltammetric change. On one hand, slight complexation of cobalt by sodium gluconate [12] shifts the reduction potential and decreases the peak current due to the 30% reduction in the diffusion coefficient. On the other hand, adsorption on the electrode may also contribute to the shift in reduction potential. Adsorption was considered because of the small oxidation charge recorded during cyclic voltammetry, suggesting that the high adsorption capacity of sodium gluconate on cobalt electrodes hinders cobalt oxidation. The small anodic charge was not attributed to passivation of cobalt films because no oxides were detected by either XRD or XPS [13]. When boric acid is present in the bath (bath D), only a delay in the onset of the reduction potential is observed. This delay is attributed to the adsorption of this species on the electrode because boric acid has no clear complexing capacity for cobalt ions.

The bath simultaneously containing thiourea, sodium gluconate and boric acid (bath E) showed an intermediate potential delay between those observed in thiourea and sodium gluconate or H_3BO_3 indicating that cobalt was slightly uncomplexed by thiourea (Fig. 1, curve e). Under these conditions no clear reduction peak was developed.

After selecting, from voltammetric experiments, the potential zone in which cobalt electrodeposition occurred in each bath, a potentiostatic study of cobalt deposition was performed.

Figure 2 shows the j–t transients recorded from the different baths tested. The j–t transient recorded from bath A at low overpotential showed (Fig. 2, curve a) an induction time corresponding to the formation of the first nuclei, a sharp current increase related to the growth of the deposit and a maximum subsequent current decay corresponding to the depletion of Co(II) near the electrode. As expected, by raising the overpotential, the induction time was minimised and the maximum appeared at lower deposition times (Fig. 2, curve b).

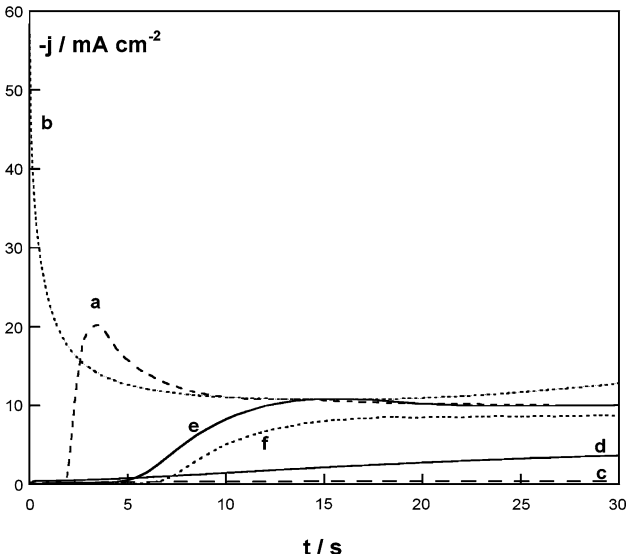

Fig. 2 j–t Transients of: (a) bath A at −840 mV, (b) bath A at −900 mV, (c) bath B at −1,000 mV, (d) bath C at −900 mV, (e) bath D at −900 mV and (f) bath E at −950 mV. Quiescent conditions

In the other baths (baths B–E), lower currents were detected at similar deposition potentials according to the shifts of the cobalt electrodeposition processes recorded during the voltammetric study. For bath B, high negative overpotentials needed to be applied to observe current (Fig. 2, curve c). In this bath, the recorded current values in the j–t transients were always lower than those recorded in the thiourea–free bath. This was due to the Co–thiourea complex formation and hence to the decrease in diffusion coefficient of the electroactive species as previously detected in voltammetric experiments.

The presence in the bath of either sodium gluconate (bath C) (Fig. 2, curve d) or boric acid (bath D) (Fig. 2, curve e) slowed down the cobalt deposition process but less than for thiourea. At −900 mV, the comparison between the recorded j–t transient from bath A (Fig. 2, curve b) and those from baths C and D (Fig. 2, curves d and e) showed that the addition of either sodium gluconate or boric acid slowed the process, with the former producing a more pronounced effect, according to the voltammetric results. When the three species were present in the bath (bath E), higher overpotential was needed to record similar currents than from baths C and D (Fig. 2, curve f).

3.2 Cobalt deposits preparation and characterization

Potentiostatic deposition of cobalt films was performed taking into account the results of the electrochemical study. Cobalt deposits between 0.5 and 5 μm (deposition charge between 1.6 and 16 C cm^{-2}) were prepared at moderate stirring conditions (100 rpm) to maintain the contribution of the Co(II) species to the electrode. A morphological study over a wide potential range was made. Structural and magnetic properties of cobalt electrodeposits prepared from the different baths at potentials corresponding to the onset of cobalt deposition were compared. From each bath, the properties of deposits of equal charge were compared.

3.2.1 Morphological analysis

The morphology of deposits prepared from baths A to E was studied. No significant modification in deposit morphology was observed as a function of deposition charge in any of the baths.

Cobalt deposits prepared from the additive-free bath (bath A) at different deposition potentials (from −870 mV to −1,150 mV) were metallic grey and presented nodular morphology (Fig. 3). As the potential became more negative a decrease in grain size was detected. This grain size decrease revealed the ease of nucleation over grain growth at high negative deposition potentials.

The presence of thiourea in the bath (bath B) induced the formation of black deposits. These deposits, even those obtained at low overpotentials, were characterized by nodular morphology with a great number of voids (Fig. 4) probably related to hydrogen evolution or hydroxide precipitation, which hinders compactness. The electrocatalytic

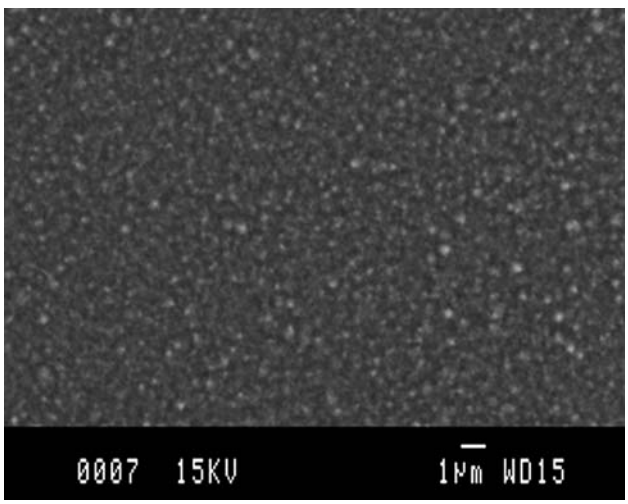

Fig. 3 Scanning electron micrograph of Co deposits of 0.5 μm prepared at −870 mV from bath A

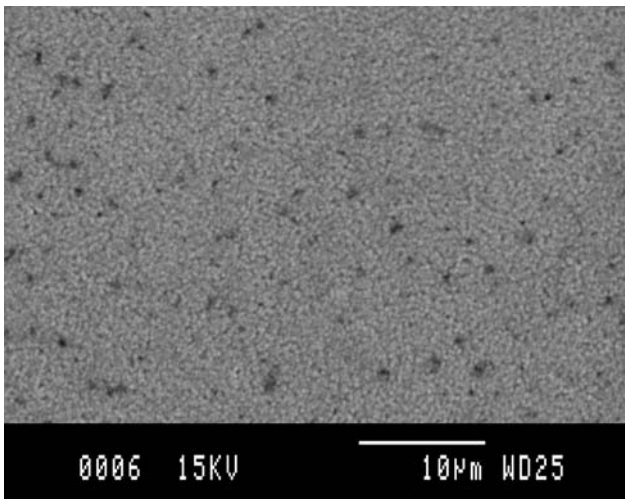

Fig. 4 Scanning electron micrograph of Co deposits of 0.5 μm prepared at −1,000 mV from bath B

behaviour of Co to hydrogen evolution may explain the high number of voids observed in the deposits prepared from this bath.

The addition of sodium gluconate or boric acid made it possible to obtain metallic grey cobalt deposits. When sodium gluconate was present (bath C) different morphologies were detected depending on the applied potential. At very low overpotentials well-separated, quasi-spherical grains were seen to grow at isolated locations over the first deposited layer with nodular morphology (Fig. 5a). A slightly higher overpotential was needed to obtain compact deposits, characterized by acicular morphology (Fig. 5b). The adsorption of gluconate during cobalt growth may be responsible for the change in deposit morphology. On the other hand, the presence of boric acid (bath D) made it possible to also obtain compact deposits with slightly faceted-grain morphology (Fig. 5c) in all conditions tested.

The simultaneous presence of boric acid and sodium gluconate in the bath containing thiourea (bath E) improved the deposit quality, showing coatings with nodular morphology (Fig. 6) but higher grain size than that observed in deposits obtained from bath A. Deposits obtained from this complex bath were crack-free and had high compactness throughout the entire range of potentials studied.

3.2.2 Crystal structure and magnetic properties

X-ray diffraction patterns and magnetic behaviour of cobalt deposits obtained from baths A to E of around 4 μm were studied The deposits were obtained at low applied potentials (from −870 mV for bath A to −1,000 mV for bath B; the potentials for the other baths were between −870 and −1,000 mV) in order to minimize the possible hydrogen reaction. The variation of these properties as a function of

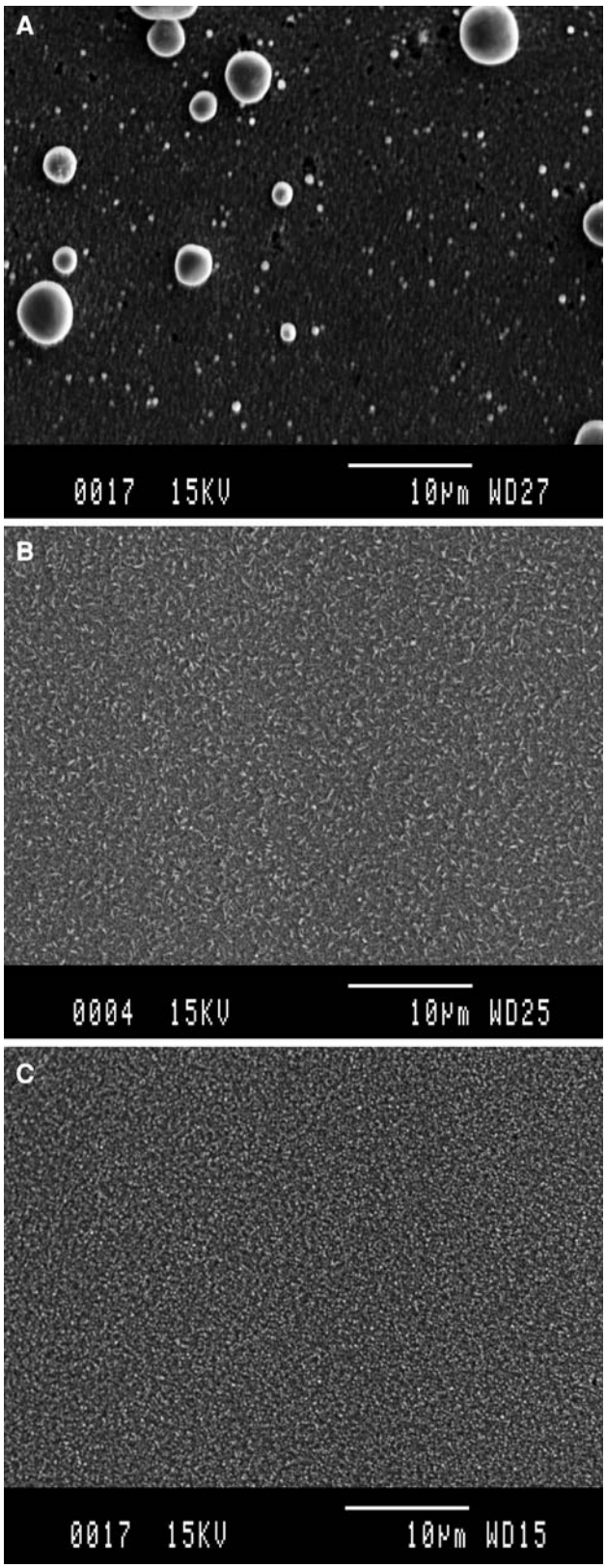

Fig. 5 Scanning electron micrographs of Co deposits of 0.5 μm prepared from (**a**) bath C at −800 mV, (**b**) bath C at −850 mV and (**c**) bath D at −850 mV

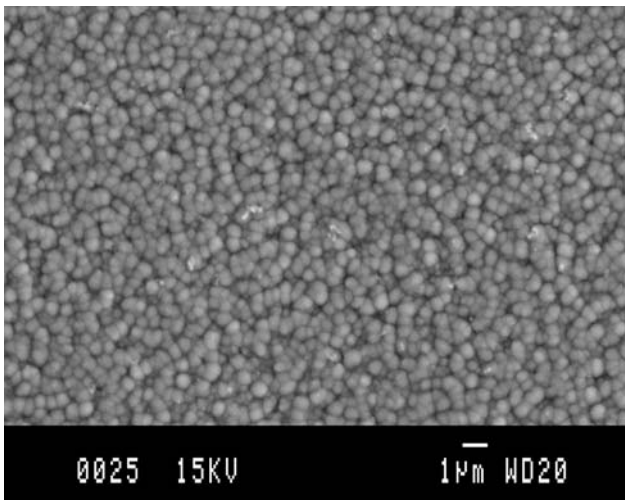

Fig. 6 Scanning electron micrograph of Co deposits of 0.5 μm prepared at −900 mV from bath E

bath composition was analysed. Cobalt deposits were removed from the vitreous carbon electrode and placed on a silicon monocrystalline substrate of low response for X-ray spectra recording.

The diffractograms of cobalt deposits prepared from the different baths, except bath B, showed narrow peaks as compared to the response of the substrate, revealing their crystalline nature. Figure 7a and b show the diffractograms of the crystalline deposits. The width of the diffraction peaks was greater than the instrumental peak linewidth, revealing the nanometric size of the crystallites. However, when cobalt deposits were obtained from bath B, the diffractogram showed practically the same response as the substrate (Fig. 7c), revealing the amorphous nature of this film.

Table 2 summarizes the information derived from the XRD patterns: structure, main planes and I/I_{max} ratio of the deposits studied. The X-ray diffractograms of the films obtained from baths A, C and D are characterized by showing a close-packed hexagonal structure (hcp) but different preferred orientation. Whereas cobalt samples obtained from baths A and D are textured with a (110) preferential orientation (but with a different peak intensity distribution), hcp cobalt phase from bath C grows with the (002) plane as preferred orientation. Positions of the peaks remained constant in all the spectra and equal to those tabulated [PDF#05-0727], implying the same lattice parameters. Due to the constancy of these parameters it could be suggested that the species are not incorporated within the lattice and that the adsorption of these species during electrodeposition is responsible for the change in the preferential orientation. Although the same structure was detected, the different orientation of the films as well as the different peak intensity distribution gave rise to

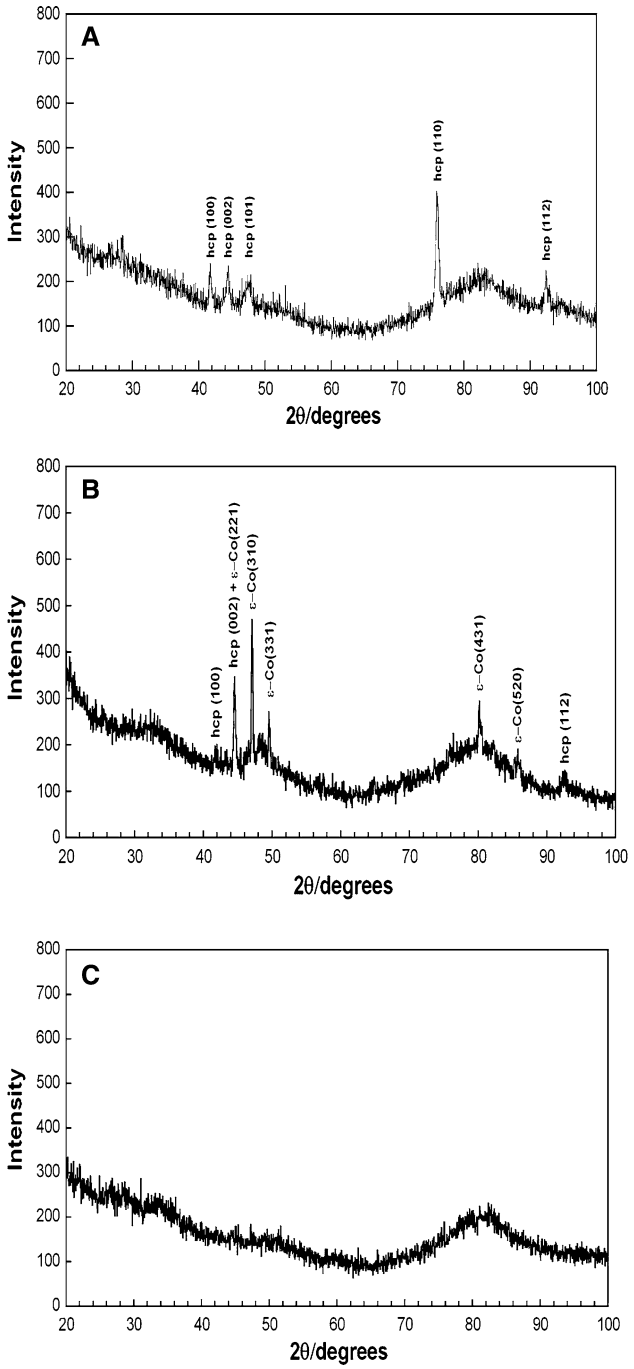

Fig. 7 XRD patterns of Co deposits of 4 μm obtained from: (**a**) bath A, (**b**) bath E and (**c**) bath B

different morphologies: nodular morphology (bath A), faceted-grain morphology (bath D) and acicular morphology (bath C).

On the other hand, when all the species were present in the solution (bath E) a primitive cubic structure (ε-Co), different from the usual hcp or fcc cobalt phases, was detected as the main phase. Coupled to this structure, some hcp phase can be observed. Also in this case, the different

Table 2 Structural properties of cobalt coatings

Bath	Structure	Planes	I/I_{max} (%)
A	hcp	(100)	37
		(002)	31
		(101)	22
		(110)	100
		(112)	31
B	Amorphous	–	–
C	hcp	(100)	36
		(002)	100
		(101)	44
		(110)	40
D	hcp	(100)	61
		(002)	16
		(101)	35
		(110)	100
		(112)	20
E	hcp + ε-Co (primitive cubic)	hcp (100)	17
		hcp (002) + ε-Co (221)	71
		ε-Co (310)	100
		ε-Co (331)	36
		ε-Co (431)	36
		ε-Co (520)	17
		hcp (112)	12

structure detected was associated with a different morphology: a nodular morphology with a higher grain size than that observed in films obtained from the simplest bath (bath A). The primitive cubic phase of cobalt (ε-Co) has been detected for cobalt nanoparticles synthesized by wet chemical synthetic routes [14, 15] or cobalt nanocrystals [16, 17] but not by electrochemical methods.

The average grain size was estimated from the full width at half maximum (FWHM) values of the diffraction peaks by using the Debye-Sherrer equation, neglecting the instrumental linewidth (which is acceptable for a nanocrystalline material) and the stress-induced line broadening. For the cobalt crystalline deposits prepared from the different baths tested, no significant differences were observed in the estimated grain size in the range 20–30 nm for all the films.

The magnetic behaviour of cobalt films was analysed by recording hysteresis loops. Figure 8 shows two representative magnetization-magnetic field dependences. A saturation magnetisation (M_s) of around 150–160 emu g^{-1} (that corresponds to the value for bulk cobalt) was obtained for all samples.

From the parallel and perpendicular hysteresis loops obtained with the SQUID, very different values of the saturation fields (H_s) were observed for parallel ($H_{s_{\parallel}}$) and perpendicular ($H_{s_{\perp}}$) fields for cobalt deposits showing hcp structure (deposits obtained from A, C and D baths)

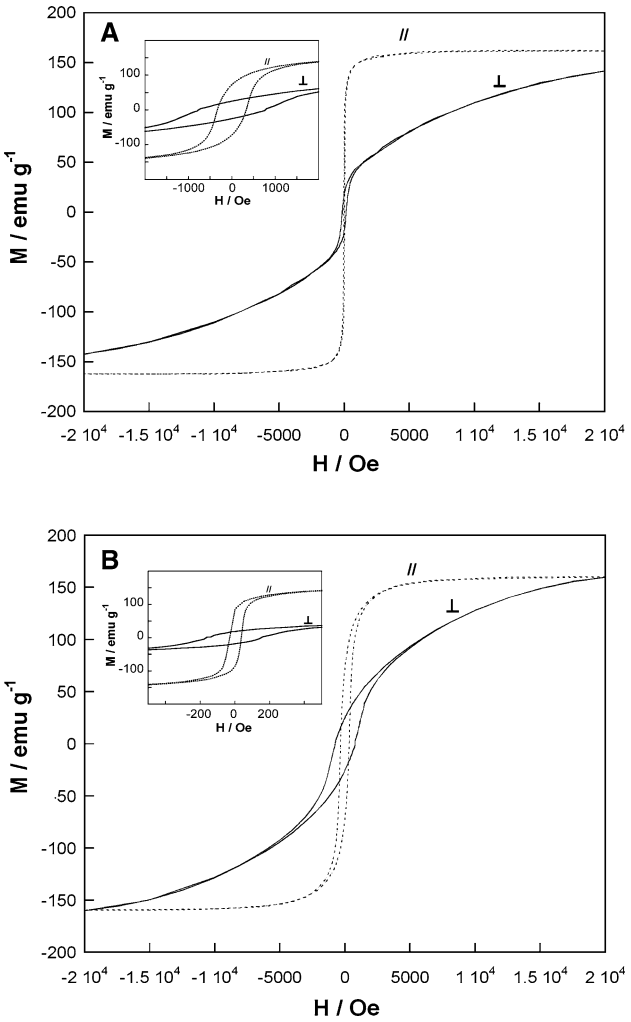

Fig. 8 Magnetisation versus magnetic field of Co deposits of 4 μm obtained from (**a**) bath A and (**b**) bath C

Table 3 Magnetic properties of cobalt coatings: Coercivity values (H_c), saturation fields (H_s), uniaxial anisotropy constant (K) and calculated angle of the resulting anisotropy with respect to the film normal (θ)

Bath	H_c (∥) (Oe)	H_c (⊥) (Oe)	H_s (∥) (Oe)	H_s (⊥) (Oe)	K (J cm^{-3})	θ (°)
A	31	149	11,000	40,000	2.36	55
B	15	25	–	–	–	–
C	344	767	15,000	32,000	2.07	45
D	86	183	12,000	40,000	2.43	54
E	117	100	13,000	15,000	0.21	5

(Fig. 8; Table 3), revealing the magnetic anisotropy of these films. An easier magnetization direction in the parallel-applied field was observed. The anisotropy was not parallel to the applied field. A high uniaxial anisotropy constant (K) and the angle of the resulting anisotropy with respect to the normal film (θ) were estimated for these deposits using the expressions [18]:

$$H_{s_{\parallel}} = 2K\cos^2\theta/M_s \quad (1)$$

and

$$H_{s_{\parallel}} + H_{s_{\perp}} = 4\pi M_s + 2K/M_s \quad (2)$$

The values of K were greater than that corresponding to pure hcp cobalt ($K = 0.45$ J cm^{-3}) [19] probably due to internal stress. A spontaneous orientation of the film parallel to the magnetic field confirmed the strong uniaxial anisotropy, in addition to the usual shape anisotropy expected for thin films [19].The calculated angle θ was 45–55° in the three cases.

Less difference between M–H loops with the magnetic field perpendicular or parallel to the film plane was observed for cobalt amorphous films prepared from bath B or cobalt ε-Co + hcp obtained from bath E, suggesting no significant magnetic anisotropy in these films. Regarding the unusual primitive cubic cobalt phase, the calculated value ($K = 0.21$ J cm^{-3}) is close to that found in the bibliography for nanocrystals with cubic ε-Co structure embedded in an amorphous carbon matrix [20]. A clearly different value of the calculated θ was obtained for these films. On the other hand, the value of K for amorphous cobalt cannot be calculated because of the lack of magnetic anisotropy associated to the short-range order.

Noticeable differences were also detected in coercivity values (H_c) for the cobalt films prepared in the different electrolytic baths (Table 3), both in the easy and the hard axis of magnetization. The highest coercivity observed was in cobalt films obtained from bath C and the lowest value was measured in the cobalt deposits obtained from bath B. Whereas cobalt deposits from baths A and D, with the hcp structure and the same preferred orientation, show similar H_c values, the cobalt deposits obtained from bath C, also with hcp structure, show a much higher value mainly associated to the change in the preferential orientation. A different value of coercivity was also observed for deposits prepared from complex bath E, associated with the structural change induced for the components of the bath. The lowest value of coercivity was detected in the amorphous films obtained from bath B. For these amorphous deposits, the lack of macroscopic magnetocrystalline anisotropy implies a relatively easy magnetization rotation. Furthermore the absence of microstructural discontinuities (grain boundaries or precipitates), on which magnetic domains can be pinned, makes magnetization by wall motion easy and, hence, coercive fields of a few oersteds are achieved.

4 Conclusions

Electrodeposition has been shown to be a suitable technique for obtaining cobalt films with tailored magnetic

properties, because the different species tested (boric acid, gluconate and thiourea) induced different structural properties and even amorphous nature in the deposits. Moreover, structural changes are reflected in the different morphologies observed.

The electrochemical study allowed us to detect the dependence of the cobalt electrodeposition process on bath composition. Coherent and uniform cobalt deposits were obtained from baths containing boric acid or gluconate. Although the presence of only thiourea did not favour the formation of uniform cobalt deposits the combination of thiourea with gluconate and boric acid made it possible to obtain coherent films in a wide range of potentials. The baths tested favoured the appearance of singular orientations with different types of magnetic behaviour. The use of these different species allowed us to modulate the magnetic response of the cobalt deposits.

Cobalt films obtained from baths A and D showed hcp structure with (110) as preferred orientation. The similar structural characteristics in both cases justify the similar coercivity values (around 150 Oe).

The highest value of H_c (around 380 Oe) was observed in cobalt coatings of hcp structure, (002) preferred orientation and acicular morphology obtained from bath C. The lowest H_c (around 15 Oe) was detected in cobalt films obtained from bath B due to the amorphous nature of these deposits.

A primitive cubic phase (ε-Co) was detected in cobalt obtained from the most complex bath (bath E), revealing that an unusual structure of cobalt films can be induced by the simultaneous presence of complexing agents and adsorbed species.

Depending on the bath composition, it was then possible to obtain cobalt electrodeposits with different magnetic properties. While the presence of thiourea induced the formation of soft magnetic films, sodium gluconate made it possible to obtain harder magnetic coatings. An intermediate behaviour was detected when all the species were present in the bath. Thus the possibility of developing new electrodeposition baths containing the species tested with the objective of preparing Co containing films with tailored magnetic properties is open.

Acknowledgements This paper was supported by contract MAT-2006-12913-C02-01 from the *Comisión Interministerial de Ciencia y Tecnología (CICYT)*. J. García-Torres also thanks the Departament d'Innovació, Universitats i Empresa of the Generalitat de Catalunya and Fons Social Europeu for financial support.

References

1. Higashi K, Fukushima H, Urkawa T, Adaniga T, Matsudo K (1990) J Electrochem Soc 137:3418
2. Osaka T (2000) Electrochim Acta 45:3311
3. Moina CA, de Oliveira-Versic L, Vazdar M (2004) Mater Lett 58:3518
4. Brückner W, Thomas J, Hertel R, Schäfer R, Schneider CM (2004) J Magn Magn Mater 283:82
5. Gómez E, Vallés E (2002) J Appl Electrochem 32:693
6. Cui CQ, Jiang SP, Tseung CC (1990) J Electrochem Soc 137:3418
7. Ankara S, Majan S (1980) J Electrochem Soc 127:283
8. Gómez E, García-Torres J, Vallés E (2007) Anal Chim Acta 602:187
9. Gómez E, García-Torres J, Vallés E (2008) J Electroanal Chem 615(2):213
10. Pellicer E, Gómez E, Vallés E (2006) Surf Coat Technol 201:2351
11. Gómez E, Pellicer E, Vallés E (2003) J Electroanal Chem 556:137
12. IUPAC Stability Constants Database (SC Database) version 5.16 (2001) Ed. Academic Software cop
13. García-Torres J, Gómez E, Alcobe X, Vallés E Surf Coat Technol (Submitted)
14. Sun S, Murray CB (1999) J Appl Phys 85:4325
15. Puentes VF, Krishnan KM, Alivasatos P (2001) Appl Phys Lett 78:2187
16. Nie X, Jiang JC, Meletis EI, Tung LD, Spinu L (2003) J Appl Phys 93:4750
17. Sun S, Murray CB (1999) J Appl Phys 85:4325
18. Xiao JQ, Chien CL, Gavrin A (1996) J Appl Phys 79:5309
19. Klavunde KJ (2001) Nanoscale materials in chemistry. Wiley-Interscience, New York
20. Nie X, Jiang JC, Meletis EI, Tung LD, Spinu L (2003) J Appl Phys 93:4750

4.2. Viability of the Co-Ag electrodeposition process. Preparation and characterization of cobalt-silver films

Once the experimental conditions for silver deposition were settled, a basic study of the Co-Ag electrodeposition process was performed. After that, the capacity of electrochemistry to obtain cobalt-silver films with good prospects was also analyzed. Such experiments were performed from solutions containing 0.01 mol dm^{-3} $AgClO_4$ + 0.2 mol dm^{-3} $NaClO_4$ + 0.1 mol dm^{-3} thiourea + 0.1 mol dm^{-3} sodium gluconate + 0.3 mol dm^{-3} boric acid + x mol dm^{-3} $Co(ClO_4)_2$, where 0.02 mol dm^{-3} ≤ x ≤ 0.1 mol dm^{-3}.

The compositional results indicated that Co-Ag films with variable composition were obtained, the composition being dependent on the electrodeposition conditions: the more negative the applied potential the higher the cobalt content into the film. However, small changes in the applied potential led to great changes in cobalt incorporation which implied a difficult control on the film's composition. On the other hand, sulphur incorporation was also detected it being up to 2 wt.% in the most unfavourable conditions.

The films prepared were deeply characterized in terms of microstructure. Films with granular morphology and high roughness (of the order of a few microns) were obtained in all the conditions tested. On the other hand, *stripping* analysis revealed the heterogeneity of the deposits prepared, however this technique did not give any clue about the way in which cobalt or silver were present in the deposit. In order to gain knowledge about the oxidation state of the elements, X-Ray photoelectron spectroscopy analyses were performed not only on the film surface but also in the inner. The XPS spectra revealed that silver was in the metallic state. However, although cobalt was also found to be in the metallic state, peaks related to CoO could also be detected but mainly on the surface. Differential scanning calorimetry together with thermogravimetric analyses allowed determining the discontinuous nature of the CoO taking profit of the protective character of cobalt oxides. XRD and HRTEM together with fast fourier transform were required to exactly determine the crystalline structure of the Co-Ag deposits: fcc phase of silver, hcp-Co and a metastable hcp phase never obtained previously by electrodeposition and indexed as $CoAg_3$.

Despite the fact that the equilibrium diagram shows almost complete immiscibility of both metals, electrodeposition has been found to produce metastable phases of both cobalt and cobalt-silver films: a primitive cubic structure (ε-Co) and a hcp-$CoAg_3$, respectively. Figure 4.4 shows the unitary cells for ε-Co and hcp-$CoAg_3$. The hypothesis for the hcp-$CoAg_3$ phase to be formed is explained as follow. Cobalt crystallizes in a primitive cubic structure which is slightly less compact than the usual hcp or fcc structures for cobalt. Moreover, the interstitial sites are bigger in

size than in the other structures which may allow the incorporation of silver in it. The distortion of this primitive cubic cell by silver could lead to the hexagonal $CoAg_3$ phase.

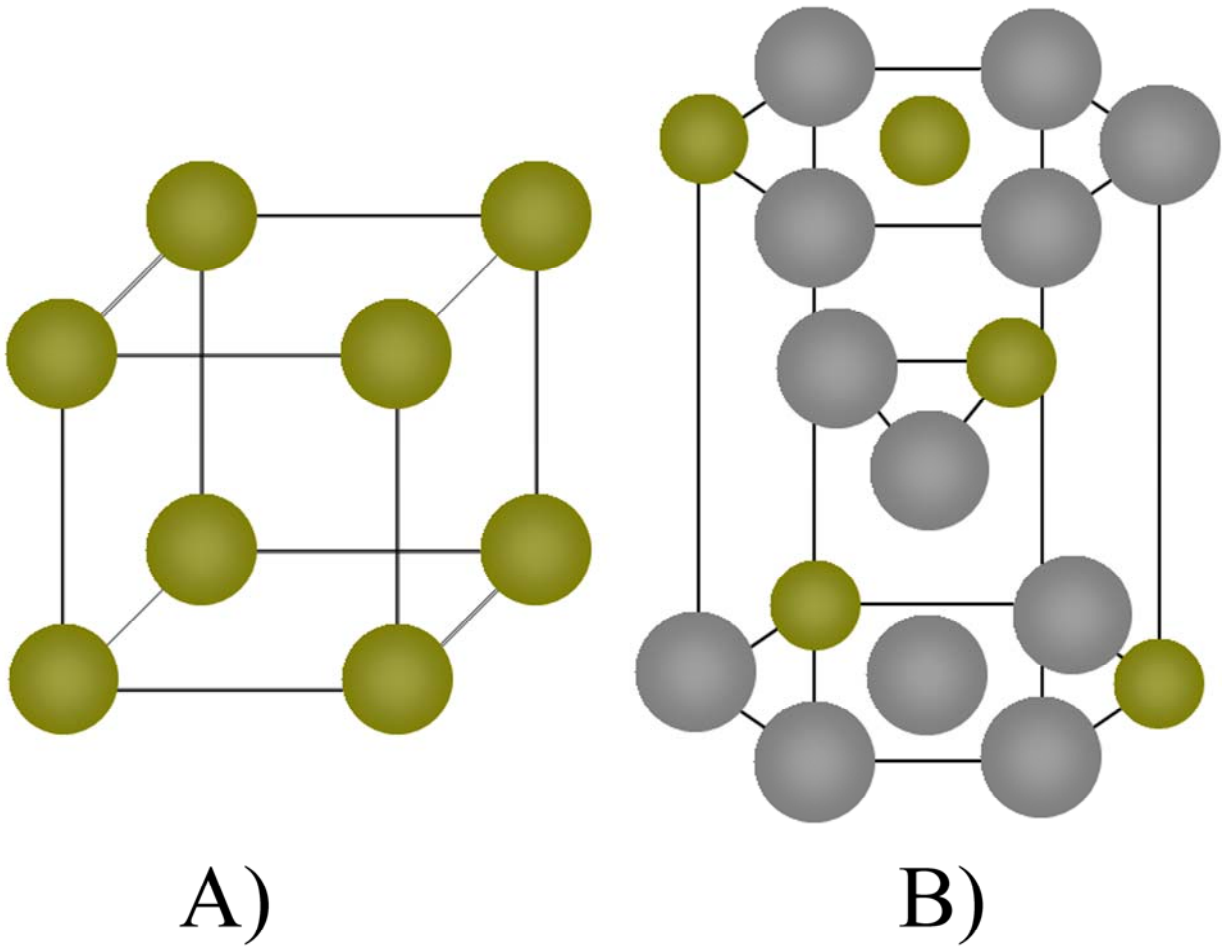

Figure 4.4. A) Primitive cubic structure of ε–Co metastable phase. B) Disordered hexagonal close-packed structure of the $CoAg_3$ metastable phase (Gray and green spheres represent silver and cobalt atoms, respectively).

Group of articles included in section 4.2.

Page 87: Electrodeposition of Co-Ag films and compositional determination by electrochemical methods

Elvira Gómez, Jose Garcia-Torres and Elisa Vallés, Analytica Chimica Acta 602 (2007) 187

Page 97: Preparation of Co-Ag films by direct and pulse electrochemical methods

Elvira Gómez, Jose Garcia-Torres and Elisa Vallés, Journal of Electroanalytical Chemistry 615 (2008) 213

Page 109: Metastable structures of Co and Co-Ag detected in electrodeposited coatings

Jose Garcia-Torres, Elvira Gómez, Xavier Alcobé and Elisa Vallés, Crystal Growth & Design 9(4) (2009) 1671

Electrodeposition of Co-Ag films and compositional determination by electrochemical methods

ANALYTICA CHIMICA ACTA 602 (2007) 187–194

available at www.sciencedirect.com

ScienceDirect

journal homepage: www.elsevier.com/locate/aca

Electrodeposition of Co–Ag films and compositional determination by electrochemical methods

Elvira Gomez, Jose García-Torres, Elisa Valles*

Electrodep. Departament Química Física, Facultat de Química, Universitat de Barcelona, Martí i Franquès, 1. 08028 Barcelona, Spain

ARTICLE INFO

Article history:
Received 14 March 2007
Received in revised form
19 September 2007
Accepted 19 September 2007
Published on line 25 September 2007

Keywords:
Heterogeneous Co–Ag deposits
Electrodeposition
Voltammetry
Stripping
Polarography

ABSTRACT

An electrolytic bath containing silver(I), cobalt(II) and different complexing agents to electrodeposit Co–Ag coatings over vitreous carbon and silicon/seed-layer substrates is proposed. *In situ* electrochemical characterization of thin deposits is performed by means of stripping (potentiodynamic or galvanostatic) methods. These techniques allow detecting the heterogeneous codeposition of cobalt and silver. Electrochemical *ex situ* methods (polarographic and voltammetric methods) are implemented to quantify the silver and cobalt percentage in the coatings. Optimal analytical parameters for voltammetric method are established.

© 2007 Elsevier B.V. All rights reserved.

1. Introduction

Nowadays the development of materials with new properties is in expansion. Additionally, the improvement of already exploited materials with new or modified properties is coming under increased scrutiny. Thus, great attention is progressively being paid to thin films and multilayers showing magnetoresistance (MR).

One system which exhibits magnetoresistance at room temperature is the Co–Ag system, and much recent research has reported on this. Thus, granular Co–Ag films have been prepared by means of physical methods such as magnetron-sputtering [1,2] ion-beam co-sputtering [3,4], high-energy mechanical alloying [5] or metal vapour vacuum arc [6]. Electrodeposition has also been recently tested as a preparation method for cobalt–silver multilayers [7], as an alternative to physical preparation techniques [8,9]. Some authors have also proposed the electrodeposition as a possible method for preparing Co–Ag granular films [10–12], although at present, work of this nature is limited to sporadic electrochemical studies.

Silver and cobalt are almost insoluble in each other both in solid and liquid states [13]. Due to the potential applicability of electrodeposition as a technique to obtain films and to modify their properties, our final objective is the preparation of Co–Ag heterogeneous films by means of this technique. In order to obtain magnetoresistance, the deposit should present a composition range between 10 and 45 wt.% cobalt, since Co–Ag materials prepared by other methods present magnetoresistance response only in this interval. Thus, the first step to achieve the aforementioned goal is to develop an electrolytic bath able to perform the simultaneous deposition of both metals. The codeposition of silver and cobalt is complicated by the big difference in their standard potentials. Therefore, cobalt was added to the bath in higher concentration than silver to favour electrodeposition of the former. Previous works of ours

* *Corresponding author*. Tel.: +34 934021234; fax: +34 934021231.
E-mail address: e.gomez@ub.edu (E. Gomez).
0003-2670/$ – see front matter © 2007 Elsevier B.V. All rights reserved.
doi:10.1016/j.aca.2007.09.040

[14,15] have proposed an electrolytic bath able to deposit silver at very negative deposition potentials. Here, our first interest is to test the possibility of simultaneously depositing silver and cobalt from such an electrolytic bath. A study of the Co–Ag electrodeposition process will be performed to analyse the electrochemical behaviour of the system in the selected bath.

Once the electrochemical behaviour of the system is known, the deposit composition must be determined in order to relate it with deposit properties. Different electrochemical techniques (*in situ* and *ex situ*) will be tested. Since polarography does not allow the simultaneous determination of cobalt and silver, due to the likeliness of mercury oxidation, the second objective in this work is to attempt to develop a voltammetric method able to quantify silver by a simple and sensitive electrochemical procedure. Cobalt was analysed by polarography.

2. Experimental

The study of the electrodeposition process and deposit preparation-characterization was performed in a conventional three-electrode cell using a microcomputer-controlled potentiostat/galvanostat Autolab with PGSTAT30 equipment and GPES software. Chemicals used were $AgClO_4$, $Co(ClO_4)_2$, CSN_2H_4 (thiourea), H_3BO_3, $C_6H_{11}NaO_7$ (gluconate) and $NaClO_4$, all of analytical grade. All solutions were freshly prepared with water treated with a Millipore Milli Q system, de-aerated with argon and maintained under argon atmosphere during the electrochemical experiments. The pH of the selected bath to electrodeposit was maintained at 3.7. In all cases temperature was maintained at 25 °C.

Working electrodes were vitreous carbon (Metrohm) and silicon with Ti/Ni seed layer (Si/Ti(100 nm)/Ni(50 nm)) supplied by IMB-CNM. The vitreous carbon electrode was previously polished to a mirror finish by using alumina of different grades (3.75 and 1.87 μm) and ultrasonically cleaned for 2 min in water before each experiment. The silicon-based substrata were cleaned with acetone followed by ethanol and later with water. The counter-electrode was a platinum spiral. The reference electrode was Ag|AgCl|NaCl 1 M mounted in a Luggin capillary containing 0.2 M $NaClO_4$ solution. All potentials were referred to this electrode.

Voltammetric scans and voltammetric or galvanostatic *stripping* experiments were used to analyse the deposition process. Only one cycle was run in each voltammetric experiment. *Stripping* analyses were always performed immediately after deposition either in the deposition solution itself or in a thiourea- and silver(I)-free solution. All potentiodynamic *stripping* experiments were made at a scan rate of 10 mV s^{-1}. Galvanostatic *stripping* was carried out at a current of 32 μA cm^{-2}. Deposits were prepared potentiostatically on silicon-seed layer under stirring conditions (ω = 800 rpm) using a magnetic stirrer.

Compositional analyses were performed by means of polarographic and voltammetric techniques using a Methrom 757 VA Computrace and the same equipment was used for electrochemical study respectively. A dropping mercury electrode (DME) was used as working electrode in the polarographic technique and a vitreous carbon was used in the voltammetric. The analysis of deposits was carried out after dissolving them in 32 wt.% nitric acid. Temperature was kept at 25 °C except when temperature influence was studied.

3. Results and discussion

3.1. *Electrochemical study of the Co–Ag electrodeposition process*

A preliminary study of the electrodeposition process was performed on a vitreous carbon electrode by using the solution optimized for silver deposition [14] but adding cobalt(II). This study allowed us to select 0.1 M as total cobalt(II) concentration, so that deposition bath composition was: 0.01 M $AgClO_4$ + 0.1 M $Co(ClO_4)_2$ + 0.1 M thiourea + 0.1 M gluconate + 0.3 M H_3BO_3 + 0.1 M $NaClO_4$, pH 3.7.

3.1.1. *Voltammetric study*

The study of the electrodeposition process was performed initially by cyclic voltammetry, scanning from a potential at which no current was detected at negative potentials. Different cathodic limits were used. Fig. 1 shows the voltammetric behaviour, two reduction peaks (peaks A and B) were observed prior to hydrogen evolution, as well as two oxidation features (peaks A′ and B′) were observed. When the voltammetric scan was reversed prior to the second reduction process (Fig. 1, continuous line) only one oxidation peak was recorded in the positive scan (peak A′). Peaks A and A′ appeared at the same potentials as those recorded in the cobalt-free bath [14]. Therefore, peaks A and A′ were related to silver deposition and silver oxidation, respectively.

When the cathodic limit was lengthened a new reduction process (peak B) as well as the corresponding oxidation process (peak B′) were recorded. When the scan was reversed at

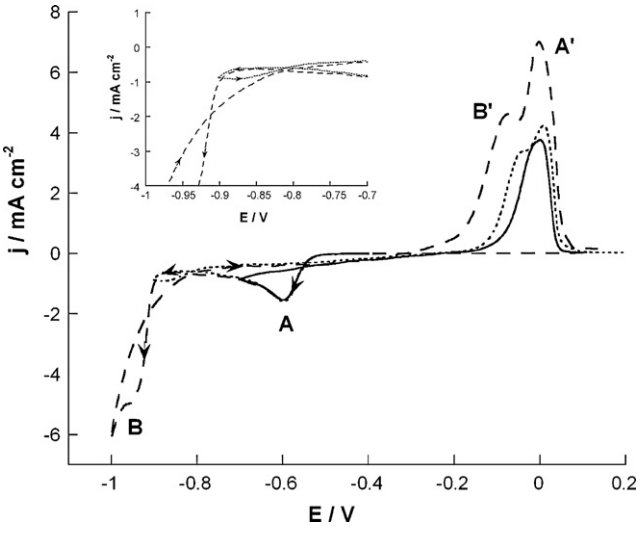

Fig. 1 – Cyclic voltammograms of 0.01 M $AgClO_4$ + 0.1 M $Co(ClO_4)_2$ + 0.1 M thiourea + 0.1 M gluconate + 0.3 M boric acid + 0.1 M $NaClO_4$ solution, pH 3.7. Initial potential −0.4 V. Different cathodic limits: Continuous line, −700 mV; pointed line, −900 mV; and dashed line, −1000 mV. Scan rate 50 mV s^{-1}.

the beginning of the second reduction peak (peak B), a nucleation loop was observed (Fig. 1, pointed line). This indicated a new nucleation process that took place over the first electrodeposited silver layer. Upon decreasing the negative limit, the reduction current increased, but no clear reduction peak was developed due to the nearness of proton reduction (Fig. 1, dashed line). So, by means of the voltammetric study it could be concluded that peak B was related with cobalt deposition, B′ being the corresponding oxidation peak associated with the deposit formed in peak B.

From these voltammetric experiments it is possible to determine the potential range in which silver and cobalt codeposition took place, thus defining the working zone for deposit preparation. As can be observed in Fig. 1, potential range between −800 and −1000 mV would allow Co–Ag codeposition over glassy carbon with relatively low hydrogen reaction.

3.1.2. *In situ electrochemical characterization*

Deposits prepared potentiostatically at different deposition potentials were analysed by means of anodic linear sweep voltammetry (ALSV) in order to characterize the kind of deposit obtained in the initial deposition stages. Low charge deposits (few nanometers thick) were analysed. The ALSV technique has already been shown to be very useful in the characterization of deposited alloys [16,17].

Fig. 2 shows the different responses of the voltammetric *stripping* analysis depending on oxidation bath composition. When the deposits were oxidized in the preparation bath (Fig. 2, dashed line) one oxidation feature, asymmetric and wide, was recorded. When a thiourea- and silver(I)-free bath was used, the stripping response showed two peaks, the less cathodic peak is related to silver oxidation, whereas the more cathodic one (with a shoulder on its right side) was related

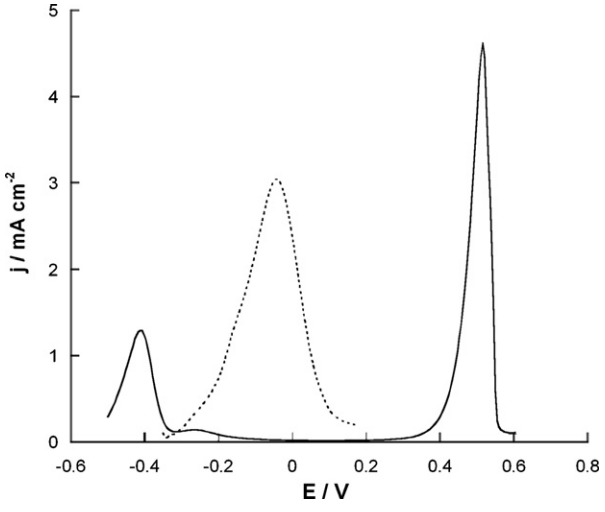

Fig. 2 – Voltammetric *stripping* curves of a Co–Ag deposit prepared potentiostatically at −850 mV and oxidized in different baths. Oxidation bath: dash line, 0.01 M $AgClO_4$ + 0.1 M $Co(ClO_4)_2$ + 0.1 M thiourea + 0.1 M gluconate + 0.3 M boric acid + 0.1 M $NaClO_4$ solution, pH 3.7; continuous line, 0.1 M $Co(ClO_4)_2$ + 0.1 M gluconate + 0.3 M boric acid + 0.1 M $NaClO_4$ solution, pH 3.7. Scan rate 10 mV s^{-1}.

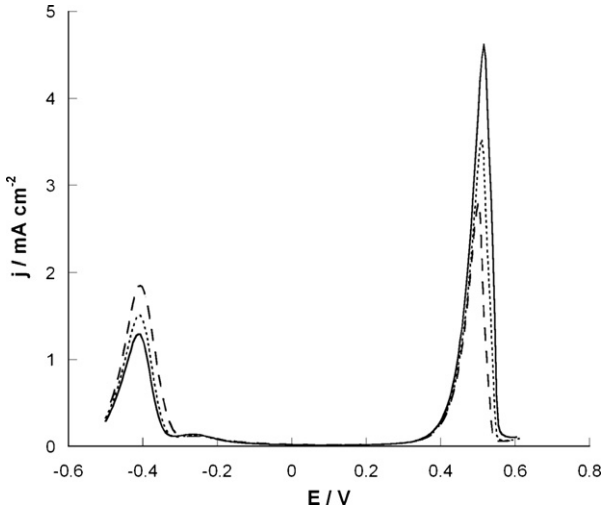

Fig. 3 – Voltammetric *stripping* curves of Co–Ag deposits prepared potentiostatically at different potentials and at Q = −0.13 C cm^{-2}: continuous line, −850 mV; pointed line, −870 mV; and dashed line, −900 mV. Oxidation bath 0.1 M $Co(ClO_4)_2$ + 0.1 M gluconate + 0.3 M boric acid + 0.1 M $NaClO_4$ solution, pH 3.7. Scan rate 10 mV s^{-1}.

to cobalt oxidation (Fig. 2 continuous line). This assignment is made since the positions of these peaks fitted well with those of the oxidation peaks of pure-silver and pure-cobalt deposits in this same bath. These results allowed us to assume the heterogeneity of the deposits obtained as well as to point out the interference effect provoked by simultaneous reduction of Ag(I) at potential values at which the *stripping* was done and by thiourea. It is known that thiourea adsorbs easily over this kind of substrates [18] delaying the cobalt oxidation. On the other hand, the complexing capacity of thiourea over silver [19] favoured the silver oxidation process. These opposite effects of thiourea over cobalt and silver provoked an overlapping of both peaks.

To confirm the assignment of peaks recorded in the thiourea- and silver(I)-free bath, a series of deposits was prepared varying applied potential. At potentials at which only silver deposition occurred, a progressive increase in the deposition time implied an increase in the charge recorded under the less negative peak. For a fixed deposited charge, at those potentials at which the co-deposition was possible, upon decreasing the applied potential an increase was observed in the charge under the more negative peak as well as a decrease in the more positive one (Fig. 3). Thus, cobalt percentage in the deposits increases on decreasing deposition potential.

Similar information was obtained by means of galvanostatic *stripping*. When the analysis was performed in the same preparation bath, a single plateau was observed (Fig. 4a, dashed line). But when the *stripping* took place in the thiourea- and silver(I)-free bath three plateaux were recorded corresponding to the two main peaks and the shoulder of the most cathodic peak observed in the voltammetric *stripping* (Fig. 4a, continuous line). It was also observed that a decrease in either applied potential or deposited charge (or both) was associated to a change in the width of the plateaux (Fig. 4b).

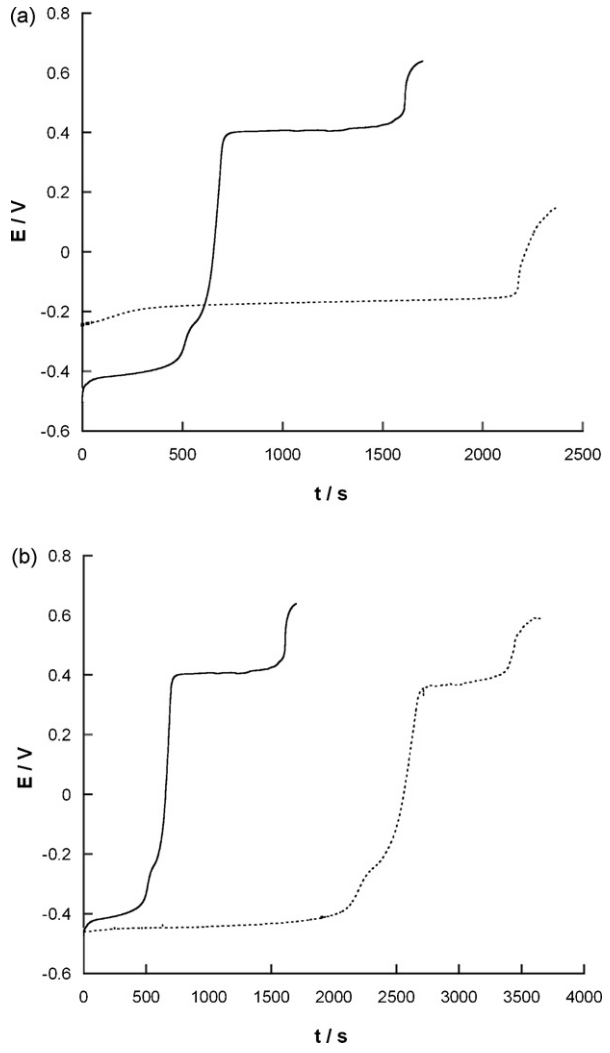

Fig. 4 – (a) Galvanostatic *stripping* curves of Co–Ag deposits prepared potentiostatically at −900 mV and at $Q = -0.15\ C\ cm^{-2}$ and oxidized at $0.03\ mA\ cm^{-2}$ in different oxidation baths: dash line, 0.01 M $AgClO_4$ + 0.1 M $Co(ClO_4)_2$ + 0.1 M thiourea + 0.1 M gluconate + 0.3 M boric acid + 0.1 M $NaClO_4$ solution, pH 3.7; continuous line, 0.1 M $Co(ClO_4)_2$ + 0.1 M gluconate + 0.3 M boric acid + 0.1 M $NaClO_4$ solution, pH 3.7. (b) Galvanostatic *stripping* curves of Ag–Co deposits prepared at: continuous line, −900 mV and $Q = -0.15\ C\ cm^{-2}$ and dashed line, −910 mV and $Q = -0.40\ C\ cm^{-2}$ and oxidized in 0.1 M $Co(ClO_4)_2$ + 0.1 M gluconate + 0.3 M boric acid + 0.1 M $NaClO_4$ solution.

The *stripping* results show that the deposits formed at potentials corresponding to voltammetric peak B contained silver and cobalt. The fact that the *stripping* peaks/plateaux remained at fixed positions independently of the applied potential indicates the heterogeneous nature of the deposit. At the lower applied potentials at which the simultaneous Co–Ag codeposition might occur, a cobalt peak/plateau was detected after a short period of time during which only silver was deposited due to the ease of its deposition in contrast to the difficulty of cobalt reduction at these lower potentials.

Stripping analysis performed for low deposition charges (of the order of 5 mC) provided us with only qualitative information about the composition of the deposits because their total oxidation was not reached. The Q_{ox}/Q_{red} ratio was around 80% for low deposition charges, and this ratio decreased as either the deposition charge increased or the preparation potential decreased. On the other hand, the Q_{ox}/Q_{red} ratio was not exceeded even when decreasing the scan rate at values lower than $1\ mV\ s^{-1}$. The lowest Q_{ox}/Q_{red} values were probably due to the simultaneous hydrogen reaction over the cobalt freshly deposited. For this reason, it was necessary to develop a quantitative method to determine cobalt and silver percentages in the deposits, especially in thick deposits (between 5 and 15 μm). With the aim to determine deposit composition by means of electrochemical methods, a polarographic method to analyse cobalt and a voltammetric method for silver determination were implemented.

3.2. *Analysis method for silver and cobalt determination in Co–Ag coatings*

3.2.1. *Analysis of silver by cyclic voltammetry*

We propose that the cyclic voltammetry will be a straightforward tool to analyse silver content in Co–Ag deposits using the standard addition method. Silver content analysis was conducted in the potential range between 0 and +0.6 V cycling initially to negative values in order to record the reduction peak observed in silver(I) solutions. This peak corresponds to a diffusion controlled process of silver ions towards the electrode [14].

The analysis was performed using glassy carbon as working electrode and 0.2 M sodium perchlorate solution as a supporting electrolyte. Perchlorate was selected because it does not present a complexing effect. As previously observed, peak current does not depend on pH in the interval 1–5 [14], so solution pH was maintained at about 2–3. Standardized silver solutions were used to check out the procedure.

After recording two consecutive cyclic voltammetries, it was observed that the reduction process in the second scan was greatly advanced and the peak current increased, clear evidence that silver was not completely oxidized during the anodic sweep. As a consequence of this incomplete oxidation, the nucleation was easier on the remaining silver over the electrode therefore a higher current was achieved earlier. This happened even when the scan was lengthened to potentials previous to oxygen evolution. In these conditions it was necessary to establish a protocol that ensured the regeneration of the electrode superficial state. Many attempts were made to regenerate the original situation of the electrode. Polishing treatment was ruled out as the variation of the electrode roughness might cause modification in the effective area value and thus make it impossible to relate the current recorded in subsequent experiments. The best way to remove the deposit was found to be by means of potentiostatic oxidation, and different applied potentials and time duration were tested. Total regeneration of the electrode surface was achieved holding the potential at 0.6 V for 60 s after a voltammetric scan. Good reproducibility was obtained after 60 s of stirring and bubbling and 60 s of settling.

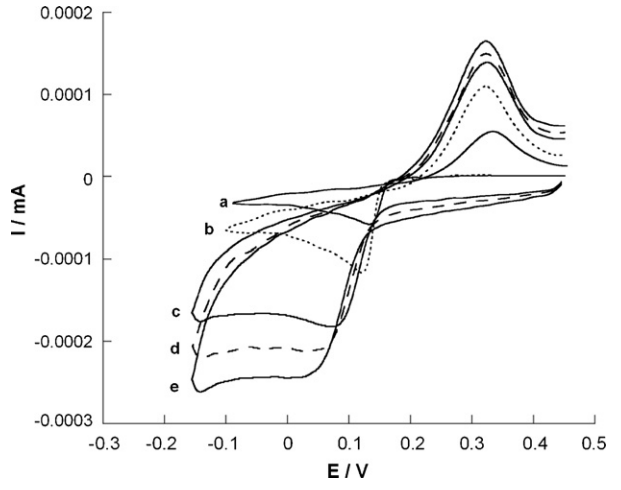

Fig. 5 – Cyclic voltammograms of 0.2 M $NaClO_4$ + 3.6 mg L^{-1} $AgClO_4$, pH 2 solution at different scan rates of: (a) 10 mV s^{-1}, (b) 20 mV s^{-1}, (c) 50 mV s^{-1}, (d) 70 mV s^{-1}, and (e) 90 mV s^{-1}.

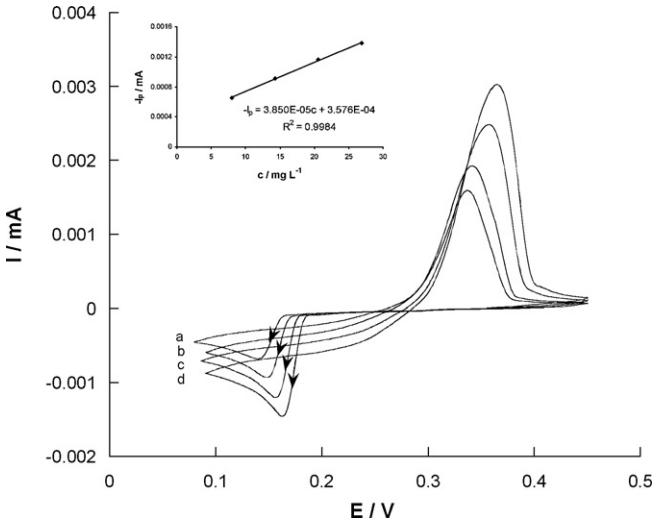

Fig. 6 – Cyclic voltammograms of 0.2 M $NaClO_4$ + x mg L^{-1} $AgClO_4$, pH = 2 solution: curve (a) x = 8; curve (b) x = 14.3; curve (c) x = 20.6 and curve (d) x = 26.9. Scan rate 20 mV s^{-1}. Inset shows the linear dependence of current peak vs. silver(I) concentration.

Once the electrode reproducibility was ensured and before establishing analytical parameters, we set the optimization of conditions at which voltammetric curves (scan rate, temperature) were recorded.

3.2.1.1. *Effect of scan rate.* As was expected, when the scan rate was increased the peak current increased and the peak potential shifted towards more negative potentials. On decreasing silver concentration to low values (of the order of 3 mg L^{-1}) a loss of definition in the peak shape was observed (Fig. 5 curves a–c), a clear mass control process being detected only at scan rates equal to or less than 20 mV s^{-1} (Fig. 5 curves d and e). Upon increasing concentration, well-defined peaks were observed independently of scan rate. In view of these experimental features and taking into account that the lower the scan rates the lower the peak currents that would imply higher measurement error, the scan rate selected was 20 mV s^{-1}.

3.2.1.2. *Effect of temperature.* Taking into account the important temperature influence on the silver reduction peak observed in previous studies [15], a control of temperature was considered necessary when recording the voltammetric response. As stated above, an increase in temperature of a few degrees provoked an increase in peak current, but for low silver(I) concentrations such an increment gave rise to a loss in peak definition and it became difficult to establish unequivocally its maximum. In these conditions a temperature of 25 °C was sufficient to record a clear peak in all concentration ranges.

3.2.1.3. *Validation of the method.* To check whether the selected conditions gave rise to a reliable quantification, the method was validated by applying the standard addition method. Silver(I) solutions of known concentration (standard silver solutions) were added to the unknown concentration solution. The plot of current peak value versus added concentration yielded the concentration of the problem solution. Different concentrations were tested in order to check whether the method was a sensible and reliable one in a wide concentration range.

Fig. 6 shows the dependence of the peak current versus increments in silver(I) concentration. By fitting cathodic peak current against silver(I) concentration, a close fit to linearity can be observed, indicating that the method was concentration sensitive.

In order to characterize the reliability of this method, solutions of known concentration of silver(I) were analysed following the established protocol and by carrying out three additions from a standard solution. Several concentrations in the selected range were tested to assure that the method was valid. Fig. 7 shows how the method developed led to a calculated Ag(I) concentration of 3.11 mg L^{-1}, when the concentration present in the cell was 2.97 mg L^{-1}(after adding 0.2 mL of a standard solution of 374 mg L^{-1} to 25 mL of supporting electrolyte). In the same way, reproducibility of results was evaluated by repeatedly analysing the concentration of fixed solutions. Agreement was achieved between the real values and the experimental ones, the relative standard deviation value (R.S.D.%) being 5% (Fig. 7).

3.2.1.4. *Analytical characterization.* In order to obtain the analytical parameters of this voltammetric method, silver(I) solutions of known concentration were analysed. It was observed that for concentrations up to 2 mg L^{-1} a linear relation between current peak and silver(I) concentration was obtained, 2 mg L^{-1} being the lowest concentration at which a reliable analytical signal can be recorded. This value is the quantification limit, although not the detection limit. Under 2 mg L^{-1}, voltammetric response was observed but not as a clear peak, hence, this result allowed for detection but no for quantification. So it can be concluded that this method

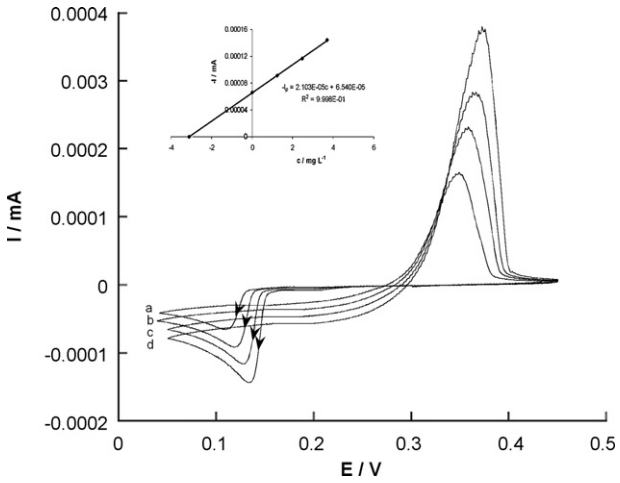

Fig. 7 – Cyclic voltammograms corresponding to (a) test solution; (b)–(d) consecutive standard additions of 1.24 mg L^{-1} $AgClO_4$. The inset shows the plot for the concentration determination by the standard addition method.

can detect concentrations higher than 0.5 mg L^{-1}, this concentration being the detection limit, but not quantitative for concentrations under 2 mg L^{-1}.

3.2.1.5. *Interferences*. It was decided to investigate the possible effect of cobalt(II) presence in the solution on the quantitative determination of silver(I) by this method. After dissolution of the prepared Co–Ag samples, cobalt(II) and silver(I) will coexist in the solution. Thus, silver(I) concentration was also analysed from solutions where both ions of known concentration were present. No differences were observed in spite of the presence of cobalt(II).

The metallic species (nickel and titanium) coming from the seed layer were also present in the solution after dissolving the Co–Ag deposit, but for voltammetric silver analysis these were not considered as possible interferences due to their low concentration and the great difference between their standard potentials with that of silver.

3.2.1.6. *Method description*. From a previous study, the specific procedure for silver determination in Co–Ag electrodeposited films was established. The analysis was carried out in a volume of 25 mL of 0.2 M $NaClO_4$. At first, the solution was deaerated with argon for 20 min, kept under argon atmosphere and thermostatized at 25 ° C. An accurately polished vitreous carbon electrode was used to perform the determination.

Ag(I) analysis includes different steps. Once the cyclic voltammetry of the blank solution was recorded, a known volume of the dissolved sample was added to the cell and the solution was stirred for 2 min. After that, the cyclic voltammetry for the sample was recorded in the selected potential range. A key stage in the analysis method was the regeneration of the electrode surface. For this, before each addition of a selected volume of the standard solution, the substrate must be oxidized potentiostaticaly at 0.6 V for 60 s. To assure good reproducibility the solution must be stirred and bubbled for 60 s and must be settled for another 60 s. Next, a selected volume of the standard solution was added and the cyclic voltammetry recorded. After each cyclic voltammetry the regeneration process was performed. At least three additions must be made. Peak current versus added concentration was plotted. The Ag(I) concentration in the sample was determined by the standard addition method.

3.2.2. *Analysis of cobalt by polarography*

Polarography is a method that determines cobalt with great accuracy. Polarographic experiments were carried out in 1.0 M CH_3COONH_4 and 1.0 M NH_3 solution as a supporting electrolyte. Differential pulse polarography (DPP) was used. A drop time of 0.4 s and a superimposed pulse of −50 mV were selected. Potential was scanned from −1 to −1.35 V. Room temperature and a volume cell of 20 mL were selected. The standard addition method was used to determine the quantity of cobalt.

A preliminary step in cobalt characterization by polarography was the study of the interference effect of ions coming from the seed layer (nickel and titanium). According to the standard potentials of the metals, the closest one to cobalt and the one which could thus interfere was nickel. To evaluate this possibility scans in the range −0.8 V and −1.40 V were recorded. As can be observed in Fig. 8, two different peaks were recorded. The peak at −1.2 V was related to cobalt reduction because of successive additions of standard solution of cobalt(II) increased its height, while the small peak at −0.95 V was related to nickel reduction. These peaks did not overlap in any experimental conditions.

Since the polarography method shows a wide linearity range and a low detection limit, the analytical parameter worth evaluating in the selected bath was reproducibility. In order to characterize reproducibility, repetitive measurements were carried out for a concentration of 1.0 mg L^{-1} cobalt(II) in the bath, ±0.1 mg L^{-1} being the dispersion value.

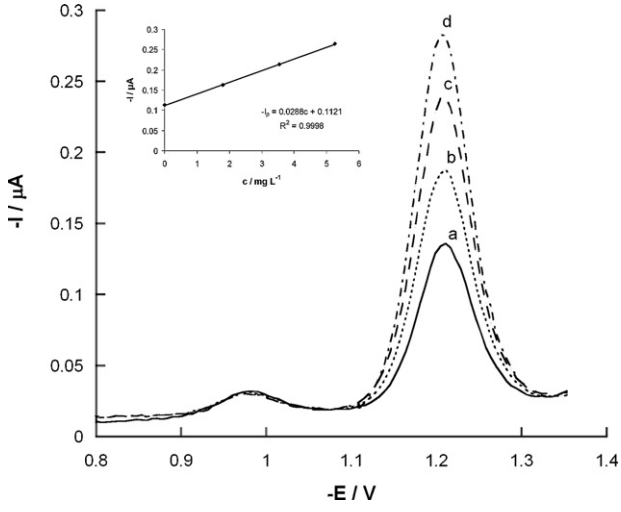

Fig. 8 – DDP polarograms of 1.0 MCH_3COONH_4 and 1.0 M NH_3 solution as supporting electrolyte in which was added: curve (a) 0.5 mL of dissolved Co–Ag deposit prepared potentiostatically at −800 mV over silicon/seed-layer substrata. Curves (b)–(d) additions of 0.3 mL of a standard cobalt solution of 154 mg L^{-1}. Scan rate 10 mV s^{-1}.

Table 1 – Percentage of cobalt in Co–Ag deposits of 13.3 C cm^{-2} prepared potentiostatically under stirred conditions over silicon/seed-layer substrates

E (mV)	wt.% Cobalt
−830	56
−810	46
−800	33
−790	25
−770	11
−750	2

3.3. *Determination of silver and cobalt in electrodeposited coatings*

In order to illustrate the application of both methods, samples proceeding from the dissolution of Co–Ag deposits were analysed. The deposits were prepared potentiostatically under stirring conditions on silicon with Ti/Ni seed layer. Different potentials (between −730 and −850 mV) were applied to assure a different percentage of both metals in the deposits.

The deposits were dissolved in 0.5 mL of nitric acid of 32 wt.%; after that water was added to a total volume of 5 mL. 0.5 mL aliquots of this solution were analysed by both electrochemical methods implemented in order to determine silver and cobalt content.

Following the procedure previously described a good response with standard additions and a good reproducibility in the recorded signals was obtained. After plotting the peak current versus metal concentration a close fit to linearity was obtained for both methods.

Our results confirmed that a decrease in the applied potential was associated to an increase in the cobalt percentage in the deposit, and that the potential range between −750 and −830 mV leads to deposits with percentages in the 2 < Co wt.% < 56 range (Table 1). As our range of interest for cobalt is 10–45% (potentially useful to observe magnetoresistive response), the potential interval to get this cobalt range is 750–810 mV.

4. Conclusions

Electrodeposition was developed by selecting adequate electrodeposition parameters for an electrolytic bath containing silver(I), cobalt(II), thiourea, boric acid and gluconate suitable for Co–Ag coatings. The potential ranges at which either single deposition of silver or codeposition of both metals were determined by cyclic voltammetry. The potential at which the codeposition process started on silicon seed-layer is −750 mV. These data make it possible to select the adequate potential range for deposit preparation.

The *stripping* method makes it possible to detect the initial stages of deposits formation. The deposition bath was unsuitable to perform the *stripping* characterization (due to interference effects of both silver(I) and thiourea). However, in the absence of both species it was possible to characterise low-charge deposits, two main peaks/plateaux then being recorded, corresponding to both cobalt and silver oxidation and thus demonstrating the heterogeneity of the deposit. It was also detected that at the lower applied potentials the simultaneous deposition took place over the first silver deposited and that a high incorporation of cobalt in the deposits was favoured by decreasing the deposition potential value.

Electrochemical methods were tested for quantitative determination of silver and cobalt percentages in Co–Ag electrodeposits. A voltammetric method was proposed for silver quantification, whereas a polarographic one was used for cobalt determination. Analysis of both metals was performed after simultaneous dissolution of the Co–Ag deposit and the corresponding Ti/Ni seed layer.

The voltammetric analysis method for silver determination was implemented over vitreous carbon electrode, proving to be valid over a wide concentration range. If accurate temperature control, low scanning rate and a pH value around 2–3 are maintained, this technique is feasible and easy to use for silver detection due to its high selectivity, excellent sensitivity and simple operation, the quantitative range being wider than that required for our research. This method could therefore be used on those silver alloys in which the voltammetric response of the alloy components are separate enough to record a reliable analytical silver signal in order to avoid interferences.

The polarographic determination of cobalt in the deposits is highly selective (we observed no interference effects due to other ions present in the samples), and high sensitivity is recorded, the variation coefficient being close to that of the voltammetric method.

The usefulness of electrochemical methods to analyse the composition of Co–Ag coatings over silicon/seed-layer substrates is demonstrated. The electrochemical technology analysed is not only useful to prepare thin films materials but also as an analytical tool of the prepared electrodeposits.

Acknowledgements

This paper was supported by contract MAT-2006-12913-C02-01 from the *Comisión Interministerial de Ciencia y Tecnología (CICYT)*. J.M. García-Torres also thanks the Departament d'Innovació, Universitats i Empresa of the Generalitat de Catalunya and the Fons Social Europeu for financial support.

REFERENCES

[1] A.E. Berkowitz, J.R. Mitchell, M.J. Carey, A.P. Young, D. Rao, A. Starr, S. Zhang, F.E. Espada, F.T. Parker, A. Hutten, G. Thomas, J. Appl. Phys. 73 (1993) 5320.
[2] J.Q. Wang, G. Xiao, Phys. Rev. B 49 (1994) 3982.
[3] J.H. Du, Q. Li, L.C. Wang, H. Sang, S.Y. Zhang, Y.W. Du, D. Feng, J. Phys. Condens. Matter. 7 (1995) 9425.
[4] S. Arana, N. Arana, F.J. Gracia, E. Castaño, Sensor Actuator A-Phys. 123–124 (2005) 116.
[5] A.J. Fagan, M. Viret, J.M.D. Coey, J. Phys. Condens. Matter. 7 (1995) 8953.
[6] S.P. Wong, M.F. Chiah, W.Y. Cheung, N. Ke, J.B. Xu, Nuc. Instrum. Meth. B 148 (1999) 813.
[7] S. Valizadeh, G. Holmbom, P. Leisner, Surf. Coat. Technol. 105 (1998) 213.
[8] T. Veres, M. Cai, S. Germain, M. Rouabhi, F. Schiettekatte, S. Roorda, R.W. Cochrane, J. Appl. Phys. 87 (2000) 8513.

[9] S.E. Paje, M.A. Arranz, J.P. Andrés, J.M. Riveiro, J. Phys. Condens. Matter. 15 (2003) 1071.
[10] H. Zaman, A. yamada, H. Fukuda, Y. Ueda, J. Electrochem. Soc. 145 (1998) 565.
[11] S. Kenane, E. Chainet, B. Nguyen, A. Kadri, N. Benbrahim, J. Voiron, Electrochem. Commun. 4 (2002) 167.
[12] S. Kenane, J. Voiron, N. Benbrahim, E. Chainet, F. Robaut, J. Magn. Magn. Mater. 297 (2006) 99.
[13] Alloy Phase Diagram In: Hugh Baker (Eds.), ASM Handbook. Vol 3. ASM International. Ohio 1992.
[14] E. Gómez, J. García-Torres, E. Vallés, J. Electroanal. Chem. 594 (2006) 89.
[15] E. Gómez, J. García-Torres, E. Vallés, Mater. Lett. 61 (2007) 1671.
[16] V.D. Jovic, R.M. Zejnilovic, A.R. Despic, J.S. Stevanovic, J. Appl. Electrochem. 15 (1988) 511.
[17] A.R. Despic, V.D. Jovic, in: P. Horsman, B.E. Conway, R.E. White (Eds.), Modern Aspects of Electrochemistry, Vol. 27, Chap. 2, Plenum Press, New York, 1995.
[18] B. Reents, W. Plieth, V.A. Macagno, G.I. Lacconi, J. Electroanal. Chem. 453 (1998) 121.
[19] A. Bellomo, D. de Marco, A. de Robertis, Talanta 20 (1973) 1225.

Preparation of Co-Ag films by direct and pulse electrochemical methods

Available online at www.sciencedirect.com
ScienceDirect
Journal of Electroanalytical Chemistry 615 (2008) 213–221
Journal of Electroanalytical Chemistry
www.elsevier.com/locate/jelechem

Preparation of Co–Ag films by direct and pulse electrochemical methods

Elvira Gomez *, Jose Garcia-Torres, Elisa Valles

Electrodep., Departament de Química Física and Institut de Nanociència i Nanotecnologia de la Universitat, de Barcelona, Martí i Franquès, 1, 08028 Barcelona, Spain

Received 13 September 2007; received in revised form 4 December 2007; accepted 20 December 2007
Available online 31 December 2007

Abstract

A new electrolytic bath containing sodium perchlorate, thiourea, sodium gluconate, boric acid and silver and cobalt salts, able to favour simultaneous electrodeposition of silver and cobalt, has been developed. A systematic analysis of the effect of cobalt(II) concentration, applied deposition potential, hydrodynamic conditions and electrochemical techniques was made. From this bath, Co–Ag deposits of different composition have been prepared and characterized. Granular deposits were obtained from all the electrochemical deposition procedures tested; more compactness and uniformity were attained when the deposits were obtained by pulse plating method. Electrochemical and compositional characterizations indicated that heterogeneous cobalt–silver deposits were prepared containing some oxi- and/or hydroxylated cobalt species.
© 2008 Elsevier B.V. All rights reserved.

Keywords: Electrodeposition; Cobalt–silver; Film characterization; Pulse plating

1. Introduction

The study of granular materials containing fine magnetic particles embedded in a non-magnetic metallic matrix has produced widespread experimental and theoretical work, due to the potential application of these materials in magnetic sensors and read-head devices [1–6]. In this line, the Co–Ag system present interest because, at equilibrium, cobalt is immiscible with silver, thus giving easily sharp interfaces between the magnetic clusters and the non-magnetic matrices [7]. Preparation of Co–Ag films has been made by a variety of techniques well suited to commercial manufacture, such as molecular beam epitaxy (MBE), sputtering, laser pulsed deposition or mechanical alloying [8–13].

Electrodeposition could be an interesting alternative for Co–Ag films preparation, because it can allow the preparation of deposits of variable composition. Some studies of the Co–Ag system electrodeposition from sulphate and halide baths have been performed, all of them using fixed deposition conditions [14–18]. The aim of the work is to present a systematic study of Co–Ag preparation from a new electrolytic bath in order to favour the simultaneous electrodeposition of cobalt and silver and to modulate the deposits composition. The tested bath was selected on the basis of a previously-developed one containing thiourea as the main complexing agent [19], sodium gluconate and boric acid (*Ag bath*) that was able to deposit Ag at suitable negative potentials [20]. The interest is the preparation of uniform Co–Ag deposits of several microns (<10 μm) thick with adjustable cobalt percentages. The influence of different electrodeposition techniques in the composition and morphology of deposits, with special emphasis on uniformity and cohesion, will be analysed.

2. Experimental

Chemicals used were $AgClO_4$, $Co(ClO_4)_2$, thiourea (CSN_2H_4), sodium gluconate ($C_6H_{11}NaO_7$), H_3BO_3 and $NaClO_4$, all analytical grade. The developed bath contained 0.01 M $AgClO_4$ + 0.1 M thiourea + 0.1 M gluconate +

* Corresponding author. Tel.: +34934021234; fax: +34934021231.
E-mail address: e.gomez@ub.edu (E. Gomez).

0022-0728/$ - see front matter © 2008 Elsevier B.V. All rights reserved.
doi:10.1016/j.jelechem.2007.12.013

0.3 M H_3BO_3 + 0.1 M $NaClO_4$ (Dis A) and variable concentrations of $Co(ClO_4)_2$. Solution pH was maintained at 3.7. According to the deposition ability of these metals it was decided to use solutions of $2 \leqslant [Co(II)]/[Ag(I)] \leqslant 10$ ratios. All solutions were freshly prepared with water first doubly distilled and then treated with a Millipore Milli Q system. Before and during experiments, solutions were deaerated with argon. Deposition was always performed at 25 °C.

Electrochemical experiments were carried out in a conventional three-electrode cell using an Autolab with PGSTAT30 equipment and GPES software. Working electrodes were vitreous carbon (Metrohm) and silicon with Ti/Ni seed layer (Si/Ti(100 nm)/Ni(50 nm)) supplied by IMB-CNM. Vitreous carbon electrode was polished to a mirror finish using alumina of different grades (3.75 and 1.87 μm) and cleaned ultrasonically for 2 min in water. Si/seed layer electrodes were firstly cleaned with acetone followed by ethanol and later with water. The counter electrode was a platinum spiral. The reference electrode was an Ag|AgCl|NaCl 1 mol dm^{-3} mounted in a Luggin capillary containing 0.2 mol dm^{-3} $NaClO_4$ solution. All potentials refer to this electrode.

Voltammetric experiments were carried out at 50 mV s^{-1}, scanning at first to negative potentials. Only one cycle was run in each voltammetric experiment. Anodic linear sweep voltammetry (ALSV) analysis was always performed immediately after deposition, scanning at 5 mV s^{-1} and from a potential at which deposition did not occur. Potentiostatic, galvanostatic and potentiostatic pulse techniques were used for deposits preparation.

Deposit morphology was observed by using a Hitachi S 2300 and Leica Stereoscan S-360 scanning electron microscopes. Roughness (R_a) of the coatings was measured point-by-point using a white-light interferometer from Zygo Corporation as a white-light interferometer Fogale-nanotec zoom surf 3D, giving a mean roughness value after a statistical analysis.

Compositional analyses were performed by means of polarographic (for cobalt analysis) and voltammetric (for silver determination) techniques [21] using a Methrom 757 VA Computrace and the same equipment used to electrochemical study, respectively. Dropping mercury electrode (DME) was used as working electrode in polarographic technique and vitreous carbon in voltammetric one. The analysis of deposits was carried out after dissolving them in 32 wt.% nitric acid. Temperature was kept at 25 °C. For some samples, elemental composition was determined with an X-ray analyser incorporated in the Leica equipment.

X-ray photoelectron spectroscopy (XPS) measurements were performed with a PHI 5600 multitechnique system and Auger spectroscopy measurements were done with a PHI 670 scanning Auger nanoprobe system. The XPS signals were evaluated quantitatively on the basis of standard spectra to yield the qualitative and quantitative composition of the film. Owing to disturbing Auger signals [22] and higher differences in the chemical shift of Co(II) and Co(III) [23], the less intense Co 2p 1/2 was used for evaluation. The binding energies (BE) of the XPS signals of all species have been corrected by assuming C1s signal at 284.6 eV. The binding energies of the standard spectra for quantification are marked in Fig. 8.

Differential scanning calorimetry (DSC) and thermogravimetric analyses (TGA) were performed at a heating rate of 2 °C min^{-1} by using a SDT 2960 Simultaneous DSC-TGA equipment of TA Instruments with Thermal Advantage as software.

3. Results and discussion

3.1. Electrochemical study of Co–Ag electrodeposition process on vitreous carbon electrode

The general trends of Co–Ag electrodeposition in the tested baths were studied on vitreous carbon electrode using voltammetric, potentiostatic and galvanostatic techniques. Fig. 1, curve a, shows the voltammogram from the optimized silver bath (*Ag bath*) under quiescent conditions, in which peak A appeared related to mass control silver deposition [20]. When cobalt(II) is present, the beginning of the silver deposition advanced, free-silver(I) concentration increased since cobalt(II) was slightly complexed with the agents present in the bath [19]. After peak A, a sharp current increase was observed related to the beginning of cobalt deposition (Fig. 1, curve b). On increasing cobalt(II) concentration the onset of the cobalt deposition-related process was advanced (Fig. 1, curve c). A new incipient peak (peak B) was observed over which immediately overlapped hydrogen evolution current, making it evident that in this medium cobalt acts as an electrocatalytic substrate to hydrogen process. When cobalt(II)

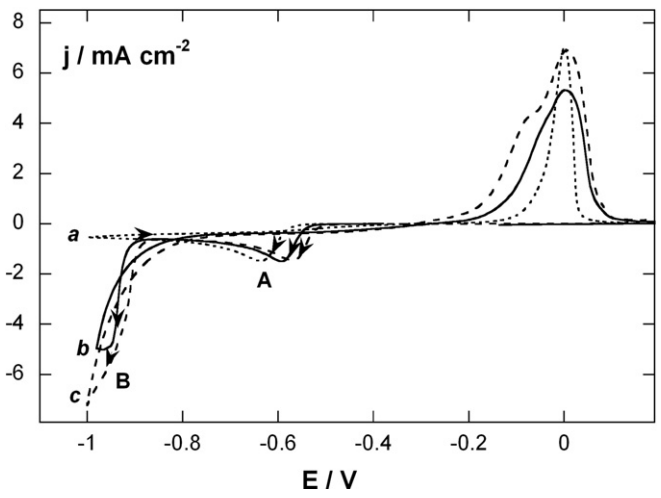

Fig. 1. Cyclic voltammograms of Dis A + x mol dm^{-3} $Co(ClO_4)_2$ solutions at: (a) $x = 0$, (b) $x = 0.05$ and (c) $x = 0.1$. Vitreous carbon electrode. $\omega = 0$ rpm.

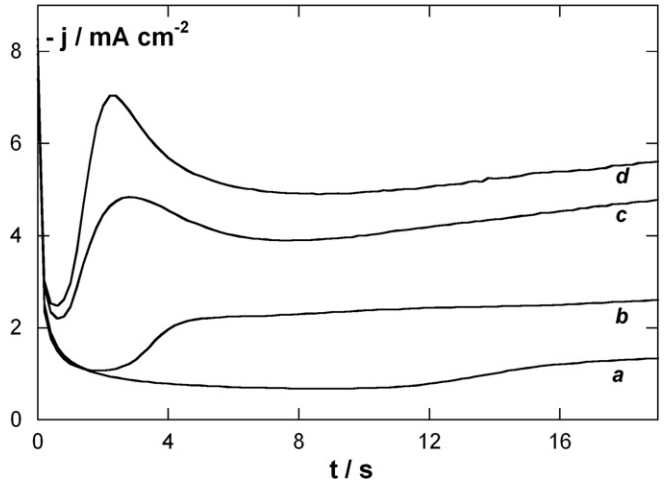

Fig. 2. j–t transients of a Dis A + 0.05 mol dm^{-3} $Co(ClO_4)_2$ solution. Deposition potential at: (a) −850 mV, (b) −900 mV, (c) −1000 mV and (d) −1050 mV. Vitreous carbon electrode. $\omega = 0$ rpm.

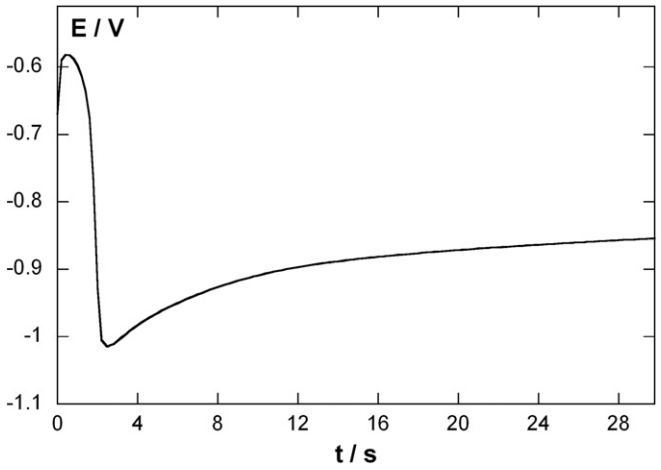

Fig. 3. E–t transients of a Dis A + 0.05 mol dm^{-3} $Co(ClO_4)_2$ solution, $j = -1.9$ mA cm^{-2}. $\omega = 0$ rpm.

was present in the solution a double oxidation peak was observed. At stirred conditions silver process-related current remained stationary in the potential zone previous to the beginning of cobalt deposition, being very sensitive to the stirring rate, unlike cobalt deposition where stirring effect was less evident.

From these voltammetric experiments it was possible to predict the potential range at which cobalt-silver codeposition took place. The upper limit was less negative as Co(II) concentration increased.

Potentiostatic and galvanostatic reduction was performed for each bath. Under quiescent conditions the j–t transients shape showed a sharp peak corresponding to a first silver deposition ($t < 0.2$ s), followed by a progressive current increase, related mainly to the beginning of cobalt deposition (Fig. 2 curves a and b), that developed to a clear second peak upon decreasing the potential. The second peak maximum appeared at lower deposition times as the applied potential was made more negative (Fig. 2, curves c and d). Elonging deposition time a smooth current increase was observed. Under stirred conditions a monotonically current increase was always observed.

As the same manner, when applying currents at which the codeposition could take place under quiescent conditions, E–t transients showed a spike ($t < 0.2$ s) corresponding to silver deposition, a potential evolution to more negative values as a consequence of silver depletion and a second spike ($t < 4$ s) corresponding to the beginning of cobalt deposition (Fig. 3). The spike's appearance was advanced flowing more negative currents. Under stirred conditions it was necessary to apply more negative current densities than in quiescent conditions to attain codeposition (i.e. a current density of −2.5 mA cm^{-2} was the threshold value for [Co(II)]/[Ag(I)] = 5 ratio solution).

Potentiostatic and galvanostatic results indicated that cobalt codeposition begun after an initial silver deposition.

3.2. Preparation and characterization of deposits obtained on silicon/seed layer substrates by direct methods

The information extracted from the basic study was tested on the substrate with technological application. Voltammetric behaviour similar to that previously observed on vitreous carbon was observed, although the processes were eased.

Samples of different thickness were prepared under different stirring rates at fixed electrodeposition conditions determining, after the compositional analysis, that a minimum of 800 rpm was necessary to allow homogeneous composition. The compositional analysis also revealed the absence of boron, being the maximum percentage of sulphur obtained at non favourable conditions lesser than 2 wt.%.

Deposits were prepared both potentiostatically (Fig. 4A) and galvanostatically (Fig. 4B) at 800 rpm from [Co(II)/Ag(I)] = 2–10 solutions showing nodular morphology (Fig. 5A and B). Deposits of −6 C cm^{-2} prepared potentiostatically presented no uniform thickness (Fig. 5A), up to R_a = 8–9 μm; similar behaviour was observed preparing them at more negative potentials. Upon increasing deposition charge (−15 C cm^{-2}), a more uniform deposit thickness was attained (Fig. 6A) but high roughness persisted (R_a = 5 μm). Deposits with more uniform thickness were obtained from the [Co(II)/Ag(I)] = 10 ratio solution. The compositional analysis of the deposits obtained from this solution revealed an important variation of composition as a function of deposition potential. Deposits prepared between −750 and −830 mV ranged in the interval 2 and 56 wt.% cobalt. Less variation in deposits composition with potential was observed for low [Co(II)]/[Ag(I)] ratio solutions.

Deposits prepared galvanostatically at the same deposition charge (−6 C cm^{-2}) than potentiostatic ones were more uniform and smoother (Fig. 5B) with roughness up to R_a = 6 μm. However, these films easily developed cracks

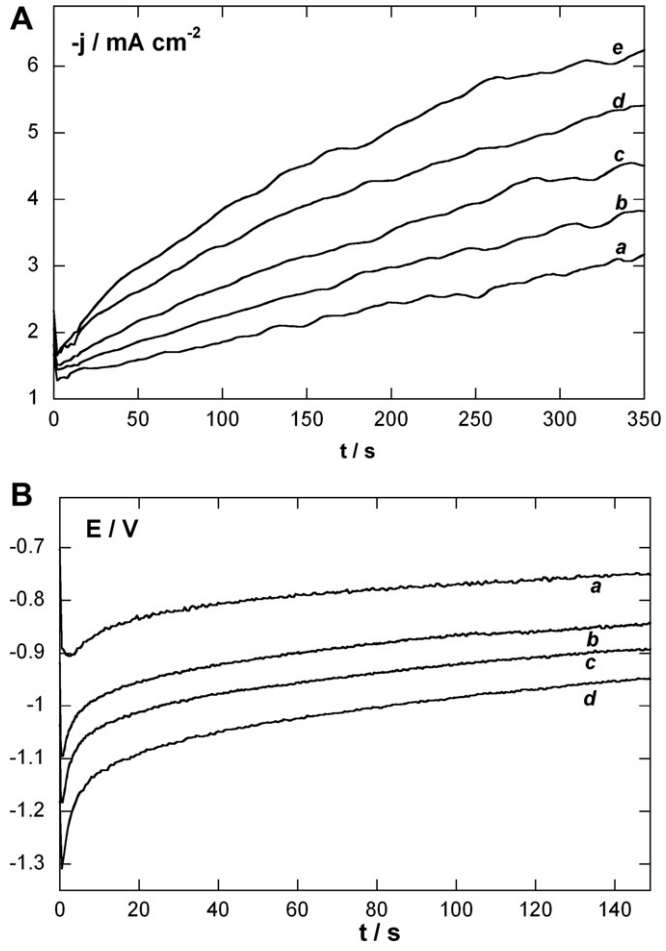

Fig. 4. From a Dis A + 0.05 mol dm^{-3} $Co(ClO_4)_2$ solution. (A) *j–t* transients at: (a) −730 mV, (b) −750 mV, (c) −770 mV, (d) −790 mV and (e) −810 mV. (B) *E–t* transients at: (a) −6.7 mA cm^{-2}, (b) −15 mA cm^{-2}, (c) −20 mA cm^{-2} and (d) −26.7 mA cm^{-2}. Si/seed layer electrode. $\omega =$ 800 rpm.

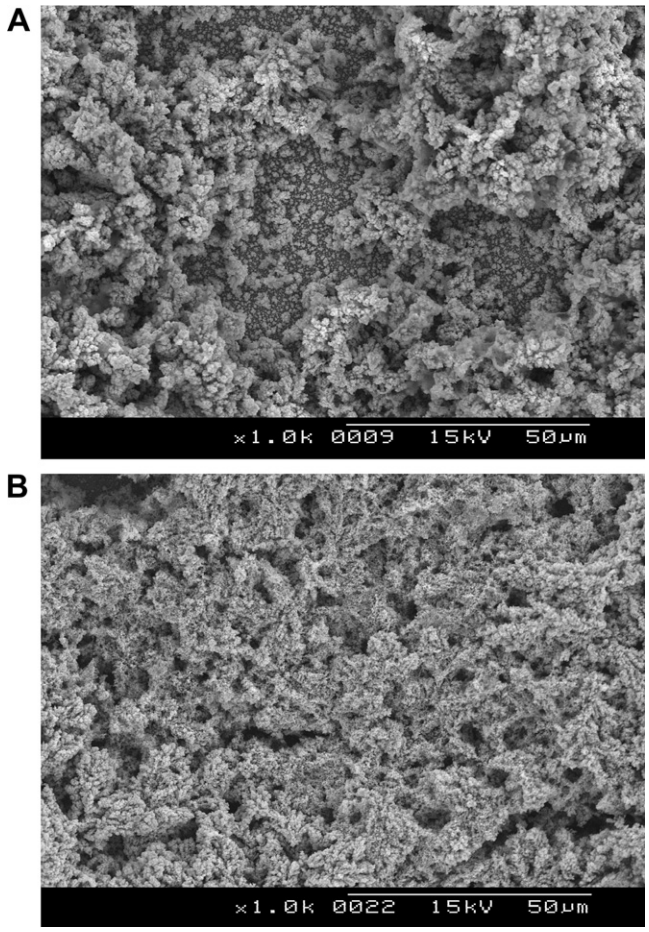

Fig. 5. Scanning electron micrographs of Co–Ag deposits prepared from a Dis A + 0.05 mol dm^{-3} $Co(ClO_4)_2$ solution at: (A) $E_{dep} = -800$ mV and (B) $j = -20$ mA cm^{-2}. $Q = -6$ C cm^{-2}. Si/seed layer electrode. $\omega =$ 800 rpm.

(Fig. 6B) when charge was increased. Moreover, the continuous increase in the potential value during the deposition process affects the composition. These facts advise against the convenience of this technique for deposit's preparation. Deposits obtained at potentials in which simultaneous hydrogen evolution occurred showed low roughness and high cobalt percentage (>60 wt.%) but a great percentage of hydroxylated species were present.

When the X-ray mapping of the deposits was recorded, a non-homogeneous signal distribution was detected along the sample. High signal density was observed in the zones with higher thickness. Nevertheless, the ratio of the signals of both metals was maintained indicating a uniform distribution of cobalt and silver into the deposits (Fig. 7). No accumulation of any of the metals in defined zones was observed.

The deposits were analyzed by means of XPS, both on surface and throughout the deposit after sputtering with argon ions during different times. The recorded XPS spectra of Co 2p and Ag 3d are shown in Fig. 8. As it can be observed, the peak Ag $3d_{5/2}$ was centred at a BE 368.28 eV with a FWHM (full width at half maximum) of 1.26 eV was very symmetric (Fig. 8A). This peak value can be compared to 368.3 eV for metallic silver and its FWHM agrees with the reported for Ag(0) [24]. The energy separation between Ag $3d_{5/2}$–Ag $3d_{3/2}$ was 5.9 eV, value that also agrees with the tabulated '[25]. The Co 2p XPS spectrum (Fig. 8B) is somewhat more complex than that of Ag 3d. The peak Co $2p_{3/2}$ is characterized by two major overlapping peaks with BE 777.96 eV (peak 1) and 780.04 eV (peak 2), in which the peak 1 is consistent with Co(0) or metallic cobalt. Meanwhile, peak 2 could be attributed to various oxides (CoO or Co_3O_4) due to the close BE of their peaks. On the other hand, the Co $2p_{1/2}$ presents the same structure than Co $2p_{3/2}$: two main peaks located at 793.23 eV (peak 3) and 795.62 eV (peak 4), in which the peak 3 agrees with cobalt in metallic form. Moreover, peak 4 fitted well with Co(II) as CoO. Apart from the main peaks, one strong associated satellite (S) to these peaks exists. In order to try to justify the presence of this oxide, the energy separations and satellite structure of the XPS spectrum for Co $2p_{1/2}$–Co $2p_{3/2}$ is crucial. The Co 2p spectra of CoO is characterized by two broad main peaks separated by a spin-orbit splitting of 15.6 eV and two intense satellites located at the high binding-energy

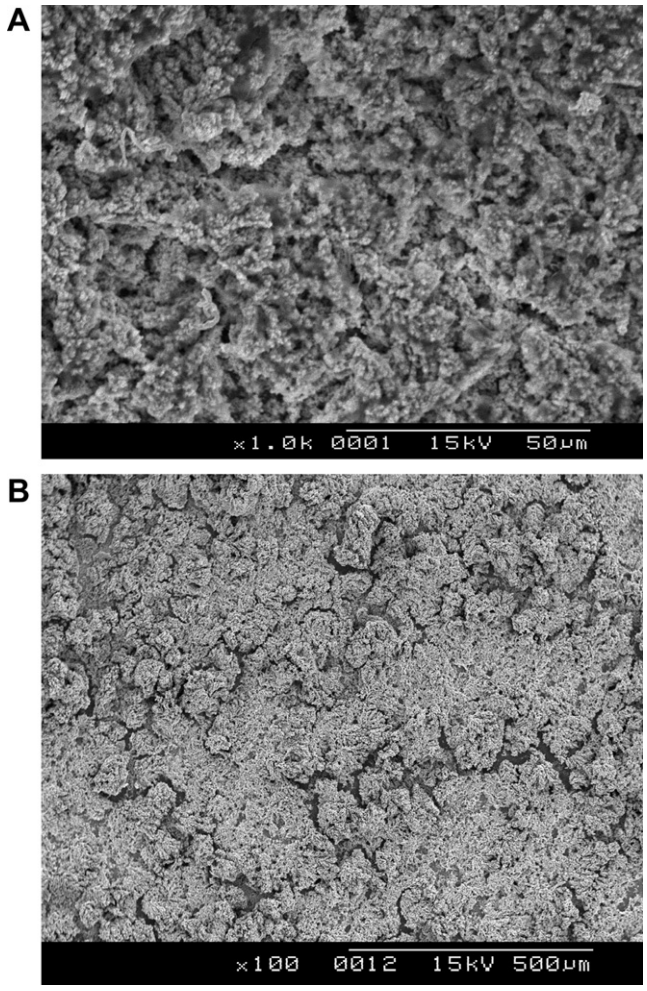

Fig. 6. Scanning electron micrographs of Co–Ag deposits prepared from a Dis A + 0.05 mol dm^{-3} $Co(ClO_4)_2$ solution at: (A) $E_{dep} = -800$ mV and (B) $j = -15$ mA cm^{-2}. $Q = -15$ C cm^{-2}. Si/seed layer electrode. $\omega = 800$ rpm.

side of the main photopeaks. In contrast, Co_3O_4 is characterized by the typical doublet separated by 15.0 eV with low intensity satellites [26,27]. According to the last explanation and to literature, spectra similar to that in Fig. 8B are typical of cobalt in CoO.

The distribution of the chemical elements throughout the film was investigated by XPS depth profiling. The elemental distribution versus sputtering time is presented in Fig. 8C. A constant composition along the film was observed for all the elements. The deposits showed always superficial oxidation (<15 wt.%) but oxide percentage diminished as the sputtering time increased reaching a stationary value. XPS results also discarded boron presence, while the maximum amount of sulphur was 1 wt.%.

Differential Scanning Calorimetry was used under different conditions in order to detect possible transformations in Co–Ag deposits. Experiments were made both in nitrogen and in air atmospheres. The temperature range scanned was 25–500 °C. Under inert conditions no features were detected, whereas when the analysis was made in air atmosphere, two endothermic peaks were recorded during

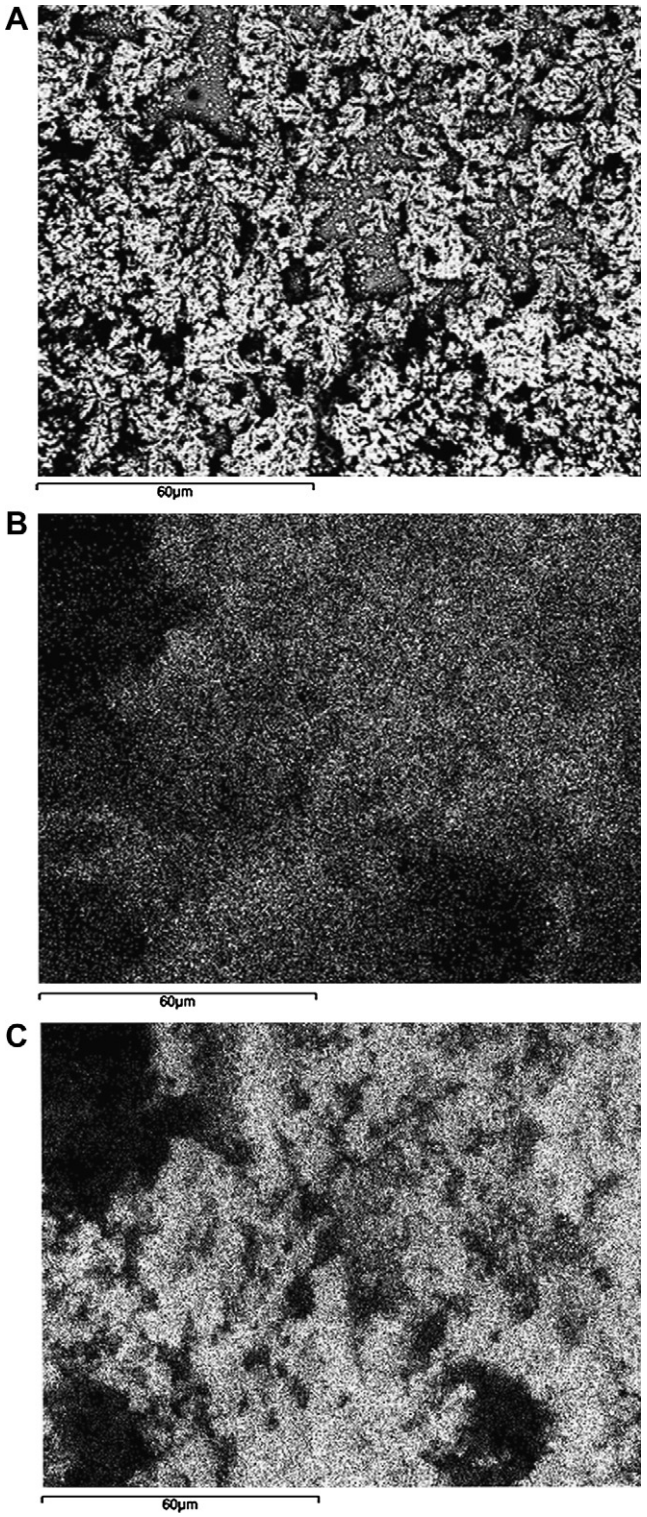

Fig. 7. (A) Deposit image, (B) cobalt X-ray mapping and (C) silver X-ray mapping of Co–Ag deposit prepared potentiostatically from a Dis A + 0.10 mol dm^{-3} $Co(ClO_4)_2$ solution $Q = -6$ C cm^{-2}.

the heating scan at 210 and 360 °C (Fig. 9A). Reversing this scan no features were observed.

In order to assign those peaks, simultaneous TGA experiments were performed in air atmosphere. As it can be observed in Fig. 9A, a weight loss of 3.5 wt.% was

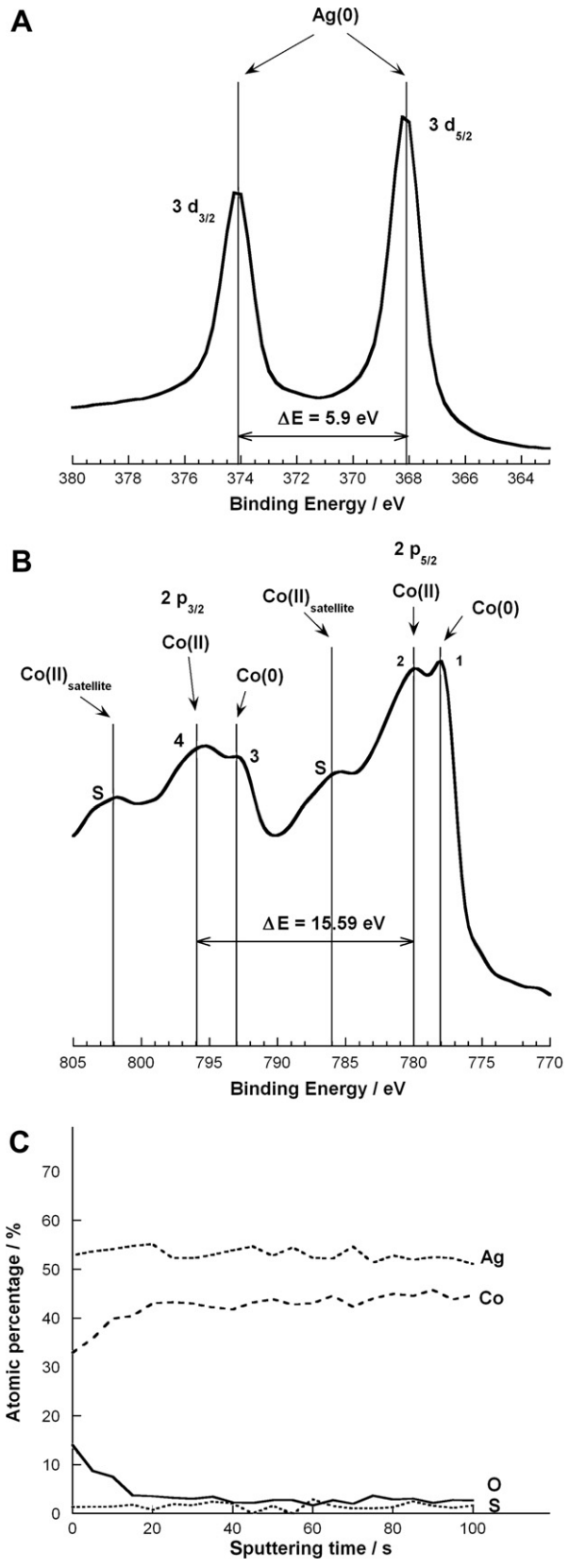

Fig. 8. (A) XPS spectrum of Ag 3d, (B) XPS spectrum of Co 2p and (C) XPS depth profile of Co–Ag deposit prepared from a Dis A + 0.1 mol dm^{-3} $Co(ClO_4)_2$ solution at −810 mV. Si/seed layer electrode. $\omega = 800$ rpm.

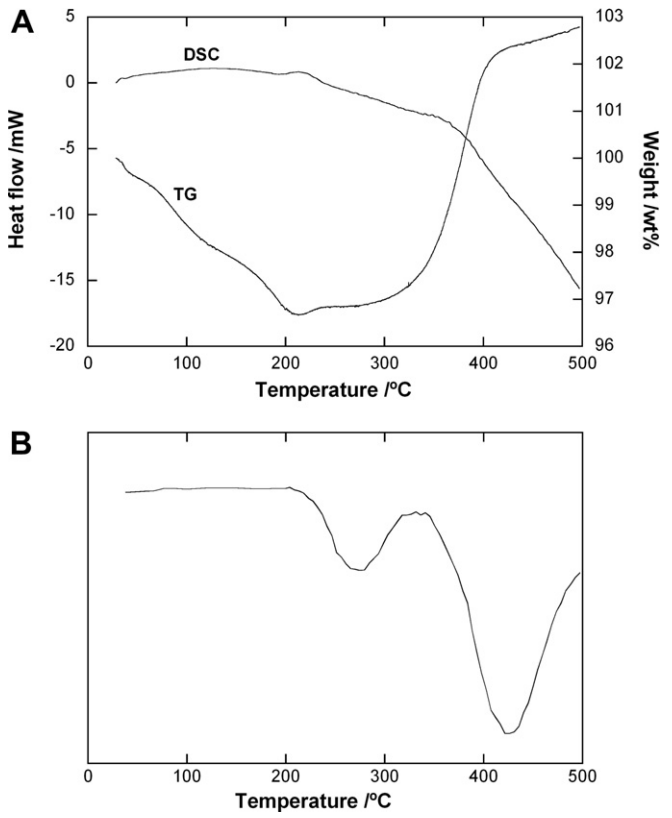

Fig. 9. (A) TG and DSC curves obtained from Co-Ag 35 wt.% and scanning from 30 to 500 °C in air atmosphere at 2° min^{-1}. (B) derivative curve of TG results.

associated with the first transition and a sudden weight increase of 6.5 wt.% was related to the second one. Derivative curves corroborated the two transitions (Fig. 9B). In nitrogen atmosphere both transitions did not occur so it was clear the oxygen presence was responsible. The first DSC peak (related to a decrease in the sample weight) could be attributed to the release, by either oxidation or decomposition of organic species that might remain trapped inside the deposit. The second DSC peak was clearly associated with cobalt oxidation. As cobalt oxide has character of protective layer (according to the Pilling–Bedworth ratio [28]), the presence of a continuous layer over the deposit would make impossible to observe any oxide peak on DSC since oxygen would not be able to traverse it. The appearance of an oxidation peak in DSC revealed the discontinuous nature of the oxide/hydroxide layer formed during film preparation.

3.3. In situ deposits characterization

In situ characterization of the deposits was carried out on vitreous carbon by ALSV (anodic linear sweep voltammetry) [29]. Deposits of charges lesser than −300 mC cm^{-2} prepared potentiostatically were oxidized scanning at 5 mV s^{-1} in $NaClO_4$ 0.2 M solution. ALSV only provided in our case qualitative information because, after the scan, some resid-

ual deposit remained over the substrate. The ratio between the ALSV oxidation charge and the reduction one recorded in the *j–t* deposition transient was lesser than 0.85. During the scan two main peaks centred at −0.45 (peak A_1) and 0.5 V (peak A_2) and a small one at 0.8 V (peak A_3) were recorded (Fig. 10, curve a). In order to assign them, pure silver as well as pure cobalt deposits prepared from solutions containing the corresponding metal and the complexing agents were oxidized. Silver gave a single peak centred at 0.5 V (Fig. 10, curve b), which fitted well with the peak A_2 recorded during Co–Ag oxidation. The oxidation of cobalt lead two peaks: the main one fitted well with the peak A_1centred at −0.45 V and the other appeared at potentials slightly less negative than the peak A_3 recorded at 0.8 V from Co–Ag system (Fig. 10, curve c).

In order to analyze the origin of both cobalt oxidation related peaks (A_1 and A_3), a series of experiments were made: pure cobalt deposits were immersed during a controlled time in $HClO_4$ 10^{-2} M solution before the *stripping* analysis. Linear voltammograms showed that the current decreased, more as the immersion time was raised. However, when cobalt deposits were immersed in NaOH 10^{-3} M solution, the peak A_1 was delayed and no significant modification of its charge was observed. While, the charge under the peak A_3 was enhanced upon increasing immersion time indicating that it probably was related to the presence of oxi- and/or hydroxilated cobalt species. These results are compatible with XPS results: the presence of both silver and cobalt in metallic form (peaks A_2 and A_1, respectively) in the Co–Ag deposits, accompanied by some oxidised species (peak A_3). This result made in evidence that the oxidised species were present in the deposit even at the first stages of the deposition process.

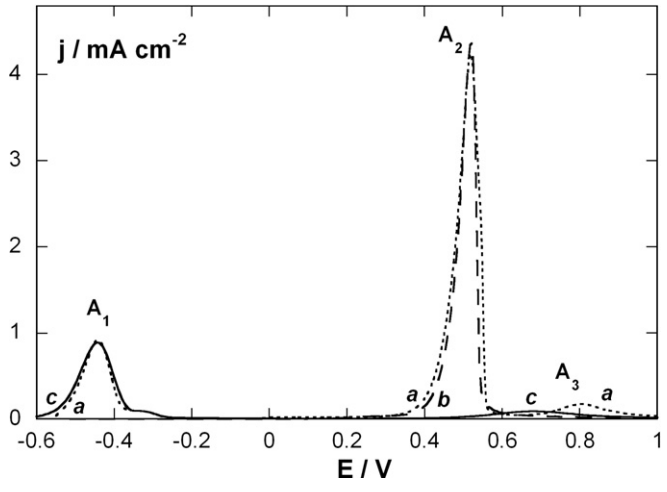

Fig. 10. Potentiodynamic stripping curves at 5 mV s^{-1} of deposits obtained from: *y* mol dm^{-3} $AgClO_4$ + 0.1 mol dm^{-3} $Co(ClO_4)_2$ + 0.1 mol dm^{-3} $NaClO_4$ + 0.1 mol dm^{-3} thiourea + 0.1 mol dm^{-3} sodium gluconate + 0.3 mol dm^{-3} boric acid solutions, pH = 3.7. (a) for $y = 0.01$ at $E = -820$ mV, $Q = -40$ mC cm^{-2}. (b) for $y = 0.01$, $E = -620$ mV, $Q = -11$ mC cm^{-2} and (c) $y = 0$, $E = -950$ mV, $Q = -8$ mC cm^{-2}. Vitreous carbon electrode. $\omega = 100$ rpm.

3.4. Deposits preparation by pulse method

Pulse plating method was tested as a mean to improve the deposit quality since our main interest was focused on attaining uniformity just from the beginning of deposition process and to increase the deposit cohesion.

For different [Co(II)/Ag(I)] ratio solutions the pulse potential method was used varying potential value and pulse length. Moderate stirring (100 rpm) sufficed to maintain constant the contribution of the metallic ions to the electrode. Silver potential was selected at values more negatives than those at which mass control process begins (−570 and −610 mV for [Co(II)/Ag(I)] = 10 and 5, respectively), while cobalt potential values were chosen over those corresponding to the beginning of its deposition process (−870 and −910 mV deposition started for [Co(II)/Ag(I)] = 10 and 5, respectively). In order to minimize hydrogen evolution the applied potential for cobalt deposition was higher than −1000 mV. It was observed that partial currents of each metal increased slightly in every cycle as a consequence of an increase in the effective deposit surface, but their ratio remained constant along successive

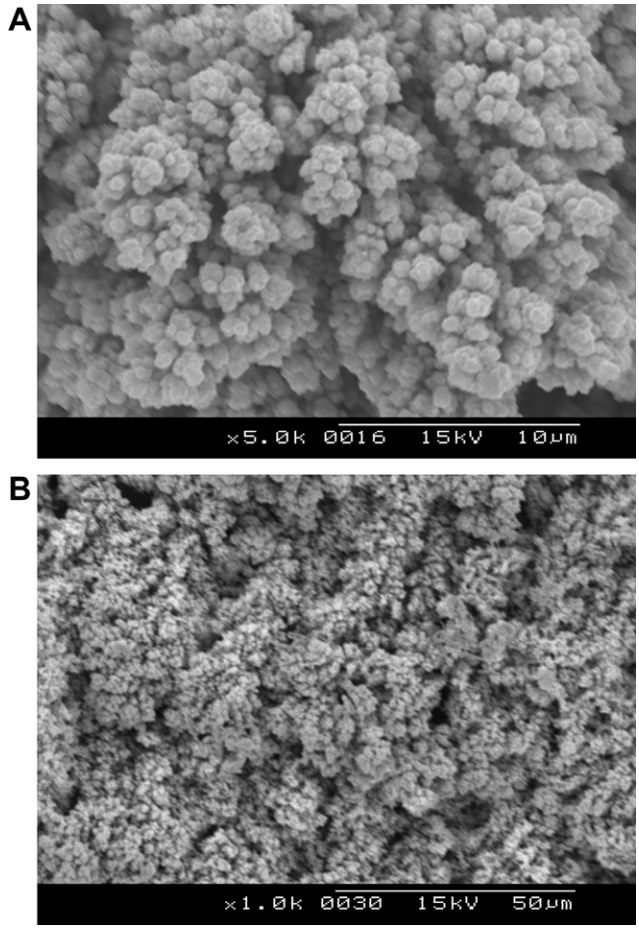

Fig. 11. Scanning electron micrographs of Co–Ag deposits obtained from a Dis A + *x* mol dm^{-3} $Co(ClO_4)_2$ solutions by alternate pulses: (A) for $x = 0.05$ and $E_{Ag} = -650$ mV, $t_{Ag} = 10$ s, $E_{Co} = -950$ mV, $t_{Co} = 0.5$ s and (B) for $x = 0.1$ and $E_{Ag} = -620$ mV, $t_{Ag} = 10$ s, $E_{Co} = -900$ mV, $t_{Co} = 0.5$ s. Si/seed layer electrode. $\omega = 100$ rpm.

cycles, fact that would mean that both Co and Ag percentages in the deposit was maintained.

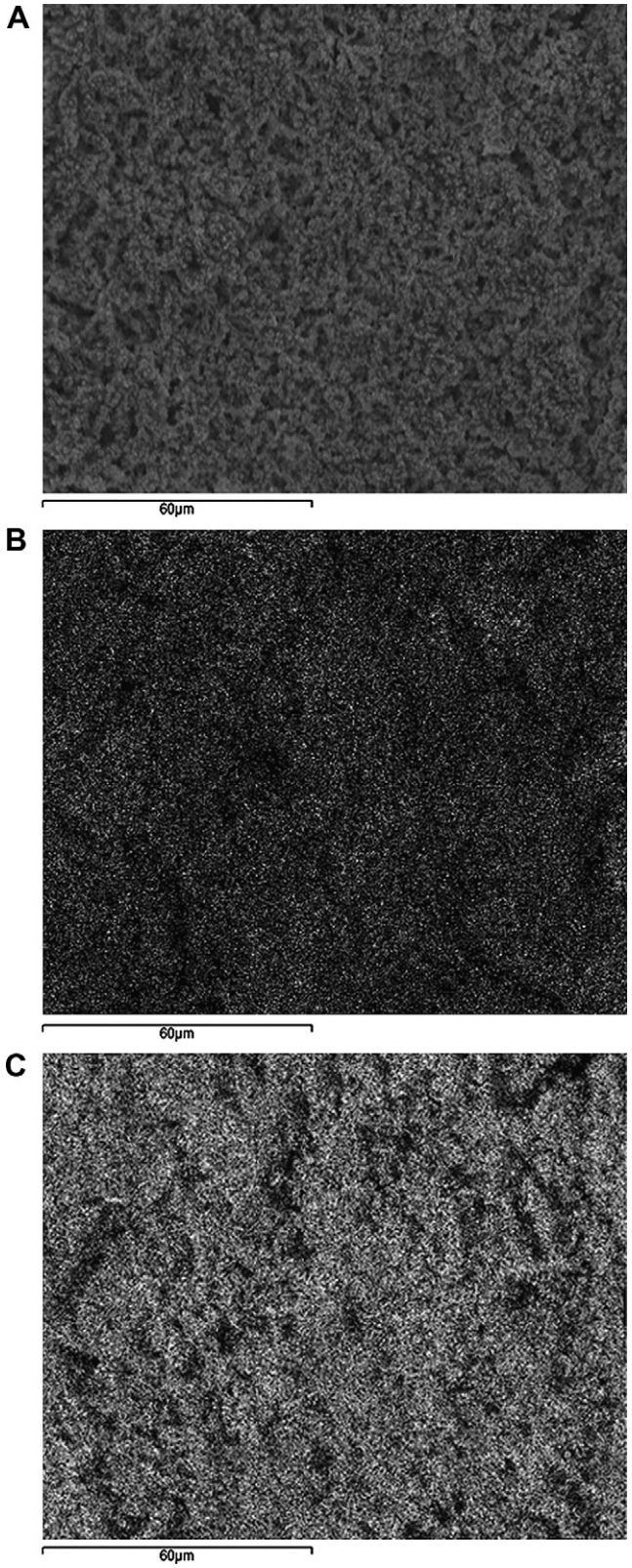

Fig. 12. (A) deposit image, (B) cobalt X-ray mapping and (C) silver X-ray mapping of Co–Ag deposit prepared by pulse plating from a Dis A + 0.10 mol dm^{-3} $Co(ClO_4)_2$ solution. $Q = -4$ C cm^{-2}.

Imaging the deposits prepared by pulse plating also revealed nodular morphology (Fig. 11A). However, an improvement of the deposits was evident even to the naked eye because they were more uniform (Fig. 11B). Roughness values were always lesser than 4 μm. The decrease of the roughness with respect to deposits prepared from direct methods was clear. Pulse plating method favoured less rough Co–Ag deposits formation even from low deposited charges.

Maintaining fixed silver deposition conditions ($E_{Ag} = -650$ and -620 mV for [Co(II)/Ag(I)] = 5 and 10, respectively, pulse length 10 s) but varying pulse length and potential for cobalt deposition, deposits showed similar aspect and morphology. However, smoothness of deposits improved by using the [Co(II)/Ag(I)] = 5 solution. By limiting the cobalt deposition time to 0.5 s, deposits of relatively low cobalt percentage were obtained, percentages lesser than 8 wt.% from [Co(II)/Ag(I)] = 5 and 15 wt.% from [Co(II)/Ag(I)] = 10 solutions were obtained depositing around −1 V, being necessary to increase the cobalt pulse length to increase cobalt content. X-ray mapping of the deposits prepared by pulse plating (Fig. 12) revealed homogenous distribution of both metals into the deposit. As a difference that it was observed from deposits prepared by continuous techniques, uniform signal distribution along the scanned area was observed as a consequence of the higher compactness.

These findings open a window of possibilities, since it seems possible by varying cobalt concentration, applied potential and deposition time to modulate Co and Ag percentage in the deposits. So that, any composition can be obtained balancing these parameters.

4. Conclusions

The incorporation of cobalt(II) in the silver deposition bath previously developed allowed Co–Ag codeposition. Cobalt(II) concentrations were selected higher than silver(I) one in order to approach the deposition potentials of these metals. For each cobalt(II) concentration an optimal potential deposition range was selected in order to optimize deposit quality.

Co–Ag deposits prepared by means direct deposition methods (potentiostatic and galvanostatic) were very rough and show nodular morphology. Uniformity in deposits thickness increases by raising the deposition charge. Deposit composition was very sensitive to electrodeposition conditions, so that an accurate control of the deposition parameters was needed to ensure a given cobalt percentage. The XPS revealed the presence in the deposits of cobalt and silver in metallic form and some oxi- and/or hydroxylated species. Electrochemical characterization in a free-complex bath confirmed the heterogeneity of the deposit showing two clear oxidation peaks related to cobalt and silver oxidation and a small band related to some kind of oxi- and/or hydroxylated cobalt species.

The use of pulse plating method improved deposit cohesion and reduced roughness. The deposits are characterized by a total coverage even at low deposited charges. In all conditions they showed the nodular morphology observed previously in those deposits prepared by direct methods. The modulation of the pulse plating parameters (potential, pulse length) allows controlling codeposition process.

Acknowledgements

This paper was supported by contract MAT-2006-12913-C02-01 from the *Comisión Interministerial de Ciencia y Tecnología (CICYT)*. The authors wish to thank the Serveis Cientificotècnics (Universitat de Barcelona) for the use of their equipment and Núria Cinca and Marc Torrell for their help in the interpretation of DSC and TGA results. J.M. Garcia-Torres also thanks the Departament d'Innovació, Universitats i Empresa of the Generalitat de Catalunya and Fons Social Europeu for financial support.

References

[1] Ch. Wang, Y. Rong, T.Y. Hsu, J. Magn. Magn. Mater. 305 (2) (2006) 310.
[2] Ch. Wang, Y. Rong, T.Y. Hsu, Mater. Sci. 24 (2) (2006) 351.
[3] C.P. Lungu, I. Mustata, A.M. Lungu, O. Brinza, V. Zaroski, V. Kuncser, G. Filoti, L. Ion, J. Optoelectron. Adv. Mater. 7 (5) (2005) 2507.
[4] S. Fukami, N. Tanaka, T. Shimatsu, O. Kitakami, Mater. Trans. 46 (8) (2005) 1802.
[5] V.G. Kravets, L.V. Poperenko, I.V. Yurgelevich, A.M. Pogorily, A.F. Kravets, J. Appl. Phys. 98 (4) (2005) 043705/1.
[6] V.G. Kravets, C. Bozec, J.A.D. Matthew, S.M. Thompson, J. Appl. Phys. 91 (10Pt3) (2002) 8587.
[7] Hugh Baker (Ed.), Alloy Phase Diagram ASM Handbook, vol. 3, ASM Internacional, OH, 1992.
[8] H. Hamakake, M. Wakairo, M. Ishikawa, K. Ishii, IEEE Trans. Magn. 36 (5 Pt1) (2000) 2875.
[9] K. Tonooka, O. Nishimura, Appl. Surf. Sci. 169–170 (2001) 500.
[10] R. Oksuzoglu, E. Mustafa, W. Ayhan, E. Thomas, H. Fuess, H. Hank, J. Phys. Condens. Matter 12 (44) (2000) 9237.
[11] A. Azizi, J. Arabsi, A. Dinia, Appl. Surf. Sci. 246 (1–3) (2005) 132.
[12] A. Dzhurakhalov, A. Rasulov, T. Hoof, M. Hou, Eur. Phys. J. D 31 (1) (2004) 53.
[13] J. Jedryka, M. Wojcik, S. Nadolski, H. Pattyn, J. Verheyden, J. Dekoster, A. Vantomme, J. Appl. Phys. 95 (5) (2004) 2770.
[14] S. Kenane, J. Voiron, N. Benbrahim, E. Chainet, F. Robant, J. Magn. Magn. Mater. 297 (2006) 99.
[15] S. Kenane, E. Chainet, B. Nguyen, A. Kadri, N. Benbrahim, J. Voiron, Electrochem. Commun. 4 (2002) 167.
[16] H. Zaman, S. Ikeda, Y. Ueda, IEEE Trans. Magn. 33 (5) (1997) 3517.
[17] H. Zaman, A. Yamada, H. Fukuda, Y.J. Ueda, Electrochem. Soc. 145 (2) (1998) 565.
[18] T. Watanabe, Nano-Plating, Elsevier, Oxford, 2004.
[19] IUPAC Stability Constants Database (SC Database) version 5.16. Ed. Academic Software Cop. 2001.
[20] E. Gómez, J. García-Torres, E. Vallés, J. Electroanal. Chem. 594 (2006) 89.
[21] E. Gómez, J. García-Torres, E. Vallés, Anal. Chim. Acta 602 (2007) 187.
[22] N.G. Farr, H.J. Griesser, J. Electron Spectrosc. Relat. Phenom. 49 (1989) 293.
[23] A. Foelske, H.H. Strehblow, Surf. Interf. Anal. 29 (2000) 548.
[24] E. Gulari, C. Güldür, S. Srivsnnavit, S. Osuwan, Appl. Catal. A: Gen. 182 (1999) 147.
[25] J. Chastain (Ed.), Handbook of X-ray Photoelectron Spectroscopy, Perkin–Elmer Coorp, MN, 1992.
[26] V.M. Jiménez, J.P. Espinós, A.R. Gonzalez-Elipe, Surf. Interf. Anal. 26 (1998) 62.
[27] T.J. Chuang, C.R. Brundle, D.W. Rice, Surf. Sci. 59 (1976) 413.
[28] N.B. Pilling, R.E. Bedworth, J. Inst. Met. 29 (1923) 529.
[29] V.D. Jovic, A.R. Despic, J.S. Stevanovic, S. Sapaic, Electrochim. Acta 34 (1989) 1093.

Metastable structures of Co and Co-Ag detected in electrodeposited coatings

CRYSTAL GROWTH & DESIGN
2009
VOL. 9, NO. 4
1671–1676

Metastable Structures of Co and Co−Ag Detected in Electrodeposited Coatings

Jose García-Torres,[†] Elvira Gómez,[†] Xavier Alcobe,[‡] and Elisa Vallés*[,†]

Electrodep, Departament Química Física and Institut de Nanociència i Nanotecnologia (IN²UB), Universitat de Barcelona, Martí i Franquès, 1, 08028 Barcelona (Spain), and Serveis Cientificotècnics, Universitat de Barcelona, Lluis Solé i Sabaris, 1-3, 08028 Barcelona, Spain

Received September 20, 2007; Revised Manuscript Received January 23, 2009

ABSTRACT: Silver and cobalt were simultaneously electrodeposited from a perchlorate electrolytic bath containing complexing agents and additives. Rough black Co−Ag deposits were obtained with variable composition determined by the deposition potential. The characterization of these deposits, by both X-ray diffraction and transmission electron microscopy analysis, revealed that electrodeposition in the selected bath induced metastable structures in both Co−Ag and pure-cobalt coatings. In cobalt−silver deposits, a metastable hexagonal close-packed phase (hP2) with cell parameters of $a = 2.887$ (2) Å, $c = 4.745$ (6) Å, and $c/a = 1.644$ was detected. The Co−Ag coatings exhibited ferromagnetic behavior. In cobalt deposits, a primitive cubic structure (cP20), with a cell parameter of $a = 6.093$ (1) Å, was detected.

Introduction

Heterogeneous structures of ferromagnetic and nonmagnetic metals, such as multilayers and granular films, have attracted a great deal of attention because of their technological implications in spin-valve systems, magnetic sensors, or read-head devices, among other applications. These systems are characterized by showing magnetoresistance (MR). Magnetoresistance is a change of electrical resistance when an external magnetic field is applied. For these systems to be magnetoresistive, there must be sharp interfaces between the ferromagnetic and the nonmagnetic metal.

In this regard, a Co−Ag system is potentially useful in the preparation of magnetoresistive films since complete solid solubility is precluded. This is because this system does not meet the Hume−Rothery criteria.[1] The Co−Ag equilibrium phase diagram shows that Co and Ag are almost insoluble in each other in the solid and in the liquid state and that they form no intermetallic compounds.[2] In equilibrium, Co and Ag are immiscible due to the difference in both the surface free energy and the large atomic size difference. As a result the heat of mixing is strongly positive ($\Delta H_{mix} = +28$ KJ/g atom)[3] with no tendency toward phase formation or alloying.

Different methods have been applied to prepare magnetoresistive Co−Ag films, some of which are widely used such as physical methods,[3−8] which include mechanical alloying, molecular beam epitaxy (MBE), and sputtering. Electrochemical methods[9−11] have been used less extensively.

In our laboratory, a complex bath was developed to electrodeposit cobalt and silver simultaneously.[12] A range of electrodeposition conditions were tested to prepare Co−Ag films with a wide cobalt percentage interval. The aim of the present study was to analyze the morphology, the structure, and the magnetic response of the deposits obtained, using this experimental electrolytic bath. The crystalline structure of the films prepared using electrodeposition was analyzed to assess the immiscibility of the two metals in the electrodeposited films. Partial miscibility during the preparation process is observed as has been detected for a similar Co−Cu immiscible system[13−15] that requires annealing treatment after the Co−Cu preparation process.

Although total immiscibility for the Co−Ag system has been detected during its preparation using ion-beam cosputtering[6] or mechanical alloying,[5] Fagan et al.[5] detected some regions of a metastable solid solution with a very low cobalt content around the Co grains.

The present study deals with the characterization of the Co−Ag films obtained by electrodeposition from a complex bath from a point of view of the structure, morphology, and magnetic properties. As reference, pure-cobalt deposits obtained in similar electrodeposition conditions were also analyzed.

Experimental Section

The electrodeposition of cobalt−silver coatings was performed using a freshly prepared 0.01 M $AgClO_4$ + 0.1 M $Co(ClO_4)_2$ + 0.1 M thiourea + 0.1 M sodium gluconate + 0.3 M H_3BO_3 + 0.1 M $NaClO_4$, pH = 3.7 solution (Co−Ag solution). Pure-cobalt reference deposits were prepared from a similar solution but in the absence of silver perchlorate (Co solution). All chemicals used were of analytical grade. Water was double-distilled and treated with a Millipore Milli Q system. The solutions were deaerated with argon and maintained under argon atmosphere during the electrochemical experiments. The temperature was maintained at 25 °C.

The electrodeposition was performed in a conventional three-electrode cell using a microcomputer-controlled potentiostat/galvanostat Autolab with PGSTAT30 equipment and GPES software. The cobalt−silver coatings were deposited on Si/Ti(100 nm)/Ni(50 nm) substrates supplied by IMB-CNM. They were cleaned with acetone followed by ethanol and later with water. The counter-electrode was a platinum spiral. The reference electrode was Ag|AgCl|NaCl 1 M mounted in a Luggin capillary containing 0.2 M $NaClO_4$ solution. Deposits were prepared potentiostatically in the potential range from −770 mV to −850 mV under stirring conditions ($\omega = 800$ rpm) using a magnetic stirrer.

Analyses of deposits were carried out after dissolving them in 32 wt % nitric acid. The cobalt content was analyzed with DP polarography using a Metrohm 757 VA Computrace. The silver content was determined on vitreous carbon using the voltammetric method.[12]

The phase analysis of the deposits was studied by X-ray powder diffractometry (XRD), using a Siemens D-500 diffractometer in

* To whom correspondence should be addressed. E-mail: e.valles@ub.edu. Phone: 34 934039238. Fax: 34 934021231. Web: www.ub.es/electrodep.
[†] Electrodep, Departament Química Física and Institut de Nanociència i Nanotecnologia (IN²UB).
[‡] Serveis Cientificotècnics.

10.1021/cg801167h CCC: $40.75 © 2009 American Chemical Society
Published on Web 02/27/2009

conventional Bragg−Brentano configuration. The Cu Kα radiation (λ = 1.5418 Å) was selected using a diffracted beam curved graphite monochromator. The X-ray powder diffraction diagrams were measured in the 5−105° 2θ range with a step range of 0.05° and a measuring time of 8 s per step. The structure was studied by using high resolution transmission electron microscopy (HRTEM) combined with fast Fourier transform using a JEOL 2100.

The morphology of deposits was observed using a Hitachi S 2300 and a Leica Stereoscan S-360 scanning electron microscope. For some of the samples, the elemental composition was determined using an X-ray analyzer incorporated into the Leica equipment.

A SQUID magnetometer was used to perform the magnetic measurements at room temperature.

Results and Discussion

Preparation of Cobalt−Silver and Cobalt Deposits. Different deposition potentials in the range from −770 to −850 mV were used to perform the Co−Ag electrodeposition from the Co−Ag solution. The potentials were selected from a previous voltammetric study.[12] This study revealed that simultaneous cobalt and silver deposition was possible after an initial silver deposition. Cobalt−silver deposits with cobalt percentages between 11 and 65 wt % were obtained in the selected potential range. When maintaining the stirring rate of the solution at 800 rpm, no significant variations in the composition through the thickness of the deposits were observed.

Samples of different thicknesses (ranging between 3 and 34 μm) were prepared in order to analyze any possible variation in the morphology or structure of the deposits. The thickness of the deposits was calculated from both the deposition charge and the composition of deposits, taking the efficiency of the process into account in each case. Pure-cobalt samples obtained from the same electrolytic bath (pH = 3.7) but without silver perchlorate (Co solution) were prepared as a reference for cobalt−silver deposits. Potentials corresponding to the onset of the deposition process were chosen to prepare cobalt deposits that would attain a similar deposition rate for the Co−Ag deposition process.

Characterization of Cobalt Deposits. The pure-cobalt reference deposits obtained from the Co solution bath were metallic gray with nodular morphology at low deposition charges (−13 C cm^{-2}, 3.5 μm) (Figure 1A), but they quickly turned black and developed a coral-like morphology when the deposition charge was increased (−67 C cm^{-2}, 17 μm) (Figure 1B). This morphology differs from those obtained from less complex deposition baths, which usually have a compact acicular morphology.[16]

The structure of the Co deposit was identified using X-ray diffraction. Diffractograms revealed, in addition to peaks assigned to the substrate, a collection of peaks assigned to the coating. However, these peaks do not represent either the hexagonal close packed (hcp) structure or the face centered cubic (fcc) structure of cobalt. Furthermore, they do not fit the structure for either cobalt oxides or hydroxides. After the indexation of the diffraction peaks they were all assigned to a primitive cubic phase (ε-Co) with a cell parameter of a = 6.093 (1) Å (Figure 2). The resulting cell volume (226.2 Å^3) indicates that the number of Co atoms in the unit cell should be 20. The Pearson category of this structure is therefore cP20, which gives a β-manganese structural type (PDF #001-7327). The cobalt structure detected is slightly less compact (by approximately 3%) than the usual hexagonal and cubic close packed structures of cobalt (hP2 and cF4, respectively, in Pearson nomenclature). This unusual cobalt structure has been previously detected in nanoparticles prepared by wet chemical synthetic routes[17,18] as well as in cobalt nanocrystals embedded in an amorphous carbon matrix obtained by electron-beam evaporation at high vacuum.[19] In the present study, the ε-Co phase for cobalt coatings was prepared by electrodeposition, giving a similar lattice parameter (a) to those reported in the literature.

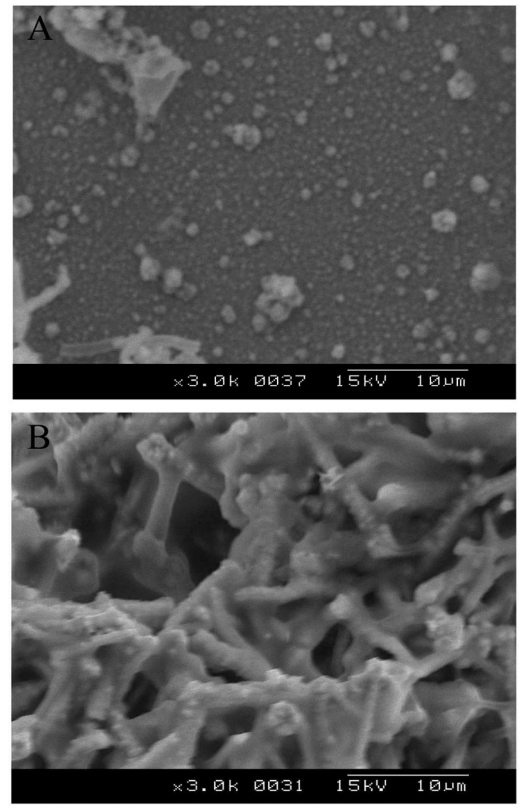

Figure 1. Scanning electron micrographs of Co deposits prepared at −1000 mV from the Co solution. (A) Q = −13 C cm^{-2}, (B) Q = −67 C cm^{-2}, ω = 800 rpm.

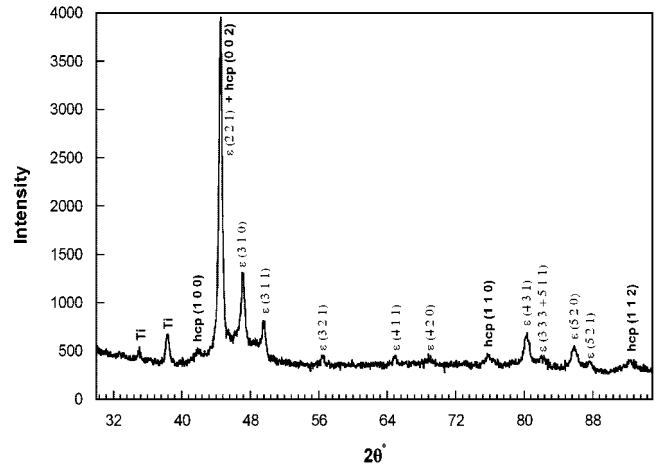

Figure 2. XRD pattern of the Co deposit corresponding to Figure 1A.

Some small peaks corresponding to the conventional hcp (hP2) cobalt structure were discovered next to some Ti peaks and the peaks that correspond to the cP20 cobalt structure. Moreover, the high background, especially in the 40−50° 2θ zone, could indicate the presence of a certain amount of amorphous cobalt.

The different cobalt structures can then be obtained using electrodeposition. Although the hcp structure (hP2) is the normal

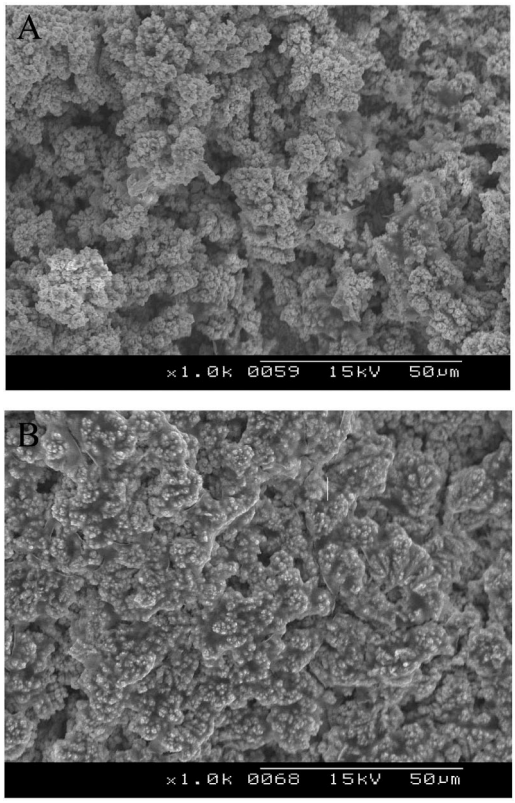

Figure 3. Scanning electron micrographs of Co−Ag deposits prepared at −800 mV from the Co−Ag solution. (A) $Q = -13$ C cm^{-2}, 35 wt % Co, (B) $Q = -67$ C cm^{-2}, 35 wt % Co. $\omega = 800$ rpm.

cobalt structure obtained at room temperature, electrodeposition can induce the fcc phase of cobalt (cF4) if a high electrodeposition rate is attained from some electrolytic baths.[16] An electrolytic bath containing perchlorate, thiourea, gluconate, and boric acid induces the primitive cubic phase (cP20), which has never been detected with electrodeposition.

The cP20 structure disappeared after the samples were annealed in a vacuum oven at 500 °C for 1 h, revealing the metastable nature of the as-deposited structure. The disappearance of the primitive cubic phase led to the stable hcp structure of cobalt. Also small peaks corresponding to cobalt oxides were detected because cobalt is extremely reactive toward oxidation and especially at high temperature.

Characterization of Cobalt-Silver Deposits. The cobalt−silver deposits prepared under the selected conditions were black and rough (Figure 3). The increase in the deposition time led to more compact deposits. Insignificant differences in morphology were observed as a function of the deposition potential.

XRD was used to characterize the Co−Ag electrodeposited coatings. The X-ray diffractograms of cobalt−silver deposits of −13 C cm^{-2} (7 μm) showed, next to some peaks attributable to the seed-layer, the peaks corresponding to the deposit (Figure 4, curve a). The indexation of these coating peaks revealed the presence of two phases: the fcc phase of silver and a hexagonal phase. The indexation of the hexagonal phase gave cell parameters of $a = 2.887$ (2) Å, $c = 4.745$ (6) Å, and $c/a = 1.644$. Neither the cobalt or cobalt oxide phases nor the unusual hcp silver structure (PDF #71-5025) were detected. The Pearson symbol for the indexed phase was hP2 (Mg structural type). Some silver based alloys such as $GaAg_3$ (PDF #28-431) or $CeAg_3$ (PDF #28-269) were also obtained in the hP2 phase.

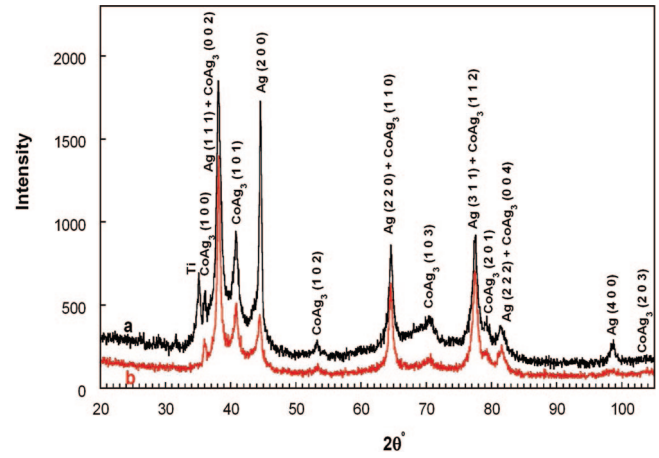

Figure 4. XRD patterns of the Co−Ag deposits from Figure 3, (a) $Q = -13$ C cm^{-2}, (b) $Q = -67$ C cm^{-2}.

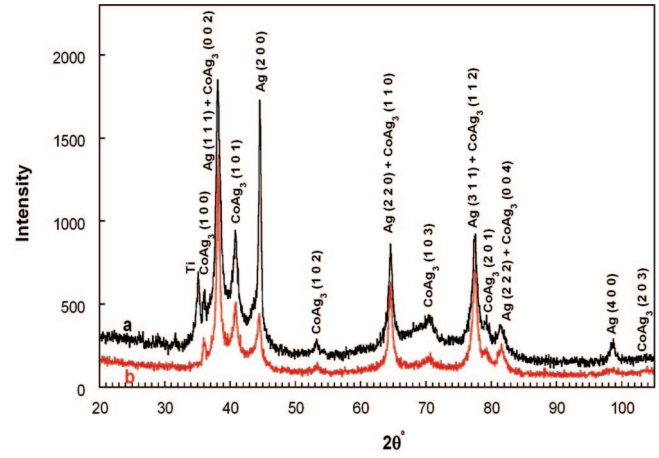

Figure 5. XRD patterns of the Co−Ag deposits of $Q = -67$ C cm^{-2} obtained from the Co−Ag solution at different potentials, (a) −770 mV, 11 wt % Co, (b) −830 mV, 56 wt % Co.

Therefore, the phase detected in this study may correspond to the $CoAg_3$ electron compound.

By increasing the deposition charge (−67 C cm^{-2}) (34 μm) no modifications were observed in the X-ray diffractograms (Figure 4, curve b) except that seed-layer peaks were not observed. On the other hand, both silver fcc and $CoAg_3$ hcp peaks remained unaltered. The same lattice parameters as those obtained for thinner deposits were detected. For as-deposited cobalt−silver deposits, this hexagonal hP2 phase was detected independently of the deposit thickness.

Similar diffractograms were obtained for the Co−Ag deposits prepared in the selected potential range (Figure 5), although a drastic decrease in some of the peaks ((2 0 0) and (4 0 0)) corresponding to the pure fcc silver phase was observed when deposition potential was decreased (Figure 5, red line). Fcc Ag and the hexagonal phase were detected throughout the experiments, although the height of the silver diffraction peaks varied with the composition of deposits depending on the deposition potential applied. The percentage of silver decreased with the decrease of the deposition potential. One important point to make here is that cobalt has not been detected in any of the experiments performed until now.

The formation of the $CoAg_3$ electrodeposited phase may be a result of the valence electron effect. For a close packed hexagonal structure, the maximum number of electron states

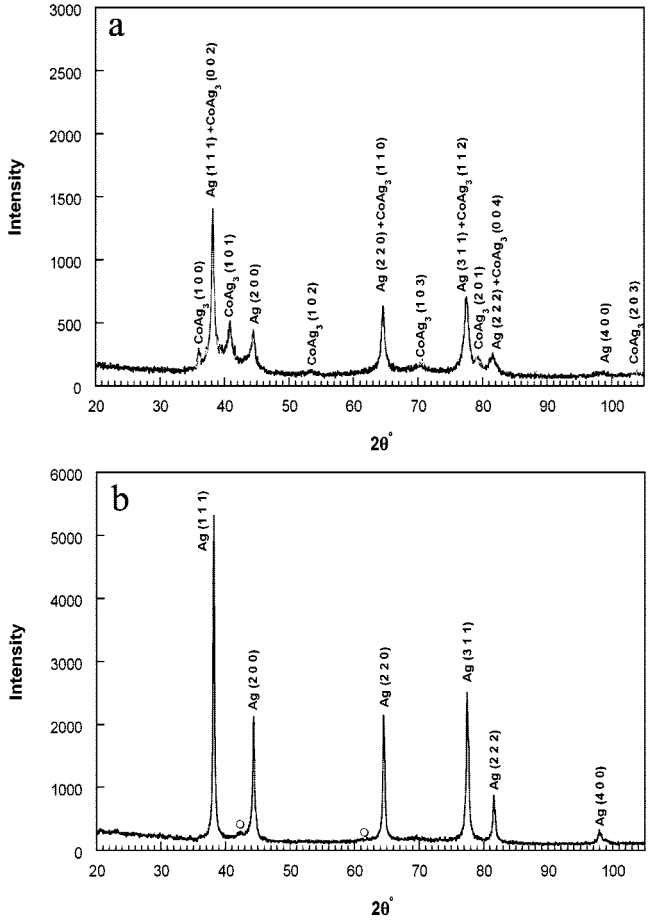

Figure 6. XRD patterns of the Co−Ag deposit of $Q = -13$ C cm^{-2} and 33 wt % Co obtained from the Co−Ag solution, (a) as-deposited, (b) after the annealing at 500 °C during 1 h.

per atom, n, filling up in the Jones' zone, can be calculated from the following equation[20]

$$n = 2 - \frac{3}{4}\left(\frac{a}{c}\right)^2\left[1 - \frac{1}{4}\left(\frac{a}{c}\right)^2\right]$$

where a and c are the lattice parameters of the hcp structure. The n value of the $CoAg_3$ hcp phase was calculated as 1.748, which was relatively close to the value of 7/4 = 1.75; therefore, the $CoAg_3$ hcp phase could be considered as a well-defined Hume−Rothery 7/4 electron compound.

Although the cobalt−silver system is totally immiscible in both metals,[2] it was possible to prepare a wide range of supersaturated solid solutions by sputter deposition.[21] In the present study, using the electrodeposition technique it was possible to form an unusual $CoAg_3$ hcp phase (hP2) in the Co−Ag system (immiscible under equilibrium conditions) and in a wide range of compositions. This structure is similar to those found in silver base alloys, such as $GaAg_3$, $CeAg_3$, and $NiAg_3$ phases.[20,22,23] Furthermore, ab initio calculations confirmed that the presence of the corresponding metastable state in the Co−Ag system and the stability of the $CoAg_3$ hcp phase may have originated from its electronic structure.[24,25] $CoAg_3$ has been previously detected in multilayers obtained using electron beam evaporation and after irradiation of the sample with a specific fluence of ions.[26]

The influence of temperature over the Co−Ag deposits was also studied. The X-ray diffractograms of samples annealed at 275 °C still showed the presence of the hexagonal phase.

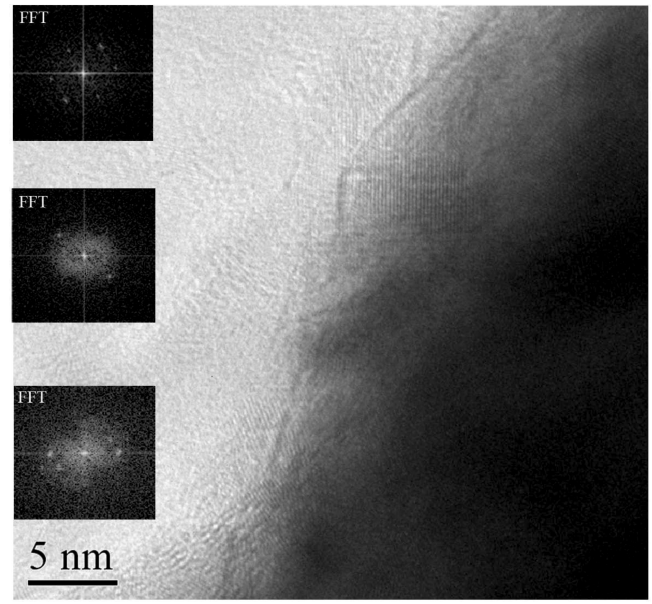

Figure 7. HRTEM micrograph of the as-deposited Co−Ag deposit of $Q = -13$ C cm^{-2} and 33 wt % Co obtained from the Co−Ag solution. The insets represent the FFT patterns that are the result of averaging the whole image.

However, when the annealing of the samples was performed at 500 °C, several differences were observed in the diffractograms with respect to those of the as-deposited samples (Figure 6). The peaks corresponding to the $CoAg_3$ phase disappeared. Both height and area of silver peaks increased. It is known that the annealing of the samples usually induces an increase in the crystallinity of the material, but simultaneously, the amount of silver detected increased revealing the segregation of silver from the new electrodeposited hexagonal phase. Then, the hP2 hexagonal phase detected in the as-deposited samples is a metastable phase containing probably silver and cobalt. Moreover, only small peaks corresponding to CoO were detected (○) revealing some oxidation of cobalt, but no other cobalt peaks were detected. The absence of cobalt peaks in the pattern might be determined for two reasons. On one hand, with the amorphous nature of cobalt because it has been demonstrated that by removing silver atoms from a metastable crystalline Ag-X solid solution (X = Ru, Rh, Os,...) the resulting X structure was essentially a pure amorphous structure.[27] On the other hand, Watanabe et al.[28] studied the Co−Ag system and no evidence of cobalt by XRD was observed in the composition range 0−60 at. % Co, although cobalt was crystalline with hcp structure. At this point, in order to elucidate the amorphous or crystalline nature of cobalt in the deposits after the heat treatment, XRD of annealed CoAg deposits with a high cobalt content (>60 wt % Co) was performed. Small cobalt peaks were detected, corresponding to the hcp structure. So it is worth noting here that high cobalt content in the films was needed to be detected by XRD as Watanabe et al. reported. On the other hand, and in order to corroborate the results obtained by XRD, TEM analyses were performed, as this last technique may provide additional information about the crystal structure.

Transmission Electron Microscopy. Figure 7 shows one of several HRTEM micrographs taken for the as-deposited Co−Ag films. In this micrograph, a lattice image with different sets of fringe patterns can be observed. The insets in Figure 7 represent the fast Fourier transform (FFT) patterns taken in different regions of the sample. The FFT patterns are positioned in regions

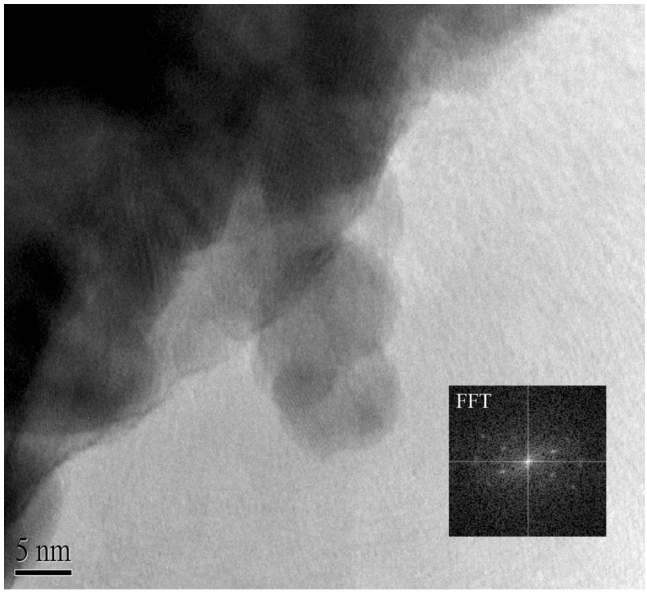

Figure 8. HRTEM micrograph of Co−Ag deposit shown in Figure 7 after the annealing at 500 °C during 1 h. The inset represents the FFT pattern that is the result of averaging the whole image.

exhibiting significant contrast differences. Each of the diffraction spots was indexed by using the previously reported lattice parameter data, from the corresponding powder diffraction files (PDF#).

The FFT images of Figure 7 allowed us to identify specific lattice fringes. On one hand, we observed *d*-spacings of 2.47 Å hcp $CoAg_3$ (100) and 2.18 Å hcp $CoAg_3$ (101) which match perfectly the $CoAg_3$ compound. Moreover, the 6-fold symmetry of the structure is apparent in the FFT image. This also indicates that the $CoAg_3$ phase crystallizes into a hexagonal close-packed lattice. These results confirm those obtained by XRD and both are strong evidence of the existence of the $CoAg_3$ metastable hcp structure in the electrodeposited films. On the other hand, *d*-spacings of 2.36 Å fcc silver (111) and 2.06 Å fcc silver (200) were detected. Although scarcely detected, *d*-spacings of 1.85 Å corresponding to hcp cobalt (111) were also present. The interplanar spacings obtained by FFT for $CoAg_3$ and Ag correspond to the more intense reflections observed by XRD, observing again the agreement between both techniques.

The TEM micrographs and the corresponding FFT patterns of the samples annealed at 500 °C during 1 h are shown in Figure 8. The analysis of the FFT patterns revealed the disappearance of the $CoAg_3$ metastable phase as the *d*-spacings of it were no longer detected. On the other hand, the FFT analyses easily reveal 1.85 Å hcp Co (101) indicating that, after annealing, all cobalt is crystalline showing hcp structure. No evidence of fcc cobalt was observed. From the FFT HRTEM micrographs it is also possible to identify the inner extents of some Moiré fringes due to the superposition of different atomic planes. The fact that cobalt reflections were difficult to observe by XRD was probably due to either a low atomic scattering factor for the X-rays compared to that for electrons or that the crystallites are very small and cannot be detected by XRD.[29]

Magnetic Properties of Co−Ag Coatings. The magnetic properties of both Co−Ag coatings and pure-cobalt coatings were determined. The magnetic properties of pure cobalt were compared with those of cobalt films obtained from other baths and published elsewhere.[16,30−32] The magnetization-magnetic field curves were recorded maintaining the samples Si/Ti/Ni/

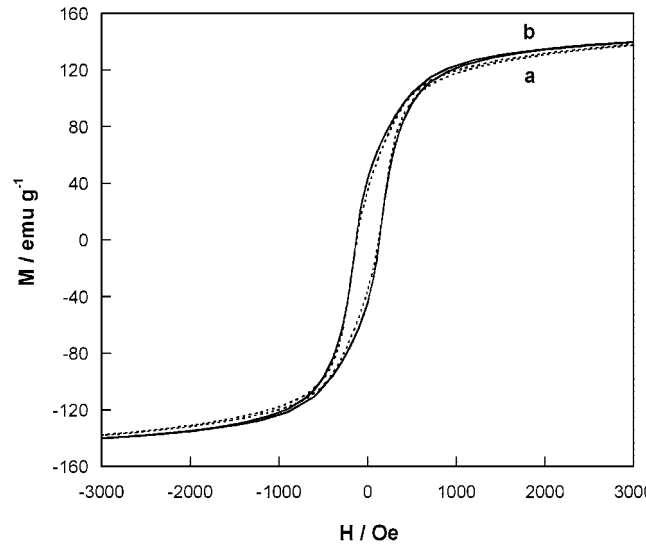

Figure 9. Magnetization versus magnetic field curves for Co deposits obtained from the Co solution at −1000 mV and different charges, (a) −13 C cm^{-2} and (b) −67 C cm^{-2}.

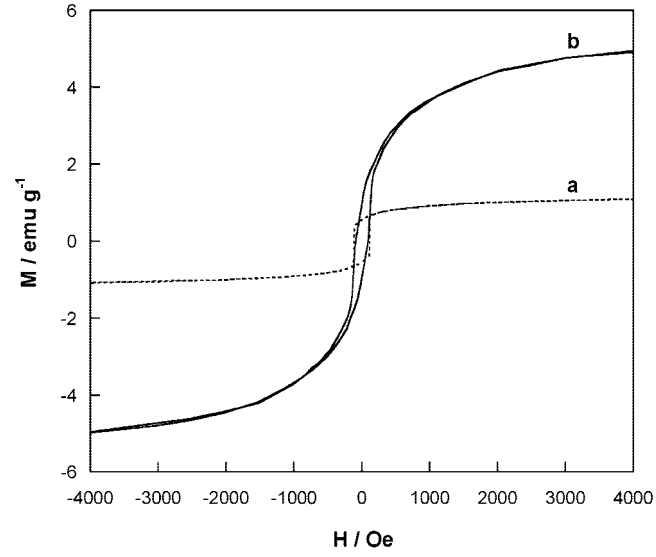

Figure 10. Magnetization versus magnetic field curves for Co−Ag deposits obtained from the Co−Ag solution and different cobalt percentages, (a) −800 mV, 33 wt % Co, (b) −820 mV, 50 wt %.

deposits parallel to the applied magnetic field. After magnetic characterization, the samples were dissolved and analyzed to determine the weight of the deposits. The magnetic response of the substrate (silicon/seed-layer) was not significant in comparison to the magnetic response of the pure-cobalt or Co−Ag coatings.

The magnetization curves of the cobalt deposits obtained from the Co solution revealed similar response for the deposits ranging from −13 to −67 C cm^{-2} (Figure 9). The saturation magnetization value, which was approximately 140−150 emu g^{-1}, corresponded to the value for bulk cobalt.[16] The coercivity value for the prepared cobalt coatings was approximately 120 Oe. Different values of coercive field were found for the cobalt electrodeposits prepared from different baths, which gave different crystalline structures. Cobalt hcp electrodeposits usually have values of coercive field in the range 200−100 Oe, depending on the current density or applied potential.[16,30,31] A

softer magnetic behavior was observed for the fcc cobalt electrodeposits, for which the value of coercive field (H_c) was approximately 40 Oe,[16] and amorphous cobalt with an H_c value of 15 Oe.[32] The cobalt deposits prepared from the Co solution in this study revealed an unusual crystalline structure with coercivity values close to those of the electrodeposits with an hcp structure.

Cobalt−silver deposits exhibited ferromagnetic behavior. In comparison with pure-cobalt films, the saturation magnetization value was low but increased with cobalt content (Figure 10). The coercive field value for the deposits of approximately 30−35 wt % of cobalt was 115 Oe.

Conclusions

This study demonstrated that the electrodeposition method is capable of inducing different crystalline structures. When a complex electrolytic bath was used, metastable crystalline structures were detected in both Co−Ag and Co electrodeposits. The experimental electrolytic bath containing perchlorate, thiourea, gluconate, and boric acid induced the formation, over the Si/Ti/Ni substrate, of cobalt coatings with crystalline structures corresponding to a primitive cubic phase (cP20). This is unlike the typical hcp or fcc cobalt structures.

Our results demonstrate that silver and cobalt can be simultaneously electrodeposited from solutions containing perchlorate, thiourea, gluconate, and boric acid. Rough black deposits of Co−Ag with different percentages were obtained, with a metastable cobalt−silver hexagonal phase (hP2). This has not been previously achieved by electrodeposition. TEM analysis indicates the presence of the metastable $CoAg_3$ as well as its disappearance after annealing at 500 °C during 1 h, leading to a hcp cobalt structure. The obtained Co−Ag deposits are ferromagnetic.

The electrodeposition technique is presented as a tool to modulate the structure and properties of the deposits obtained as a function of the experimental bath. In this study, unusual structures of Co and Co−Ag were obtained using electrodeposition in a complex bath containing a complexing agent and additives. The deposits of Co revealed a primitive cubic structure (cP20 in Pearson nomenclature), which never before has been detected using electrodeposition. On the other hand, the Co−Ag deposits revealed a hexagonal close packed structure (hP2 in Pearson nomenclature). Both phases are metastable. The magnetic properties of the electrodeposited films are included.

This study reveals the relationship between morphology, structure, and magnetic properties not only in Co−Ag deposits but also in Co deposits obtained electrochemically. The XRD patterns, SEM and TEM images, and magnetizations versus magnetic field curves are presented to demonstrate this relationship.

Acknowledgment. This paper was supported by contract MAT-2006-12913-C02-01 from the *Comisión Interministerial de Ciencia y Tecnología (CICYT)*. J.G.-T. would also like to thank the Departament d'Innovació, Universitats i Empresa of the Generalitat de Catalunya and Fons Social Europeu for their financial support.

References

(1) Hume-Rothery, W. Smallman, R. W. Haworth, C. *The Structure of Metals and Alloys*; The Institute of Metals: London, 1969.
(2) *Alloy Phase Diagram ASM Handbook*; Hugh, B., Eds.; ASM International: Cleveland, OH, 1992; Vol. 3, Chapter 2, p 27.
(3) Berkowitz, A. E.; Mitchell, J. R.; Carey, M. J.; Young, A. P.; Rao, D.; Starr, A.; Zhang, S.; Espada, F. E.; Parker, F. T.; Hutten, A.; Thomas, G. *J. Appl. Phys.* **1993**, *73*, 5320.
(4) Wang, J. Q.; Xiao, G. *Phys. Rev. B* **1994**, *49*, 3982.
(5) Fagan, A. J.; Viret, M.; Coey, J. M. D. *J. Phys.: Condens. Matter* **1995**, *7*, 8953.
(6) Du, J. H.; Li, Q.; Wang, L. C.; Sang, H.; Zhang, S. Y.; Du, Y. W.; Feng, D. *J. Phys.: Condens. Matter* **1995**, *7*, 9425.
(7) Wong, S. P.; Chiah, M. F.; Cheung, W. Y.; Xu, J. B.; Ke, N.; Ke, J. N. *Nuc. Instrum. Methods B* **1999**, *148*, 813.
(8) Arana, S.; Arana, N.; Gracia, F. J.; Castaño, E. *Sensor Actuator A-Phys.* **2005**, *123−124*, 116.
(9) Zaman, H.; Yamada, A.; Fukuda, H.; Ueda, Y. *J. Electrochem. Soc.* **1998**, *145*, 565.
(10) Kenane, S.; Chainet, E.; Nguyen, B.; Kadri, A.; Benbrahim, N.; Voiron, J. *Electrochem. Commun.* **2002**, *4*, 167.
(11) Kenane, S.; Voiron, J.; Benbrahim, N.; Chainet, E.; Robaut, F. *J. Magn. Magn. Mat.* **2006**, *297*, 99.
(12) Gómez, E; García-Torres, J; Vallés, E. *Anal. Chim. Acta* **2007**, *602*, 187.
(13) Childress, J. R.; Chien, C. L. *Phys. Rev. B* **1991**, *43*, 8089.
(14) Fedosyuk, V. M.; Kasyutich, O. I.; Ravinder, D.; Blythe, H. J. *J. Magn. Magn. Mater.* **1996**, *156*, 345.
(15) Gómez, E.; Labarta, A.; Llorente, A.; Vallés, E. *J. Electrochem. Soc.* **2004**, *151*, C731.
(16) Gómez, E.; Vallés, E. *J. Appl. Electrochem.* **2002**, *32*, 693.
(17) Sun, S.; Murray, C. B. *J. Appl. Phys.* **1999**, *85*, 4325.
(18) Puentes, V. F.; Krishnan, K. M.; Alivasatos, P. *Appl. Phys. Lett.* **2001**, *78*, 2187.
(19) Nie, X.; Jiang, J. C.; Meletis, E. I.; Tung, L. D.; Spinu, L. *J. Appl. Phys.* **2003**, *93*, 4750.
(20) Li, Z. C.; Liu, J. B.; Liu, B. X. *J. Phys.: Condens. Matter* **2000**, *12*, 9231.
(21) Sumiyama, K.; Kataoka, N.; Nakamura, Y. *Mater. Sci. Eng.* **1998**, *98*, 343.
(22) Duwez, P.; Willens, R. H.; Klement, W, Jr *J. Appl. Phys.* **1960**, *31*, 1137.
(23) Pandey, V.; Ramachandrarao, P. *Surf. Coat. Technol.* **1987**, *30*, 401.
(24) Kong, Y.; Guo, H. B.; Yan, H. F.; Liu, B. X. *J. Phys. Chem. B* **2005**, *109*, 9362.
(25) Guo, H. B.; Liu, B. X. *J. Mater. Res.* **2004**, *19* (5), 1364.
(26) Amirthapandian, S.; Panigrahi, B. K.; Srivastava, A. K.; Gupta, A.; Nair, K. G. M.; Nandedkar, R. V.; Narayanasamy, A. *J. Phys.: Condens. Matter* **2002**, *14*, L641.
(27) Hauser, J. J. *Physical Review B* **1983**, *28* (8), 4860.
(28) Watanabe, T. *Nano-plating: Microstructure Control Theory of Plated Films and Data Base of Plated Film Microstructure*; Elsevier: Amsterdam, 2004.
(29) Sakuma, H.; Tai, H.; Ishii, K. *IEEJ Trans* **2008**, *3*, 375.
(30) Gómez, E.; Pellicer, E.; Vallés, E. *J. Electroanal. Chem.* **2001**, *517*, 109.
(31) Gómez, E.; Pellicer, E.; Alcobé, X.; Vallés, E. *J. Solid State Electrochem.* **2004**, *8*, 497.
(32) García-Torres, J.; Gómez, E.; Vallés, E. *J. Appl. Electrochem.* **2009**, *39*, 233.

CG801167H